# THE FLUID CHARACTERISTICS OF BENTONITE SUSPENSIONS.

By

Carl Kerby Stoddard

Thesis submitted to the Faculty of the Graduate School
of the University of Maryland in partial
fulfillment of the requirements for the
degree of Doctor of Philosophy

1941

UMI Number: DP71132

# ABSTRACT.

Carl Kerby Stoddard, Doctor of Philosophy, 1941.

Major: Chemical Engineering

Title of Thesis: The Fluid Characteristics of Bentonite
Suspensions.

Directed by Dr. Wilbert J. Huff.

Pages in thesis,      . Words in abstract,


A study of the peculiar fluid characteristics of bentonite
suspensions was conducted by ascertaining the shearing stress
transmitted by the suspensions when they were submitted to a
constant and sustained rate of shear. The use of the variables,
shearing stress and rate of shear was suggested by a considera-
tion of the fundamental requirements of the concept of viscosity.
In order to express the results of the shearing stress and rate
of shear variables in the absolute units of dynes per square
centimeter and reciprocal seconds respectively, it was necessary
to calibrate the instrument by means of refined petroleum oils
whose viscosities were accurately known. The instrument used
was built according to a design suggested by C. W. Goodeve which
embodied a rotating conical sample cup into which an identical
cone frustrum was coaxially suspended from a torsion wire. De-
flections of the torsion wire were observed for given separa-
tions between the shearing surfaces at a constant rate of ro-
tation when the sample occupied the annular space. The calibra-
tion of the instrument demonstrated that the shearing action of
the conical surfaces approached closely the ideal case envisioned

91262

by the definition of the coefficient of viscosity.

The measurements made upon bentonite suspensions showed that the shearing stress would attain a constant value under the influence of the sustained rate of shear for a sufficient length of time. This constant value is considered to be the result of an equilibrium between the development of structure by the forces that cause gelation and the destructive action of the shearing surfaces. The relation between the shearing stress and rate of shear for the equilibrium condition showed that the fluid behavior was non-Newtonian and was best described by a parabolic equation. The presence of thixotropy was shown by a hysteresis loop obtained by a cyclic increase and decrease of the rate of shear. The ability of the bentonite suspensions to develop a rigid structure and exhibit a yield point was measured and considered in relation to the fluid behavior. It was concluded that yield value is a property of the solid state and cannot be shown on a rheological diagram which is the graph of the variables, shearing stress and rate of shear. This is equivalent to a denial of the Bingham hypothesis. The yield value was established by means of shearing stress-shear determinations which also indicated the presence of elastic behavior and relaxation effects. A diagrammatic explanation of the relation of the solid state to the fluid state in terms of the variables, shearing stress, shear, and rate of shear, is given.

# TABLE OF CONTENTS.

# TABLE OF CONTENTS CONTINUED.

# LIST OF FIGURES.

# LIST OF FIGURES CONTINUED.

# LIST OF FIGURES CONTINUED.

# LIST OF TABLES

# LIST OF TABLES CONTINUED.

## TABLE OF SYMBOLS USED.

$\mathcal{V}$ = volume of efflux in time t.

$P$ = pressure head.

$R$ = radius of capillary. cm.

$L$ = length of capillary. cm.

$\eta$ = coefficient of viscosity.

$F$ = force tangentially on a plane surface.

$A$ = area.

$v$ = linear velocity, centimeters per second.

$x$ = distance over which a shear is acting.

$\tau$ = shearing stress, dynes per sq. cm. acting tangentially.

$\sigma$ = rate of shear, seconds$^{-1}$.

$\varphi$ = amount of shear, centimeters.

$t$ = time, seconds, minutes or hours.

$G_T$ = moment of force opposing the shearing of a viscous
material by means of concentric cylinders, measured
by the energy stored in a torsion wire, ergs.

$\ell$ = length of cylinder on which a shearing force is acting. cm.

$R_1$ = the radius of an inner cylinder, cm.

$R_2$ = the radius of an outer cylinder, cm.

$\omega$ = angular velocity, radians per second.

$\tau_B$ = shearing stress at the yield point on the Bingham type
of diagram.

$\tau_L$ = shearing stress at some lower point sometimes called
the lower yield value.

$\tau_U$ = shearing stress at the beginning of linearity, called
the upper yield value.

$R_E$ = effective radius of the inner cone, cm.

$r$ = any intermediate radius between the cones, cm.

$F_v$ = total viscous force acting on inner cone frustrum, dynes.

$G_v$ = The moment of force or couple generated by the viscous drag of a fluid, ergs.

$\delta$ = deflection of the inner cone, degrees.

$T$ = torsional constant of the wire, ergs per degree.

$\Omega$ = angular velocity, revolutions per minute.

$\tau_m$ = the mean shearing stress between concentric cylinders.

$\sigma_m$ = the mean rate of shear between concentric cylinders.

$d$ = the normal separation between two concentric cylindrical shearing walls, cm.

$Q$ = a factor determined by the value of
$$\frac{2\pi}{60}\left[\frac{R_E + \frac{1}{2}d}{d}\right]$$

$h$ = the verticle distance measured by the micrometer head, cm.

$k$ = the wire constant for converting deflection readings into shearing stresses.

$\sigma$ = total rate of shear, sec$^{-1}$.

$\sigma_\lambda$ = constant rate of shear due to asymptotic variation of rate of shear with separation, d.

$m$ = slope of the straight line relationship between deflections and rates of shear, $\sigma$ , obtained with the standard oils.

$\theta$ = period of oscillation of torsional pendulum, seconds.

$I$ = moment of inertia.

$e$ = restoring couple acting on the angular displacement from rest position of the torsional pendulum, ergs per radian

$M$ = mass of disk, gms.

$R_e$ = Reynold's number.

$\rho$ = density, grams per cubic centimeter.

# INTRODUCTION.

The use of bentonite and similar clay materials because of their unique fluid behavior when suspended in water has become of considerable importance in recent years. Perhaps the most outstanding illustration from the standpoint of scope and monetary value is the use of bentonite and bentonitic clay suspensions in drilling for petroleum. Considerable expenditures of time, thought and money are made directly upon the mud-fluid that performs several very useful services as the hole is being drilled into the various rock formations. The efficiency of these services is closely related, and in some cases, directly dependent, upon the fluid condition of the mud material.

The colloidal properties of bentonite suspensions afford a common denominator for the similarity of fluid behavior of many other heterogeneous materials that are important to technology. The ceramic industry is in many ways concerned fundamentally with the fluid properties of clay dispersions, casting slips, enamels and glazes, etc. The useful performance of paints, printing inks, plasters and resins, is in all cases, closely related to the fluid behavior. The pumping of ground cement rock, sewage sludges, and ore pulps present problems to the engineer that are the results of the fluid properties of colloidal and semicolloidal materials. The process for the separation of coal and other minerals from the valueless constituents of an ore by means of the sink and float effect

in suspensions of high density depends upon the maintenance of a medium of sufficient fluidity and the proper overall density.  Careful control is necessary since the two factors act in opposition to each other.

The measurement and study of the fluid properties of these and similar materials has given recent impetus to the somewhat forgotten science of rheology.  The term rheology is new to many; but is defined in the latest edition of Webster's Dictionary as the science of the flow and deformation of matter.  It has a connotation towards the less conspicuous and not so well understood flow and fluid properties of the more complex systems such as listed above.  There is some reason to suspect that part of the information available on the flow of these materials is wrong.  The need for exact fundamental investigation is great for it is admitted that many of the past investigations have been based upon empirical and arbitrary approaches, frequently born of the extreme necessity of the rheological measurement.  It is felt that the opportunity afforded the recent investigation is unique since the instrument used is admirably suited to measure fluid properties in fundamental units, and that, also, the results will be of particular interest to those who make use of the fluid properties of bentonite and of general interest to the subject of rheology as a whole.

# CHAPTER I

## THE VISCOSITY CONCEPT.

In order to proceed to a logical study of the fluid
properties of a bentonite suspension, it is necessary to
have clearly in mind the fundamental philosophy of the shear-
ing concept that forms the basis for the measurement of the
liquid state. The use of a single number, the coefficient
of viscosity, to express the degree of the fluid state of
a material rests upon such firmly established theory, that
there has arisen a tendency to overlook the importance of the
shearing relationships to viscous measurements. In the fol-
lowing, the shearing concept is traced through the classical
work that established the laws of flow and makes possible the
viscometric methods used today. It is to be understood in
the pages to follow that turbulent flow is excluded as a pos-
sibility except where it is expressly indicated as such.

Newton[1] in 1729 wrote of the shearing forces trans-
mitted by fluids in motion and formulated the hypothesis:
"That the resistance which arises from the lack of slipperi-
ness [viscosity] is proportional to the velocity with which
the parts of the liquid are separated from one another".
On the basis of this hypothesis he conceived certain propo-
sitions which he was able to demonstrate by his rigorous
mathematical reasoning. He did no experimental work; and

---

[1] Isaac Newton, Principia ii, section VII (1729)

it seems he was content with his hypothesis only as a mental experiment necessary for his mathematical deductions.

Experimental evidence to verify this assumption did not appear until years afterwards, when in 1842 and 1846, Poiseuille published his conclusions on the flow of water through capillary tubes.[2] Poiseuille did not offer the equation that today is designated by his name, but merely indicated the relations between the pressure head, length and diameter of the tube, and the volume of efflux in a given time by means of the following equation.

$$Q = K \frac{PR'}{L} \tag{1}$$

where:

$Q$ = volume of efflux in time t.

$P$ = pressure head.

$R$ = radius of the capillary.

$L$ = length of the capillary.

$K$ = a constant which is proportional to the viscosity and is characteristic of the liquid.

It was not long after that Wiedemann[3] published a deduction of Poiseuille's Law. His pupil Hagenbach[4] gave it in a more precise form four years later which is virtually

[2]Poiseuille, Comptes rendus 11: 961, 1041 (1840)
    ibid 12: 112 (1842)

[3]Wiedemann, Pogg. Ann. 99, 221 (1856)

[4]Hagenbach, Pogg. Ann. 109, 385 (1860)

the same as is used in modern text-books on physics. The derivation will not be given here but it is desirable to bring attention to the assumptions (as listed by Barr) that are used in the mathematical derivation of the Poiseuille equation.

It is assumed: (1) that the flow is everywhere parallel to the axis of the tube; (2) that the flow is steady, initial disturbances due to accelerations from rest having been damped out; (3) that there is no slip at the wall of the tube, i. e., the fluid in contact with the wall of the tube is at rest; (4) that the fluid is incompressible; (5) that the fluid will flow when subjected to the smallest shearing force, the viscous resistance being proportioned to the velocity gradient.[5a]

On this basis the derivation proceeds to the expression that today is designated as Poiseuille's equation:

$$Q = \frac{\pi P R^4}{8 L \eta} \tag{2}$$

where:        $\eta$ = the coefficient of viscosity.

Newton's hypothesis appears in the latter part of the 5th assumption. It is not clear whether or not Wiedemann and Hagenbach were aware that this assumption has been previously ennunciated by Newton, but at least they were aware of its significance in relation to fluid flow.

The correctness of Newton's assumption is demonstrated by the wide use of the Poiseuille equation for the determination of the coefficient of viscosity, $\eta$ . The science of viscometry is based upon this hypothesis and resulting

---

[5a] Guy Barr, A Monograph of Viscosity, (London, Oxford University Press, 1931), p. 13.

constancy of $\eta$ has been many times demonstrated.

As a result of the exact understanding of the Newtonian hypothesis, the definition of the coefficient of viscosity is possible in terms of absolute quantities. This definition, which is due to Maxwell, is given here as enunciated by the British Engineering Standards Association:[6]

> The coefficient of viscosity of a fluid is the numerical value of the tangential force on unit area of either of two planes at unit distance apart when the space between these planes is filled with the liquid in question and one of the planes moves until unit velocity in its own plane relatively to the other.

This statement is given mathematically by the following equation

$$F = \eta \frac{A v}{x}$$

(3)

where:

$F$ = the force acting tangentially on the plane.

$A$ = area over which the force acts.

$v$ = velocity with which the plane moves.

$X$ = distance between planes.

From Equation 3, the dimension of viscosity are obtained in the following manner:

$$\eta = \frac{Fx}{Av} = \frac{(m l t^{-2})(l)}{(l^2)(l t^{-1})} = m l t^{-1}$$

(4)

---

[6] British Engineering Standards Association, Specifications No.188, 1929.

In the C.G.S. system, the term poise has been almost universally adopted in accordance with the suggestion of Deeley & Parr.[7]  A somewhat more convenient unit is the hundredth of a poise or the familiar centipoise.  It so happens that water at a temperature of 20°C has a viscosity of almost exactly one centipoise.

Equation 3 is the mathematical expression of Newton's hypothesis.  It can be written in this form

$$\tau = \eta \frac{dv}{dx} \tag{5}$$

where:   $\tau$ = the force acting tangentially per unit area.

The velocity gradient term $\frac{dv}{dx}$ is general and can be applied to the flow in a tube wherein the velocity varies parabolically from zero at the wall to a maximum at the center.  In the ideal case of the above definition, the velocity of flow varies linearly from the stationary plane to the moving plane.

It can be shown[8] that the velocity gradient $\frac{dv}{dx}$ of Equation 5 is numerically equal to the rate of shear, $\sigma$ existing between the planes $dx$ distance apart moving with a velocity difference $dv$ .  Rate of shear is defined by

---

[7]Deeley and Parr, Phil. Mag. 26:85 (1913)

[8]First Report on Viscosity and Plasticity, Committee for the Study of Viscosity, Academy of Sciences at Amsterdam. (New York City, Nordemann Publishing Company. 2nd ed.,1939) p. 6.

this equation:

$$\sigma = \frac{d\varphi}{dt}$$

(6)

where:    $\sigma$ = rate of shear, reciprocal seconds.

         $\varphi$ = amount of shear, cm.

         $t$ = time in which the shear occurs, sec.

Accordingly Equation 5 becomes:

$$\tau = \eta \, \sigma$$

(7)

This equation represents the useful form for expressing the shearing relation that is necessary to the concept of viscosity. It states that the shearing stress is directly proportional to the rate of shear, the term $\eta$ being the coefficient of proportionality, i. e. the viscosity. This again is the hypothesis conceived by Newton although he at that time had no concern for a means of measuring the "lack of slipperiness" of liquid. As stated before, this useful consequence of Newton's hypothesis was not realized until after the observations of Poiseuille and the mathematics of Hagenbach indicated its reality.

It is possible to put the Poiseuille equation into the form of Equation 7, thus showing the relationship of the forces and shearing motion of a liquid flowing through a tube. This is shown in the following manner.

$$\frac{RP}{2L} = \eta \, \frac{4Q}{\pi R^3}$$

(8)

In Equation 8, the term $\frac{RP}{2L}$ represents the force or shearing stress existing at the wall and the term $\frac{4Q}{3R^3}$ becomes the value of the rate of shear existing between the wall and the center of the tube.

CHAPTER II

THE GRAPHICAL REPRESENTATION.

The graph of the equation,

$$\tau = \eta \sigma \qquad (7)$$

is a straight line extending upwards to the right from the
origin as shown in Figure 1a. The slope of the straight
line is the viscosity of the fluid which Figure 1a might
represent. Such diagrams are commonly called rheological
diagrams.
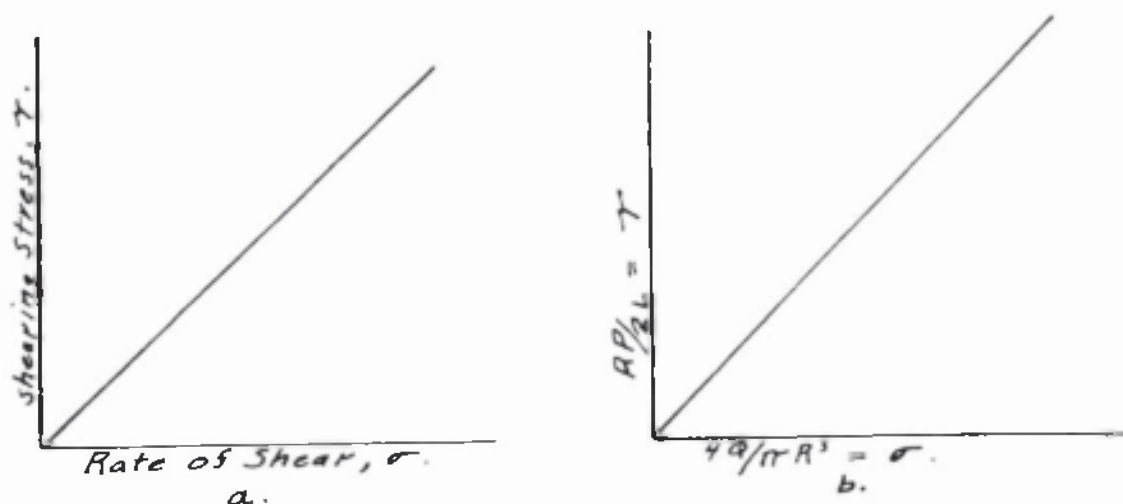


Figure 1. Rheological Diagrams for Newton's relation-
ship and flow of viscous materials through tubes.

In a similar fashion the Poiseuille expression,

$$Q = \frac{\pi\, P R^4}{8 L \eta} \tag{2}$$

as arranged in Equation 8, allows the plotting of the
rheological diagram.  In this case the stress term, $\frac{RP}{2L}$
is plotted as the ordinate and the rate of shear term $\frac{4Q}{\pi R^3}$,
as the abscissa as shown in Figure 1b.

Since flow of a simple liquid through a tube proceeds
as a special form of the simple shear defining the viscosity
concept, measurements of the efflux per unit time, plotted
with the corresponding pressure, yield points that fall on
a straight line, such diagrams are frequently found in the
literature.  However, if the values of efflux and pressure
are reduced to consistent values of rate of shear and shear-
ing stress by combination with the terms for radii and
length in accordance with Equation 8, the points will all
fall on the same straight line for a given liquid even when
tubes of different dimensions are used.[9]  This applies, of
course, for conditions of flow that are not turbulent.

The ideal condition represented by the shearing between
parallel planes pictured in the definition above of the
coefficient of viscosity given is not easy to realize ex-
perimentally.[10]  However, the Couette type of viscometer

---

[9] M. Reiner, Physics, 5:326 (1934)

[10] First Report on Viscosity and Plasticity, op. cit.
pp. 75-6

offers a close approximation in which two coaxial cylinders are used instead of the parallel planes.[10] One cylinder revolves in respect to the other and the force that acts on the fixed cylinders as a result of the continuous shearing is related to the velocity gradient.

The derivation of the Couette equation is given in many places[5b] and will not be repeated here. The assumptions are the same as those necessary for the Poiseuille equation except that the flow is considered as being in parallel layers, concentric to the axis of the cylinder. The equation is as follows:

$$\frac{G_T}{2\pi R_1 R_2 \ell} = \eta \, \frac{2\omega R_1 R_2}{R_2^2 - R_1^2} \tag{9}$$

where:    $\eta$ = coefficient of viscosity, poise.

$G_T$ = moment of force opposing the shearing, ergs.

$\ell$ = length of the cylinder on which the force is acting, cm.

$R_1$ = radius of the inner cylinder, cm.

$R_2$ = radius of the outer cylinder, cm.

$\omega$ = angular velocity, radians per second.

Equation 9 is a linear equation that shows the relation between the shearing stress given by the left hand term and the rate of shear as given by the term $\frac{2\omega R_1 R_2}{R_2^2 - R_1^2}$ on the right side. This is predicated on the basis that $G_T$ and $\omega$ are the variables. When Equation 9 is plotted on linear cordinates, the customary linear figure is obtained, the slope of which is the numerical value of the coefficient of viscosity.

---

[5b]Guy Barr, op. cit. p. 222.

This is shown by Figure 2.
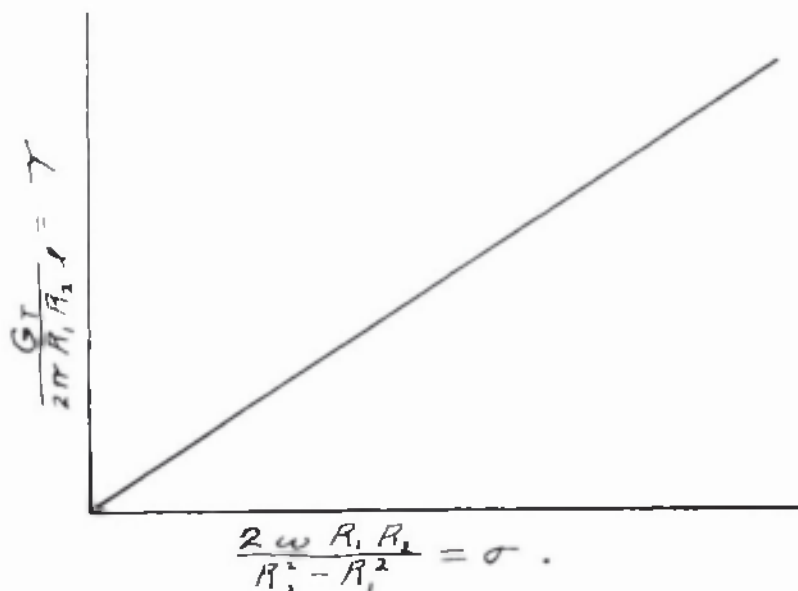


Figure 2. Rheological Diagram for the Couette Equation.

In the foregoing, it has been brought out that the concept of viscosity arises from the measurement of the forces that are transmitted by a fluid when subjected to a sustained shearing action. In the case of simple liquids it has been amply demonstrated that the force transmitted is directly proportional to the intensity of the shearing (i.e. the rate of shear). This was first expressed as a hypothesis by Newton and subsequently found to be a fact as the result of the contribution of Poiseuille, Hagenbach, Couette, etc.

The constant of proportionality was recognized by Maxwell as a convenient measure of the consistency of liquids and has come to be designated as the coefficient of viscosity. Equation 7 is the mathematical relationship between the force and the rate of shearing when applied to the simple fluids. Diagramatically this is shown by Figure 1a. It is now common to designate the fluids that conform to this equation as Newtonian liquids. By the same token, fluids that do not conform to the linear relationship between shearing stress and rate of shear are called non-Newtonian liquids. Sometimes the term anomalous fluids is used; however, this term is not apt because the designation of anomaly is a matter of definition.

It was Hatschek [11] who first suggested that there is no a priori reason that the relationship between the force and the rate of shear should be linear. In other words the relation between the shearing force and a rate of shear, may be represented by this equation:

$$\tau = f(\sigma) \tag{10}$$

It so happens that this general expression is a simple relationship (as shown by Equation 7) for the vast majority of the simple liquids. However, certain materials such as colloids, bitumens, honey, paints, clay suspensions, etc.

---

[11] E. Hatschek, The Viscosity of Liquids. (London, Bell and Sons, 1928) p.215

do not show obedience to the simple linear relationship between rate of shear and stress as is given by Equations 7, 8 and 9. It is found that the coefficient of viscosity is not a constant and is in reality some unknown function of the rate of shear, in general decreasing as the rate of shear increases. A further complication to the fluid properties of these materials arises from the observation that the materials under certain conditions will not relieve a small applied stress as a true liquid will but sustain it more or less indefinitely, i. e. the material possesses a rigidity. Hysteresis effects were also observed in the attainment of equilibrium between the two factors, rate of shear and shearing stress. Urgency of the need of the measurements usually affected the problem of making viscometric determinations on the fluids of this type, which frequently resulted in rigorous standardization of methods valid only for simple fluids as the basis for comparison. Thus many empirical measurements were made, even though it was known that the material did not satisfy the fundamental laws which make the determination of the coefficient of viscosity possible. Further, as pointed out above, the success of the Poiseuille method has tended to divert attention from the fact that viscous measurement is a shearing process and that the constancy of the coefficient of viscosity is the effect of the linear relation between the rate of shear and shearing stress and not the cause.

With the foregoing philosophy of the viscosity concept

as a background, the work to be described in the pages to come is based on the following argument. Since the rational measurement of the fluid properties of materials depends upon the relationship between the variables, rate of shear and shearing stress, the determination of this relationship constitutes a description of the fluid properties of the material; furthermore it is not to be unexpected that a non-linear function may exist.

EXTENSION OF THE GRAPHICAL REPRESENTATION.

Figure 1 shows the graphical representation of the viscosity concept. It is the graph of Equation 7.

$$\gamma = \eta \sigma \tag{7}$$

However, as indicated above, a non-linear function may exist between the rate of shear and shearing stress variables. Thus on this basis, in Figure 3 are shown diagrammatically some of the possibilities that can be distinguished.[12]
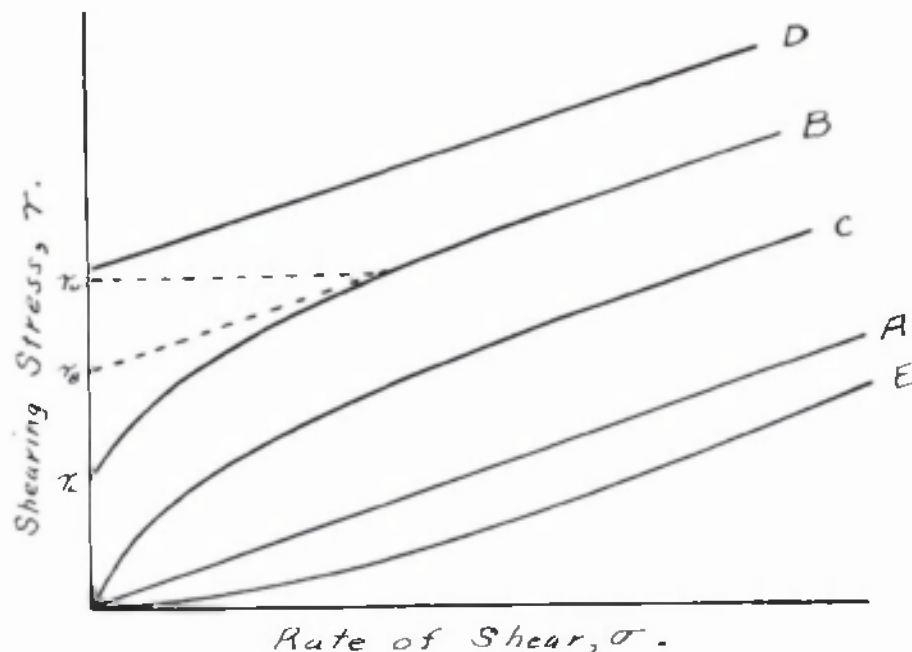


Figure 3. Rheological Diagram of Newtonian (curve A) and some Possibilities of non-Newtonian Types of Behavior (curves B C D and E)

---

[12]First Report on Viscosity and Plasticity, op. cit. pp.142-3

Curve A is the system possessing a linear proportion between rate of shear and shearing stress, which has been discussed above as Newtonian flow. Curve B represents the system that shows static rigidity and variable viscosity. The points $\tau_B$ and $\tau_L$ represent the stress associated with zero rate of shear. These have been called yield values. The yield value, $\tau_B$ is obtained when it is necessary to extrapolate from the straighter portions of the curve and the yield value $\tau_L$ is sometimes obtained by direct measurement. This curve is typical of the observations made by Bingham which will be discussed in more detail below. On curve B the reciprocal of the slope of the straight section is sometimes called mobility according to the suggestion of Bingham. Curve C represents the material that does not possess any yield value. It has been designated by some as representing the psuedo-plastic systems. In the same analogy, the system represented by curve D would be called an "ideal plastic". In this case the yield values $\tau_B$, $\tau_L$ and the stress represented by the beginning of the linear section of curve B which sometimes is called the upper yield value $\tau_U$ , all coincide at $\tau_B$ .

Curve E represents the case in which an increase in viscosity occurs with increasing rate of shear. This behavior seems to be found in nature in the case of some textile fabrics.[12]

---

[12]First Report on Viscosity and Plasticity, op. cit. pp.142-3.

This group of curves typify in general the types of flow for which there is reason to believe may exist in nature. The types of flow that may be represented by the curves other than A have not been clearly established since few experimental procedures have been amenable to reduction to rate of shear and shearing stress. Furthermore, as will be shown later, it has not been clearly understood that different results will be obtained when the shearing stress is applied to a given fluid as the independent variable, and when the rate of shear is applied as the independent variable. In other words it matters greatly which variable is dependent and which is independent.

# CHAPTER III

## DESCRIPTION OF APPARATUS.

The apparatus used in this investigation is a modification of the rotating concentric cylinder type of viscometer. It was designed by C. F. Goodeve and has recently appeared on the market, being manufactured by Messrs. Griffin and Tatlock*, Ltd of London. It is shown diagrammatically by Figure 4. A photograph of the instrument with its auxilliary apparatus is given by Figure 5. Goodeve has chosen to call the instrument a "Thixoviscosimeter" with the connotation that thixotropy can be measured. The present author cannot agree that the method proposed is a fully adequate means of measuring this phenomena; therefore in the pages to come, the apparatus will be referred to as the Goodeve instrument or the Goodeve viscometer, for a viscometer it most truly is. The following is Goodeve's description of the instrument.[13]

> The instrument comprises a container which has a conical internal surface and which is rotated at a constant speed; a frustrum of a cone is suspended or pivoted coaxially inside. The fluid between the conical surfaces imparts a moment tending to rotate the inner cone, and this moment is measured by the regular displacement of a torsion wire. The distance between the conical surfaces is altered by raising or lowering the inner cone along the axis.

> The instrument is built upon a triangular base casting, provided with leveling screws, a spirit level and a rigid pillar, as shown in Figure 4a. To this pillar is bolted a casting which acts as a protecting cover for the gears

---

[13]C. F. Goodeve. J. Sci. Inst. 16:19(1939)

and motor mounted below and which contains the
ball races supporting the lower cone A. The
motor is of the universal, governor-controlled,
constant speed type, and is arranged to swing
out from beneath the shield in order to change
the gears and thus the rate of revolution of
the cone A. This cone is made with an overhang-
ing base to protect the ball races. The con-
tainer C is a hollow cone and fits friction-
tight into the cone A, but can be readily removed
for cleaning or filling.

The inner cone B is shown in more detail in
Figure 4b. Its external conical surface is ac-
curately turned to the same angle as the inner
surface of the container. The viscous drag on
the ends is reduced by the cutaway parts and the
sharp edges. The cone is fixed to a slotted tube
D containing a thermometer whose bulb is in the
center of the inner cone. At the upper end of
this tube is mounted a drum E the periphery of
which is divided from 0 to 360°, and a chuck G
which grips the lower end of the torsion wire H.
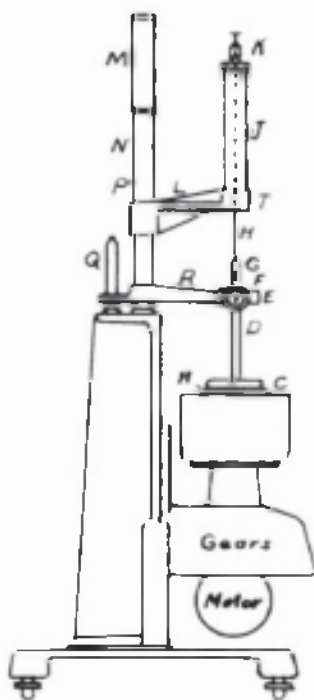


Figure 4. The Goodeve Viscometer for the Measurement of
Viscosity of Suspensions.

Figure 4b. Inner cone and Sample Cup.
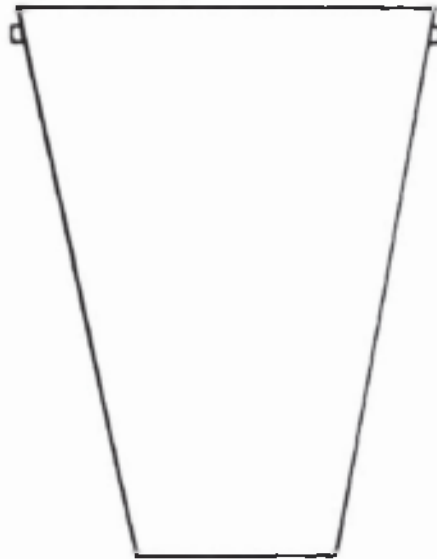


Figure 4c. Special Oversize Cup.

The upper end of the torsion wire is held by a chuck K to the column J, which in turn is securely fixed by means of the bracket L to the telescopic tube N. The position of K may be adjusted laterally over a small range to allow the cones to be centered. The tube N fits over the pillar P, and is raised or lowered by rotating the head M, which acts by means of a screw on the top of the pillar. The bracket R is fixed to the tube N and, by means of a slot working on the pillar Q, prevents the rotation of the upper part of the apparatus. This bracket also carries an eyepiece F, by means of which the angular displacement of the inner cone can be read on the drum scale

The whole structure can be conveniently raised by sliding the tube N up the pillar P until the slot disengages from the pillar Q, after which it can be rotated through some 45° and locked in the elevated position by allowing a hole in the bracket R to fit over the end of Q. The inner cone is then supported above and at the right of the container, leaving both immediately accessible.

A number of modifications and additions were made on the instrument. Chief among these was the addition of a magnetic dampening device which eliminated considerable vibration and oscillation of the suspended inner cone when the outer cup was rotating. At the equilibrium position between the restoring couple of the torsion wire and the forward drag of the viscous forces, the magnetic dampening action is zero, therefore the deflection reading is the same as would be obtained were the magnetic dampener not present. This device consisted of an aluminum disk fixed to the slotted tube carrying the inner cone and placed just below the chuck G as shown ① in Figure 5. At opposite points on its periphery were mounted two pairs of horseshoe magnets ② so that the rotation of the inner cone caused the disk to turn between
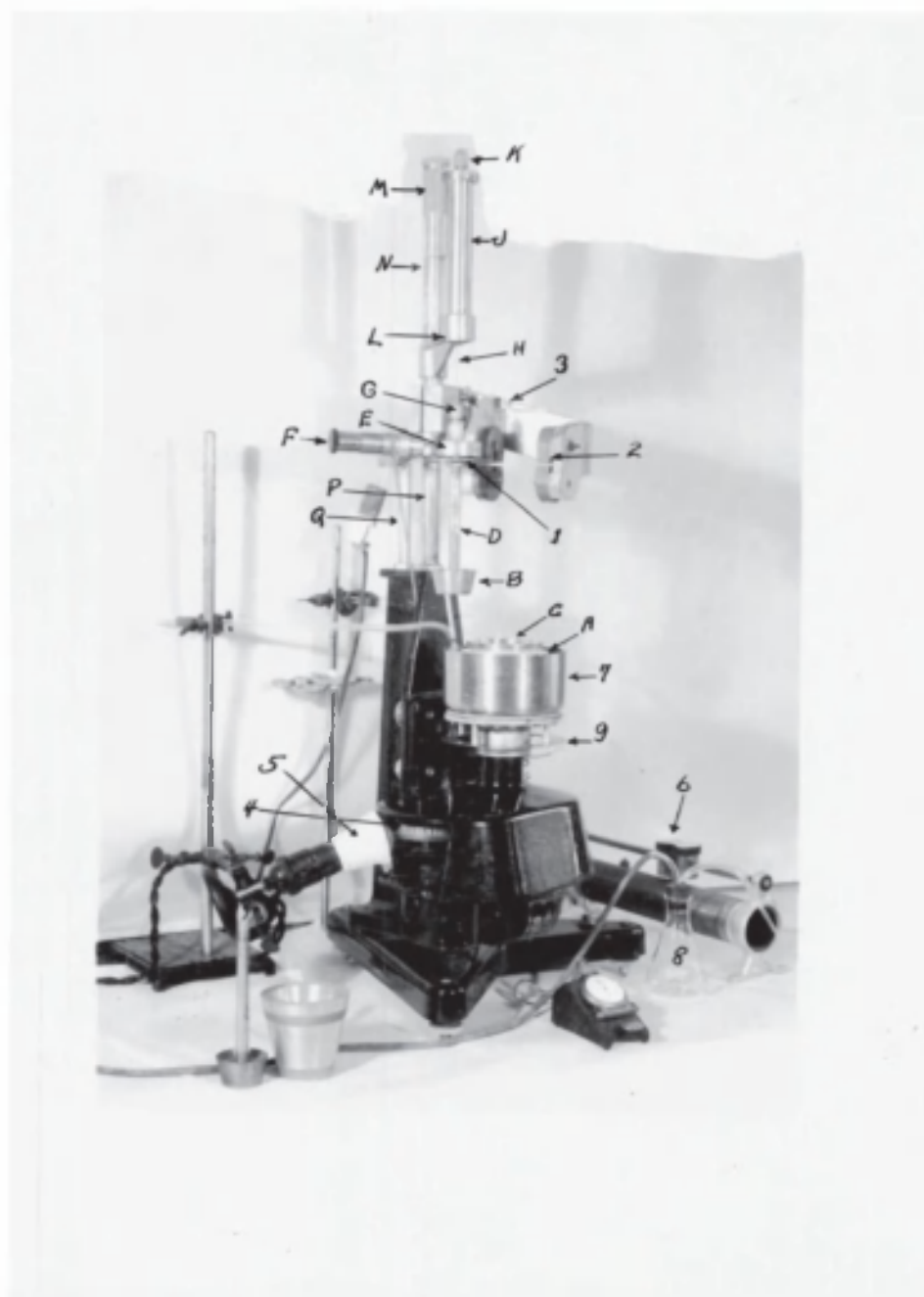
Figure 5.   Photograph of the Goodeve viscometer and auxiliary apparatus.   Head and cone assembly is in the raised position; the magnet dampener is swung away from the inner cone and torsion wire.

the poles of the magnets and thus be acted upon by the in-
duced electrical current. The magnets were of the high-
remenance alloy type, mounted with opposite poles matching.
The framework ③ supporting the magnets was clamped to the
pillar P just below the arm L and could be pivoted on the
pillar P as a turning bearing through about $40^{\circ}$, thus swing-
ing the magnets free from the disk and inner cone assembly
to allow cleaning the cup and cone and the changing of the
torsion wires. Otherwise the magnetic dampening device in
no way interfered with the normal operation of the instru-
ment.

The gears provided with the instrument allowed the
outer cup to rotate at speeds of 1.25, 5.0, 20, and 80 r.p.m.
These gears were attached to a constant speed spindle rising
vertically from the governor mechanism of the motor. A
stroboscopic speed check was obtained by fitting to this
spindle an aluminum disk ④ divided on its periphery into
40 alternate black and white strips. When this disk was
illuminated with a 5 watt neon bulb ⑤ on the 110 volt, 60
cycle current, the divisions on the drum appeared to be
stationary when it turns at 80 r.p.m. By means of a pointer
and a small mirror strategically mounted, a quick glance
would indicate whether or not the apparatus was turning at
the correct speed.

The motor was supplied with two blank leads connected
to the brushes. When a variable resistance ⑥ of about 500
ohms maximum, was placed across the brushes by means of

the provided leads, a means of speed adjustment was available. Decreasing the resistance across the brushes caused the motor to operate at a slower speed. In practice, in order to have the maximum power, it was found best to operate the motor with the greatest resistance possible across the brushes.

As a means of temperature control, a water bath jacket ⑦ was fitted around the outer cup A by means of bolt holes originally present on the instrument for that purpose. The aluminum metal parts exposed to the water were coated first with a bituminous paint to minimize corrosion. Constant temperature was obtained by arranging the end of a 200 watt low-lag knife-heating unit, not shown in the figures, to dip a few centimeters under the surface of the water in the annular space of the water jacket. This heating unit was connected in series with a 75 watt Mazda lamp to a relay. A small mercury thermostat element was immersed in the annular space and connected with the relay. By means of this arrangement a temperature control of $\pm 0.02°$ was easily obtainable in the water bath. When the room temperature was greater than that desired for the water bath and material contained in the cup, cold water from the supply tap could be introduced through a bent glass tube extending down into the annular space of the water jacket. Overflow was removed by a similar glass tube adjusted at the desired upper level, and connected to an aspirator on the water supply line. Quick adjustment

of the temperature could be made by pouring hot or cold water from a beaker into the annular space. A special thermometer, about 15 cm length reading from 0 to 40° C was clamped to dip in the water in the annular space. A heavy ringstand carried the clamping assembly for the glass water inlet and outlet tubes, the thermostat and heater.

Auxiliary equipment consisted of a number of suction flasks ⑧ interchangable on a stopper carrying two bent glass tubes by means of which the sample could be removed from the cup and the recessed part on the top side of the inner cone.

A full circle protractor ⑨ was fitted to the flange on the sample cup assembly. By means of a pointer, the angular displacements of the sample cup could be determined for comparison with the displacement transmitted by the material to the inner cone and observed through the telescopic eyepiece F. This arrangement was used for yield value observations.

A further improvement was obtained by fitting a stop in the lower chuck G so that the brass ferrule on the lower end of the torsion wire is always clamped at the same distance in the chuck. Thus, after the inner cone has been set at zero clearance with the zero reading on the head micrometer screw, and the upper chuck is clamped, the lower chuck can be released allowing the inner cone to be removed for cleaning, and replaced without necessitating a resetting of the zero on the head micrometer screw.

The preliminary experiments indicated that it was quite

difficult to obtain consistent results by shaking the material in a partially filled stoppered bottle. The labor of shaking by hand was excessive, especially for the more concentrated suspensions. For measurements to be made upon the suspensions after a definite standing period, it was almost mandatory that a reference condition of zero structure be obtainable. To meet this requirement, a device called the "structure breaker" was designed and constructed and is shown by Figures 6 and 7. Essentially it consists of a brass cylinder in which moves a perforated piston only slightly smaller than the internal diameter of the cylinder. The funnel shaped upper part contains the same volume as the cylindrical lower section. A wide base plate closes the bottom of the cylinder and affords stable support for the instrument. The rod with the piston fixed at its lower end carries a crossbar handle at its upper end and a cover disk. The cover disk is firmly fixed on the piston rod at such a point that it just covers and closes the funnel when the piston is resting flat on the bottom of the cylinder.

When used, the structure breaker is filled about 2/3 full with the material. The piston is plunged down through the material to the bottom and raised at about the same speed. The material is thus vigorously sheared by passing between the piston and the wall and through the small holes in the piston. The speed of the downward stroke is gauged by having the material squirting through the holes just rising to the cover plate. In this manner it is assured by the design of the instrument that
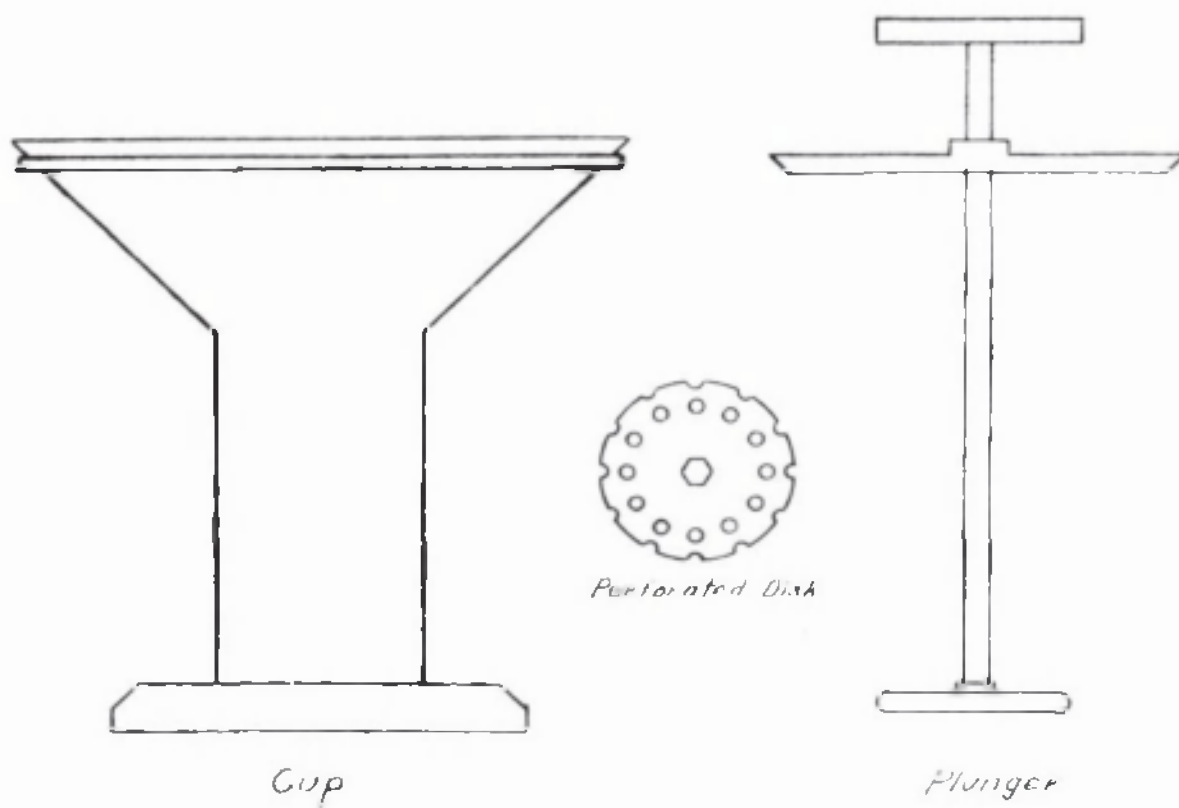
Figure 6.  Sketch Drawing of the Structure Breaker.
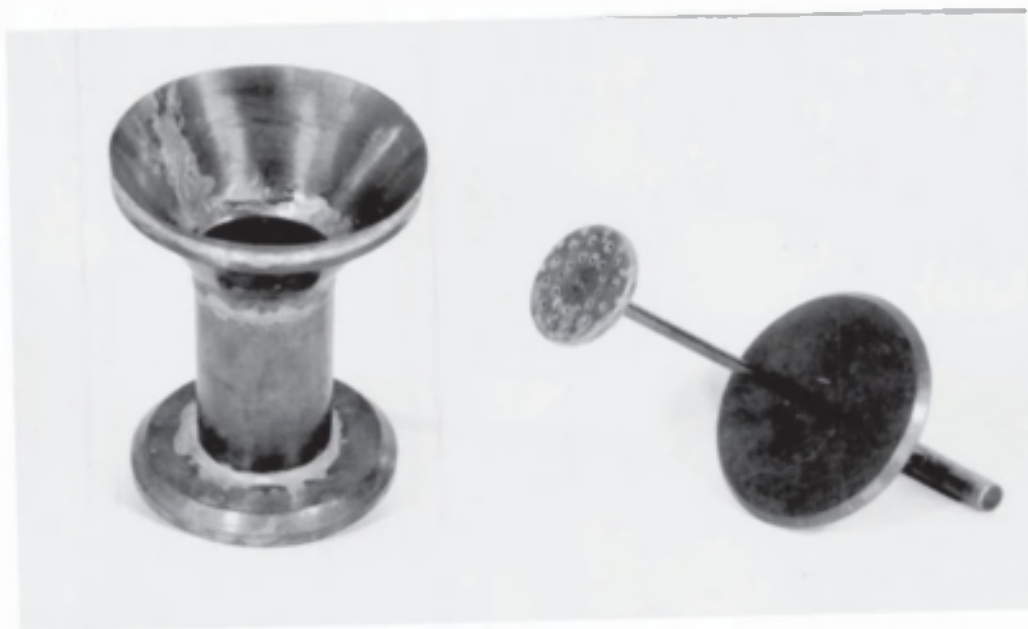


Figure 7.  Photograph of the Structure Breaker.

the material is all sheared to the same extent, and the operation occurs on all the material at the same time. Reproducible conditions of fluidity were very easily obtained with this instrument, for the bentonite suspensions.

# CHAPTER IV.

## THEORY OF THE GOODEVE INSTRUMENT.

Strictly speaking, a uniform rate of shear is obtained only by the motion of two parallel plane surfaces moving relative to one another at a constant distance. Experimentally, this ideal condition is approached closely by instruments employing rotating concentric cylinders. In this manner strictly uniform shear is not present, but a continuous or sustained rate of shear can be obtained, and if the separation between the surfaces is small compared to the radius, the deviation from the strictly uniform shear is not great.

The Goodeve instrument, being a constant-speed motor-driven instrument, offers the rate-of-shear parameter as the independent variable, with the shearing stress as the dependent variable. The rate of shear is varied by raising or lowering the inner cone by means of the micrometer screw arrangement on the head assembly. This changes the separation between the shearing surfaces and can be accomplished while the outer cup is rotating. This method of varying the rate of shear is a unique feature not found in any other viscometer.

The use of cones constitutes a further deviation from the uniformity of shear, but if the length of the frustra are short in comparison with the radius and the angle of the cone is small, an average value for the radius offers a close approximation to the conditions given by concentric cylinders. A distinct advantage is gained by the ease with which thin

layers of liquid are obtained thus tending to minimize the lack of uniformity due to curved surfaces.

Basing the theory of the instrument on the relationships developed for concentric cylinders, the following expression can be derived for the relation between the force developed by the sustained rate of shear when a Newtonian liquid is present in the annular space of the Goodeve instrument. This development follows closely the one presented by Barr.[2b]

Consider that the frustrum of the inner cone has an effective radius $R_E$, which is 1% larger than mean radius between its longer and smaller radii. This cone frustrum hangs coaxially within a similar cone, the space between being filled with a viscous liquid. When the outer cone revolves slowly the fluid will be assumed to rotate in concentric layers, with no slip at either wall. The layer in contact with the inner cone will be stationary while that at the outer wall will have an angular velocity. Let the angular velocity at any intermediate radius r, be $\omega$; the gradient of angular velocity will be $\frac{d\omega}{dr}$ . The gradient of linear velocity across a small element of the fluid at radius r will be $r\frac{d\omega}{dr}$ The force that is exerted upon the hypothetical cylinder of radius r and length $l$ by the moving fluid between it and the outer wall will be

$$F_r = \eta r \frac{d\omega}{dr} A.$$

(11)

where: $F_v$ = Total viscous force acting on inner cone frustrum, dynes.

$A$ = Side wall area of inner cone, $cm.^2$ equal to $2\pi r l$

$\eta$ = Coefficient of viscosity of the fluid.

or

$$F_v = \eta r \frac{d\omega}{dr} 2\pi r l = 2\eta \pi l r^2 \frac{d\omega}{dr} \tag{12}$$

This viscous force acts at a distance r from the axis of rotation exerting a couple on the torsion wire. Therefore the couple $G_v$, acting at the radius r is given by

$$G_v = 2\eta \pi l r^3 \frac{d\omega}{dr} \tag{13}$$

The couple due to the viscous drag is opposed by the couple due to the potential energy stored in the torsion wire. At equilibrium these two forces are equal and opposite and therefore can be equated, using the minus sign:

$$G_T = -2\eta \pi l r^3 \frac{d\omega}{dr} \tag{14}$$

Rearranging and integrating between the limits $\int_0^\omega$ and $\int_{R_1}^{R_2}$ gives

$$G_T = \frac{4\pi \eta l \omega}{\frac{1}{R_1^2} - \frac{1}{R_2^2}} \tag{15}$$

The energy $G_T$ stored in the wire is measured by observing the degrees of twist from the zero position. Then if the torsion constant T, is known for the wire the value

of $G_T$ is given by

$$G_T = \delta T \tag{16}$$

where:  $G_T$ = total energy stored in torsion wire that tends to oppose the viscous drag, ergs.

$\delta$ = angle through which the wire is twisted, degrees.

$T$ = the torsional constant of the wire, ergs/ degrees.

Substituting Equation 16 in Equation 15 and rearranging, the equation for the Goodeve instrument becomes:

$$\frac{\delta T}{2\pi \ell R_1 R_2} = \eta \frac{2\omega R_1 R_2}{R_2^2 - R_1^2} \tag{17}$$

Expressing the angular velocity in revolutions per minute instead of radians per second gives this form:

$$\frac{\delta T}{2\pi \ell R_1 R_2} = \eta \frac{2\pi}{60} \Omega \left[ \frac{2 R_1 R_2}{R_2^2 - R_1^2} \right] \tag{18}$$

where:  $\Omega$ = angular velocity, revolutions per minute.

Equation 18 is in the form that shows the linear relation between the shearing stress and the applied rate of shear. The mean shearing stress is given by the term

$$T_m = \frac{\delta T}{2\pi \ell R_1 R_2} \tag{19}$$

while the mean rate of shear is given by

$$\sigma_m = \frac{2\pi}{60} \Omega \left[ \frac{2\pi R_1 R_2}{R_2^2 - R_1^2} \right] \tag{20}$$

A plot of corresponding values of the mean shearing stress obtained for given values of the mean rate of shear using a Newtonian liquid would give a straight line as shown in Figure 3.

Since the rate of shear of the Goodeve instrument is varied by changing the separation between the cones, the use of Equations 19 and 20 can be made less cumbersome by the following simplification.

Let the term $R_1 R_2$ in Equation 19 be replaced by $R_E$ , the effective radius as defined above. This reduces the mean shearing stress to the stress at the wall of the inner cone, which is the shearing stress actually being transmitted to the torsion wire. Thusly, Equation 19 becomes

$$\tau = \frac{\delta T}{2 \pi \ell R_E^2} \tag{21}$$

If the larger radius $R_2$ (to the outer wall) is expressed in terms of shorter radius plus the separation in the following manner

$$R_2 = R_1 + d \tag{22}$$

where: $d$ = the separation between the walls, cm. Equation 20 takes the following form

$$\sigma_m = \frac{2\pi}{60} \Omega \left[ \frac{2R_1}{2R_1 + d} \cdot \frac{R_1 + d}{d} \right] \tag{23}$$

where d becomes small in comparison with $R_1$ , the term $\frac{2R_1}{2R_1 + d}$ approaches unity and can be neglected. The following equation is then obtained

$$\sigma_m = \frac{2\pi}{60} \Omega \left[ \frac{R_1 + d}{d} \right] \tag{24}$$

The term $R_1 + d$ appearing in Equation 24 represents the large radius $R_2$. A better approximation will be obtained if the smaller effective radius $R_E$, is extended to the midpoint of the space in which the shear is occurring by adding $\frac{1}{2}$ d instead of d. In this manner Equation 25 is obtained:

$$\sigma_m = \frac{2\pi}{60} \Omega \left[ \frac{R_E + \frac{1}{2}d}{d} \right] = Q\Omega \tag{25}$$

where: $$Q = \frac{2\pi}{60} \left[ \frac{R_E + \frac{1}{2}d}{d} \right] \tag{25a}$$

Equation 25 is the expression recommended by Goodeve[13] for the calculation of the rate of shear existing between the walls of the instrument when turning at constant speed. Figure 8 shows the percent increase over the rate of shear calculated by Equation 20, that is obtained when the Goodeve equation 25 is used. It is seen that the increase is less than 1% when the separation is not greater than 0.4 cm., a value seldom exceeded in this work.

The useful working equation for the Goodeve instrument accordingly is given by the following expression.

$$\frac{\delta T}{2\pi \ell R_E^2} = \eta \left[ \frac{2\pi}{60} \Omega \left( \frac{R_E + \frac{1}{2}d}{d} \right) \right] \tag{26}$$

The separation, d is obtained for the reading on the micrometer head (when correctly set at zero) by this equation:

$$d = \sin \alpha \, h = 0.20 \, h. \tag{27}$$
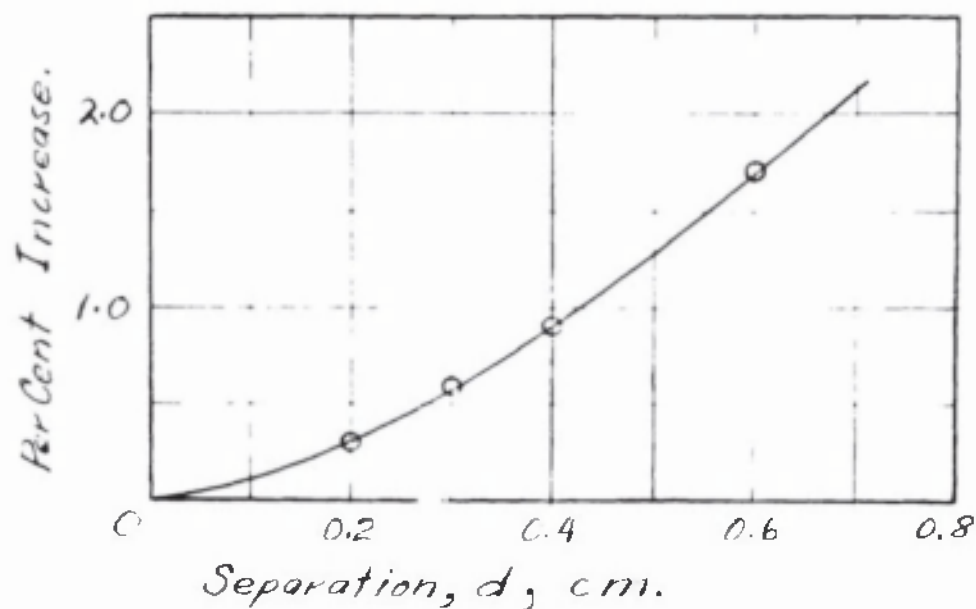
Figure 8.   Graph Showing Per Cent Increase in Rate
of Shear Obtained by Using Equ. 26 in Place of Eqn.21.
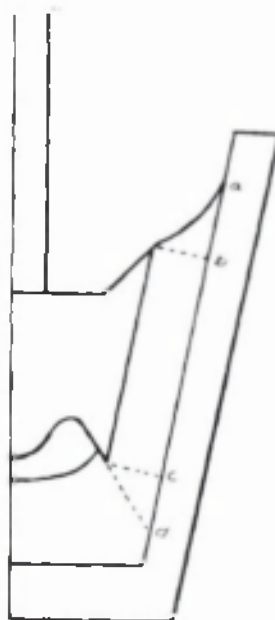


Figure 9.   Diagram Showing Location of Residual
End Effects.

where:  $\alpha$ = the angle of the cone frustrums, a constant $(11^{\circ}\ 30')$.

   $h$ = the verticle distance measured by the micrometer head, cm.

Equation 26 indicated that the shearing stress as determined by the left hand member is proportional to the rate of shear as given by the term within the brackets; the proportionality constant is the coefficient of viscosity of the liquid being acted upon by the shearing system. It now remains to demonstrate by means of experimental observations that Equation 26 is valid when the separation term d, is the independent variable, the unique feature of the Goodeve instrument. This will be shown in Chapter V.

In connection with the quantities, shearing stress and rate of shear, the units of dynes per square centimeter and reciprocal seconds will be used throughout this work. Whereas tangential force per unit area offers no great difficulty to visualize in the case of the shearing stress, reciprocal seconds in the case of the rate of shear is somewhat abstract in its connotation of the mechanical process. However, it is used in place of its more cumbersome equivalent: radians per radian second.

## END EFFECTS

In the foregoing theoretical development, the presence of drag at the ends of the inner cone was assumed to be absent. Practically, almost insurmountable difficulties stand in the way of eliminating the end effect; at least without making the instrument cumbersome. On this particular instrument, the cone feature is admirably adapted to the minimizing of the end effects. This has been accomplished by the trapping of a bubble of air in the recess under the lower end of the cone, and by removing the material from the recess at the top. However, small residual end effects remain that cannot be completely removed. At the upper surface, the liquid curves from the outer cup to the lip of the upper edge of the inner cone and doubtless some shearing force is transmitted to the torsion system by the area between a and b as shown in Figure 9. A similar situation exists in the area between c and d at the lower lip. Further, the liquid rises slightly behind the lower lip to give a slight increase to the area on the inner cone acted on by the shearing forces. It is possible that the bottom surface of the cup may also have a slight influence on the deflection of the torsion system, especially when the cone is at its lowest position in the cup. However, the position at which the end effects would be expected to be greatest, namely when the separation is small, occurs when the rate of shear and deflections are greatest, thus tending to make their relative effect less.

# CHAPTER V

## CALIBRATION OF THE GOODEVE INSTRUMENT

### Adjustment of the Instrument.

The most important adjustment of the instrument comprises centering the inner core in the sample cup. This adjustment is founded on the basis that the projection of the axis about which the lower cup assembly turns corresponds with the axis of the cones and the torsion wire and passes through the center of the upper chuck. It must be assumed that the vertical motion of the head assembly is parallel to this projected axis because no means of adjustment for this factor is provided. Thus, when the instrument is leveled the inner cone hanging from the torsion wire, will show a uniform annular spacing in the sample cup.

Since the spirit level provided on the base is not of sufficient sensitivity, the instrument was first leveled by means of the spirit level in a machinists steel square held against the vertical pillar P. Then a torsion wire and the inner cone were fitted into position and lowered into the cup until the annular space was approximately 1 mm. wide. The screws holding the upper chuck K in position on tube J were loosened and the chuck shifted laterally until uniform annular spacing between the inner cone and the cup indicated that the conical axes coincided. The screws were then firmly tightened. This adjustment was made only once. Subsequent leveling adjustments were made by operating the screws in the base until the inner cone hung concentrically in the

sample cup, the spirit level on the base being used only for rough leveling.

The upper ends of the torsion wire were fitted with a short cross-bar by means of solder, so that, the torsion wire could be firmly gripped with the fingers and raised through the upper chuck. By this means, the length of the wire was adjusted so that when the head scale reading was zero, the surface of the inner cone was just in contact with the surface of the cup. This position was indicated by the inner cone just failing to move when the outer cup assembly was rotated. This method of setting the head scale zero position was found quite satisfactory.

Experimental Determination of the Instrument Constant.

Almost any number of observations can be made upon a material being sheared in the Goodeve instrument yielding three simultaneous quantities, the head setting h, the deflection $\delta$, and the speed in revolutions per minute $\Omega$. Of these three variables, the head setting is independent for any series of measurements during which the speed is held constant, the deflection being obtained as the resultant.

By calibrating the torsion wires directly, using standard oils whose coefficient of viscosity are known accurately, constants can be determined that will allow a set of readings to be converted to viscosity (or apparent viscosity if the material is non-Newtonian). This can be done by observing the deflections obtained by a series of rates of shear applied to the standard oils and substituting the values in the following expression

$$\eta = k \frac{\delta}{\sigma} \tag{28}$$

where: $k$ = the instrument constant for conversion of deflection readings into the coefficient of viscosity.

and solving for the value of k. The standard liquids available consisted of two groups of parafine hydrocarbons obtained from the National Bureau of Standards and the Texas Oil Company, respectively. The oils from the Bureau of Standards were accompanied by certificates giving their coefficients of viscosity accurate to 0.1%. Two additional

oils were calibrated by means of an Ostwald pipette by the writer. The characteristics of these oils are listed in Table 1.

### Table 1.

#### The Characteristics of the Standard Oils and for Calibration.

| Oil | Viscosity centipoise | Density @ 25° C | Source |
|---|---|---|---|
| J | 17.19 | 0.837 | Bureau of Standards |
| K | 32.23 | 0.852 | Bureau of Standards |
| L | 75.19 | 0.873 | Bureau of Standards |
| M | 239.7 | 0.884 | Bureau of Standards |
| N | 976.5 | 0.871 | Bureau of Standards |
| O | 2708 | 0.858 | Bureau of Standards |
| A | 2.076 | 0.7975 | Texas Oil Company |
| B | 10.27 | 0.8502 | Texas Oil Company |
| C | 20.19 | 0.8722 | Texas Oil Company |
| D | 41.95 | 0.8716 | Texas Oil Company |
| E | 73.07 | 0.8677 | Texas Oil Company |
| F | 99.73 | 0.8701 | Texas Oil Company |
| E5 | 390 | 0.8773 | Calibrated by author |
| E7 | 664 | 0.8805 | Calibrated by author |

Values of the rate of shear as given by Equation 25 were calculated for a series of head settings which were adequate in giving a good coverage of the range of shearing rates available with the various speeds at which the instrument could be operated conveniently. These values are shown in Table 2 for the head settings given in column 1 and speeds of rotation of 5.0, 20, 40, and 80 revolutions per minute. Settings less than 2.0 mm. give such a small clearance between the cones that any inaccuracy of the zero adjustment is a large percent of the resulting rate of shear, therefore,

readings less than 2.0 mm. of separation were not considered advisable.  At speeds greater than 80 revolutions per minute, the liquid tends to be thrown from the cup, hence this is considered as the maximum speed at which the instrument can be operated.

The variation of the factor Q which combines the constant members of Equation 25, with the head setting is shown by Figure 10, which is useful for calculating values of for intermediate settings which are not given in Table 2.  This is done by multiplying the value of Q taken from Figure 10 by the speed at which the cup rotates.

## Table 2

### Calculated Values of Rate of Shear Using Equation 25.

| Head Setting mm. | Separa-tion d cm. | Factor Q | Rate of Shear, $\sigma_r$. | | | |
|---|---|---|---|---|---|---|
| | | | 5.0 r.pm. | 20.0 rpm. | 40 r.pm. | 80 rpm. |
| 40 | 0.80 | 0.3170 | 1.58 | 6.34 | 12.7 | 25.4 |
| 38 | .76 | .3308 | 1.65 | 6.62 | 13.2 | 26.5 |
| 36 | .72 | .3463 | 1.73 | 6.93 | 13.8 | 27.7 |
| 34 | .68 | .3636 | 1.82 | 7.28 | 14.5 | 29.1 |
| 32 | .64 | .3830 | 1.91 | 7.56 | 15.1 | 30.2 |
| 30 | .60 | .4051 | 2.02 | 8.10 | 16.2 | 32.4 |
| 28 | .56 | .4303 | 2.15 | 8.61 | 17.7 | 34.4 |
| 26 | .52 | .4594 | 2.29 | 9.19 | 18.4 | 36.76 |
| 24 | .48 | .4936 | 2.47 | 9.88 | 19.7 | 39.5 |
| 22 | .44 | .5338 | 2.67 | 10.67 | 21.3 | 42.7 |
| 20 | 0.40 | .5814 | 2.91 | 11.62 | 23.2 | 46.5 |
| 19 | .38 | .6110 | 3.05 | 12.22 | 24.4 | 48.9 |
| 18 | .36 | .6408 | 3.20 | 12.83 | 25.7 | 51.3 |
| 17 | .34 | .6753 | 3.37 | 13.51 | 27.0 | 54.0 |
| 16 | .32 | .7140 | 3.57 | 14.28 | 28.5 | 57.1 |
| 15 | .30 | .7578 | 3.79 | 15.15 | 30.3 | 60.6 |
| 14 | .28 | .8082 | 4.04 | 16.27 | 32.5 | 65.1 |
| 13 | .26 | .8664 | 4.33 | 17.30 | 34.6 | 69.3 |
| 12 | .24 | .9341 | 4.67 | 18.7 | 37.4 | 74.7 |
| 11 | .22 | 1.015 | 5.07 | 20.6 | 41.2 | 82.4 |
| 10 | 0.20 | 1.111 | 5.55 | 22.2 | 44.4 | 88.8 |
| 9 | .18 | 1.228 | 6.14 | 24.6 | 49.1 | 98.3 |
| 8 | .16 | 1.375 | 6.87 | 27.5 | 55.0 | 110.0 |
| 7 | .14 | 1.564 | 7.82 | 31.6 | 63.2 | 126.4 |
| 6 | .12 | 1.816 | 9.08 | 36.6 | 73.3 | 146.5 |
| 5.5 | .11 | 1.975 | 9.87 | 39.5 | 79.0 | 158.0 |
| 5 | 0.10 | 2.168 | 10.83 | 43.3 | 86.7 | 173.4 |
| 4.5 | .09 | 2.403 | 12.01 | 48.0 | 96.1 | 192.2 |
| 4 | .08 | 2.698 | 13.48 | 54.6 | 108.0 | 216.0 |
| 3.5 | .07 | 3.074 | 15.37 | 61.5 | 123.0 | 245.9 |
| 3 | .06 | 3.580 | 17.89 | 71.6 | 143.2 | 286.4 |
| 2.5 | .05 | 4.284 | 21.42 | 85.7 | 171.4 | 242.7 |
| 2 | .04 | 5.344 | 26.70 | 106.8 | 213.6 | 427.2 |
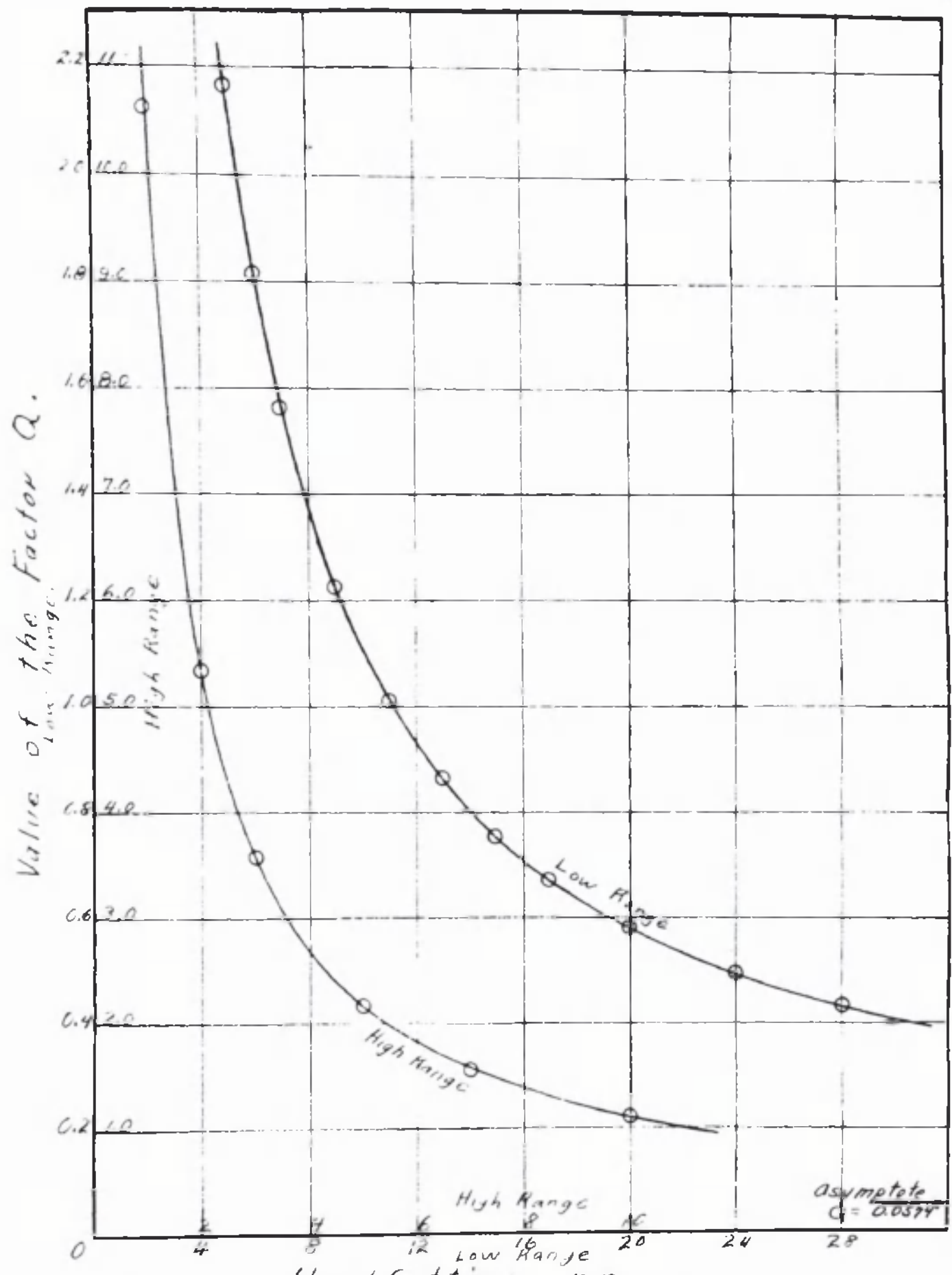
Figure 10. Variation of the Factor Q with the Head Setting.

Preliminary observation indicated the range of viscosities and speed of rotation that could be observed with a given torsion wire, arbitrarily keeping the deflections below 90° to avoid the possibility of permanent strain in the wire. The technique adopted for making the measurements for the calibration followed closely that used subsequently for the measurements made upon the bentonite sols. It was as follows:

The desired torsion wire was placed in position in the instrument, the micrometer screw being adjusted to zero in the manner described above. The torsion wire assembly was then raised by screwing the micrometer head down until the reading indicated the lowest rate of shear to be observed in accordance with a previously prepared schedule. The proper gear was placed in position and the motor assembly locked in mesh with the gear driving the sample cup. The torsion head assembly was lifted up and swung to the right, clearing the cup. The sample was poured in to about 3/5 of the volume of the cup, and when all bubbles had risen to the surface and broken, the inner cone was lowered carefully, without swinging, into the sample. The zero reading on the deflection drum was noted and recorded. The temperature of the sample as indicated by the thermometer in the stem of the inner cone was allowed to equalize with that of the water bath surrounding the sample cup. The tests were conducted at 25 ± 0.05° C and the room temperature was maintained so that it did not vary more than 1° from 25° C. When the

temperature adjustments were satisfactory the motor was started, and the excess sample in the upper recess of the inner cone was removed by means of the suction apparatus without touching or disturbing the inner cone. After the deflection of the inner cone became steady, the reading was taken. With the magnetic dampener in position the inner cone was quite steady at the lower speeds, but at the speed of 80 revolutions per minute and greater separations tendency to become uncentered was noticeable. A slight oscillation through about $0.8^\circ$ was present at all times which was found to be due to the hunting effect of the governor mechanism after the stroboscopic speed check was installed.

Successive readings were taken by lowering the torsion head to the next setting according to the previously prepared schedule. The excess oil was again removed from the recess in the upper base of the inner cone, and the deflection observed through the eyepiece. In this manner, the data shown in Table 3 was taken. The schedule shown in columns 1 and 2 of this table cover a range of rates of shears calculated by Equation 25 from approximately 20 to 400 reciprocal seconds. When it was necessary to change the speed of rotation, a generous overlap of observations at both speeds was allowed.

## Table 3

### Calibration Data

### Wire No.1

| Temperature | 25° C | | | | |
|---|---|---|---|---|---|
| Speed<br>r.p.m. | Head<br>Setting<br>mm. | Rate of<br>Shear*<br>sec⁻¹. | Deflection<br>δ<br>degrees | | Calibration No. |

| Speed r.p.m. | Head Setting mm. | Rate of Shear* sec⁻¹ | Deflection δ degrees | | Calibration No. |
|---|---|---|---|---|---|
| 80 | Oil B,<br>20<br>16<br>12<br>8<br>6<br>4<br>3<br>2 | 10.27.<br>46.5<br>57.1<br>74.7<br>110.0<br>146.6<br>216<br>286<br>427 | Zero reading<br>5.2<br>6.1<br>7.7<br>10.1<br>13.4<br>19.3<br>25.2<br>36.5 | 93.0 | Third |
| 20 | Oil K,<br>10<br>8<br>6<br>5<br>4<br>3<br>2 | 32.23<br>22.2<br>27.5<br>36.6<br>43.4<br>54.0<br>71.6<br>106.8 | Zero reading<br>6.9<br>8.1<br>10.6<br>12.5<br>15.3<br>19.7<br>28.2 | 345.7 | Third |
| 40 | 20<br>16<br>12<br>10<br>8<br>6<br>4<br>2 | 23.2<br>28.6<br>37.4<br>44.4<br>55.0<br>73.3<br>108.0<br>213.6 | 7.7<br>9.3<br>11.5<br>13.5<br>15.5<br>21.3<br>30.1<br>56.8 | | Third |
| 80 | 10<br>8<br>6<br>5<br>4<br>3<br>2 | 88.8<br>110.0<br>146.6<br>173.4<br>216.0<br>286.4<br>427.6 | 27.7<br>33.4<br>42.8<br>49.9<br>60.9<br>79.6<br>115.7 | | Third |

*Calculated by Equation 25.

Calibration Data

Wire No.1 Cont.

| Speed r.p.m. | Head Setting mm. | Rate of Shear* sec⁻¹ | Deflection δ degrees | Calibration No. |
|---|---|---|---|---|
| Oil D, | | 41.95.    Zero Reading | 244.1 | Third |
| 20 | 20 | 11.6 | 5.1 | |
| | 16 | 14.3 | 6.1 | |
| | 12 | 18.7 | 7.6 | |
| | 8 | 27.5 | 10.8 | |
| | 6 | 36.6 | 14.1 | |
| | 5 | 43.4 | 16.3 | |
| | 4 | 54.0 | 19.9 | |
| | 3 | 71.6 | 26.1 | |
| | 2 | 106.8 | 38.0 | |
| 40 | 10 | 44.4 | 18.7 | Third |
| | 8 | 55.0 | 22.1 | |
| | 6 | 73.3 | 28.4 | |
| | 5 | 86.7 | 33.1 | |
| | 4 | 108.0 | 39.9 | |
| | 3 | 143.2 | 51.5 | |
| | 2 | 213.6 | 73.4 | |
| 80 | 10 | 88.8 | 36.5 | Third |
| | 8 | 110.0 | 43.6 | |
| | 6 | 146.6 | 56.1 | |
| | 5 | 173.4 | 65.6 | |
| | 4 | 216.0 | 80.3 | |
| | 3 | 286.4 | 104.3 | |

Calibration Data

Wire No.1 Cont.

| Speed r.p.m. | Head Setting mm. | Rate of Shear* sec⁻¹ | Deflection δ degrees | Calibration No. |
|---|---|---|---|---|
| 011 L , | | 75.19. | Zero Reading | 342.7 |
| 20 | 15 | 15.15 | 11.1 | Second |
| | 10 | 22.2 | 15.1 | |
| | 8 | 27.5 | 18.2 | |
| | 6 | 36.6 | 23.6 | |
| | 5 | 43.4 | 27.3 | |
| | 4 | 54.0 | 33.3 | |
| | 3 | 71.6 | 43.6 | |
| | 2 | 106.8 | 62.8 | |
| | 1 | 212.6 | 118.5 | |
| 40 | 15 | 30.4 | 22.2 | Second |
| | 10 | 44.4 | 30.2 | |
| | 8 | 55.0 | 36.7 | |
| | 6 | 73.3 | 47.2 | |
| | 5 | 86.7 | 55.2 | |
| | 4 | 108.0 | 67.2 | |
| | 3 | 143.2 | 87.7 | |
| | 2 | 213.6 | 126.0 | |
| | | | Zero Reading | 342.2 |
| 80 | 15 | 60.6 | 45.3 | Second |
| | 10 | 88.8 | 62.4 | |
| | 8 | 110.0 | 75.0 | |
| | 6 | 146.6 | 96.6 | |
| | 5 | 173.4 | 112.3 | |
| | 4 | 216.0 | 137.6 | |
| | 3 | 286.4 | 181.0 | |

Calibration Data

Wire #2

| Speed r.p.m | Head Setting mm. | Rate of Shear* sec.$^{-1}$ | Deflection $\delta$ degrees | Calibration No. |
|---|---|---|---|---|
| | Oil B, | 10.27. Zero Reading | 51.0 | |
| 40 | 20 | 23.2 | 6.9 | Third |
| | 16 | 28.6 | 8.1 | |
| | 12 | 37.4 | 10.2 | |
| | 8 | 55.0 | 14.2 | |
| | 6 | 73.3 | 18.5 | |
| | 4 | 108.0 | 26.5 | |
| | 3 | 143.2 | 33.7 | |
| | 2 | 213.6 | 49.6 | |
| 80 | 10 | 88.8 | 24.0 | Third |
| | 8 | 110.0 | 28.4 | |
| | 6 | 146.6 | 36.3 | |
| | 4 | 216.0 | 52.6 | |
| | 3 | 286.0 | 67.6 | |
| | 2 | 427.2 | 98.8 | |
| | Oil K, | 32.23. Zero Reading | 178.5 | |
| 20 | 20 | 11.6 | 10.4 | Third |
| | 16 | 14.3 | 12.2 | |
| | 12 | 18.7 | 15.2 | |
| | 8 | 27.5 | 21.5 | |
| | 6 | 36.6 | 27.7 | |
| | 5 | 43.6 | 32.7 | |
| | 4 | 54.0 | 40.1 | |
| | 3 | 71.6 | 52.6 | |
| | 2 | 106.8 | 76.8 | |
| 40 | 10 | 44.4 | 37.2 | Third |
| | 9 | 49.1 | 40.2 | |
| | 8 | 55.0 | 44.4 | |
| | 7 | 63.2 | 50.5 | |
| | 6 | 73.2 | 57.6 | |

## Calibration Data

### Wire #2 Cont.

| Speed r.p.m | Head Setting mm. | Rate of Shear* sec$^{-1}$ | Deflection $\delta$ degrees | Calibration No. |
|---|---|---|---|---|
| | Oil K, | 32.23. Zero Reading | 0.0 | |
| 20 | 15 | 15.1 | 12.3 | Second |
| | 10 | 22.2 | 17.2 | |
| | 8 | 27.5 | 20.8 | |
| | 6 | 36.6 | 26.5 | |
| | 5 | 43.4 | 31.1 | |
| | 4 | 54.0 | 38.0 | |
| | 3 | 71.6 | 49.3 | |
| | 2 | 106.8 | 71.9 | |
| | 1 | 212.6 | 134.5 | |
| | Oil D, | 41.95. Zero Reading | 164.1 | |
| 20 | 20 | 11.6 | 14.0 | Third |
| | 14 | 16.3 | 18.3 | |
| | 10 | 22.2 | 24.1 | |
| | 8 | 27.5 | 29.1 | |
| | 6 | 36.6 | 37.4 | |
| | 4 | 54.0 | 54.4 | |
| | 3 | 71.6 | 71.1 | |
| | 2 | 106.8 | 104.5 | |
| | Oil L, | 75.1 Zero Reading | 344.5 | |
| 5.0 | 15 | 3.8 | 7.4 | Second |
| | 10 | 5.6 | 10.3 | |
| | 8 | 6.9 | 12.3 | |
| | 6 | 9.1 | 15.9 | |
| | 5 | 10.8 | 18.6 | |
| | 4 | 13.5 | 22.8 | |
| | 3 | 17.9 | 29.5 | |
| | 2 | 28.7 | 42.7 | |
| | 1 | 53.15 | 85.0 | |
| 20 | 15 | 15.15 | 30.0 | Second |
| | 10 | 22.2 | 41.5 | |
| | 8 | 27.5 | 50.0 | |
| | 6 | 36.6 | 64.3 | |
| | 5 | 43.4 | 75.1 | |
| | 4 | 54.0 | 91.5 | |
| | 3 | 71.6 | 119.0 | |
| | 2 | 106.8 | 172.5** | |
| | | Zero Reading | 344.3 | |
| 40 | 15 | 30.3 | 59.3 | Second |
| | 10 | 44.4 | 81.3 | |
| | 8 | 55.0 | 99.3 | |
| | 6 | 73.3 | 132.3 | |
| | 5 | 86.7 | 149.3 | |
| | 4 | 108.0 | 183.3 | |

**After this large deflection the inner cone returned to a zero reading of 344.3, indicating for the short time no appreciable permanent set occurred in the wire.

The calibration data given in Table 3 for torsion wires 1, 2, and 3, are shown graphically by Figures 11a, 11b, 11c respectively. The calculated values of rates of shear from column 3 are given as abscissa with the corresponding deflections from column 5 as ordinates. It is evident that the points for a given oil at a given speed fall on a straight line. At speeds less than 80 revolutions per minute, the lines are parallel but shifted to the right. It appears that the shift is proportional to the speed of rotation.

It is seen that extrapolation of the straight lines of Figures 11a, 11b, 11c to zero deflection gives negative intercepts on the rate of shear axis. Also, for a given speed, the lines for the oils of different viscosity all meet at the same point on the negative rate of shear axis. The value of these intercepts are found to be proportional to the speed of rotation.

According to Figures 11a, 11b, 11c those finite deflections remain for a given oil when the rate of shear has dropped to zero. It is known that the oils used do not have any observable yield value therefore this condition is not physically possible.

The experimental procedure used to reduce the rate of shear is to increase the distance between the shearing surfaces, the speed remaining constant. By this token, zero rate of shear is attained by making the separation infinitely great. The application of this reasoning to the simplified Equation 25 shows that the rate of shear will decrease
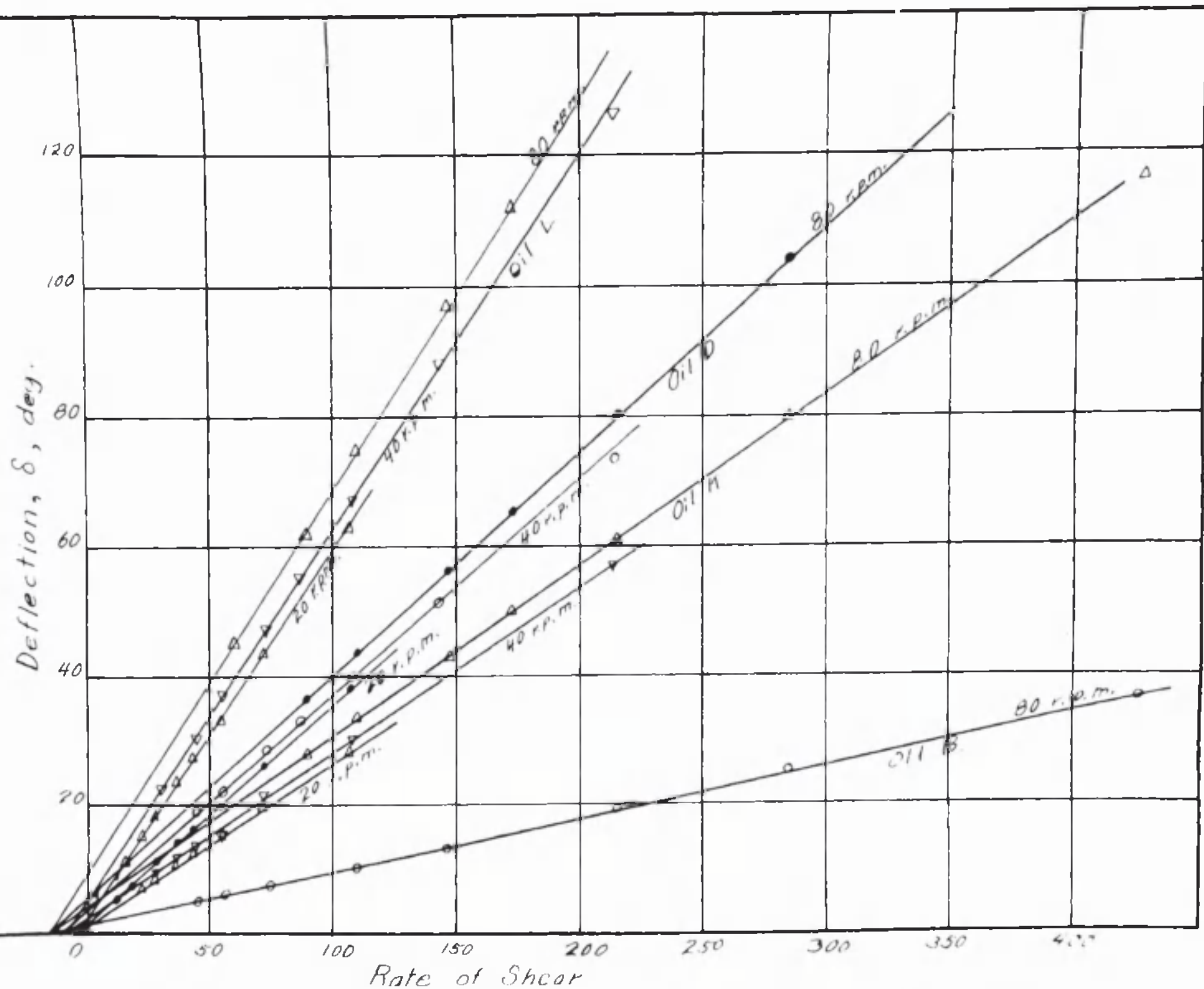
Figure 11a. Graph of the Calibration Data of Wire No. 1
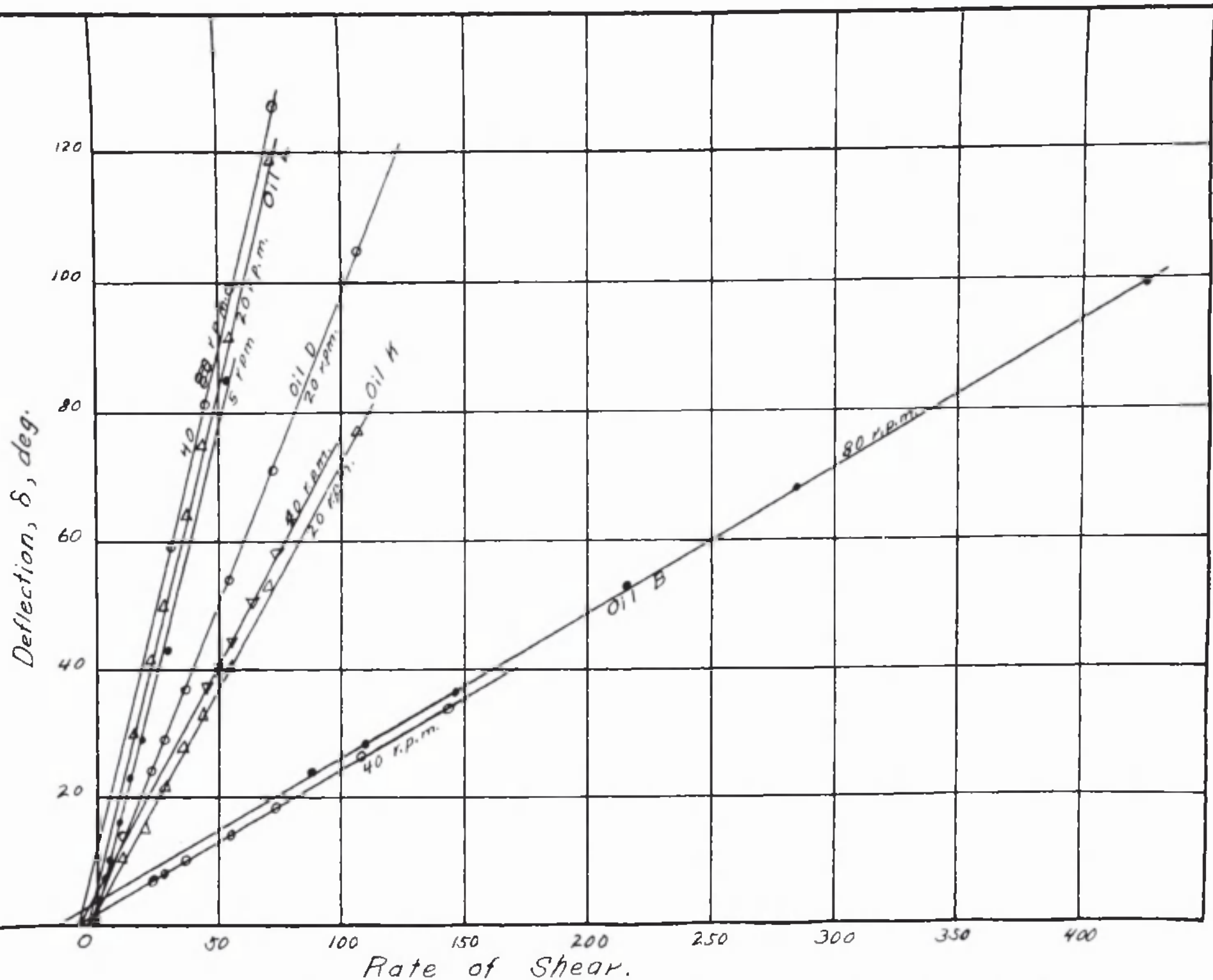
Figure 11b. Graph of the Calibration Data of Wire No. 2.
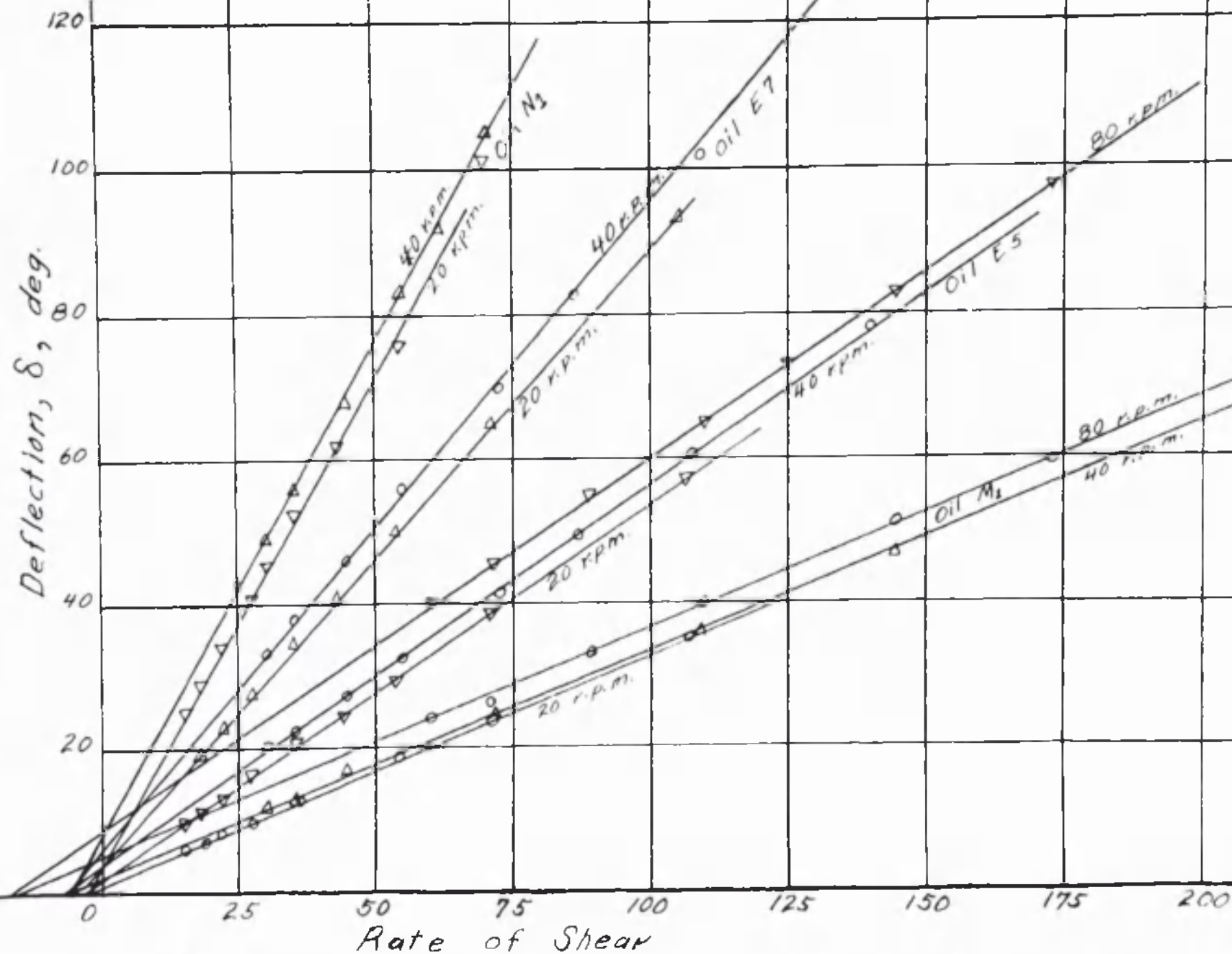
Figure IIc. Graph of the Calibration Data of Wire No. 3.

asymptotically to a constant value as the separation becomes large. Examination of the unsimplified form of the rate of shear Equation 20, indicates that the rate of shear will become vanishingly small when the separation becomes great. Figure 12 shows a graphic comparison between these two equations for calculating the rate of shear. The factor Q represents the rate of shear obtained per revolution of the cup per minute and is seen to be very nearly the same for both equations for separations up to about 1 cm. The preliminary experiments have indicated that small changes in deflection would be produced with relatively large changes in head settings above 20 mm.; therefore the upper limit was arbitrarily taken as 20 mm. which corresponds to a separation of 0.4 cm. Figure 12 indicates that the difference between the rates of shear obtained by Equations 20 and 25 is negligible for the range of head settings that are less than the equivalent separation of 0.40 cm., i. e. a head setting of 2.0 cm. Since this range was never exceeded, it cannot be concluded that the negative rate of shear intercepts of Figures 11a, 11b, 11c, are due to the use of Equation 25 in the place of Equation 20. They must be ascribed to some other cause.

At any constant rate of shear Figures 11a, 11b, 11c, show three deflections for a given oil of constant viscosity when three different velocities of revolution are used. Theory demands that they should be the same, for the deflection should

Figure 12. Graph Showing the Difference Between the Rate of Shear at various Separations Calculated by the Simplified Eqn 25 and the theoretical Eqn 20

Separation, $d$, cm.

$Q$, (rate of shear per revolution.)

Upper limit of experimental range

Calculated by Eqn 20

Calculated by Eqn 25

0.33 0.40 0.50 0.667 1.0 2.0

0 0.1 0.2 0.3 0.4 0.5 0.6 0.7
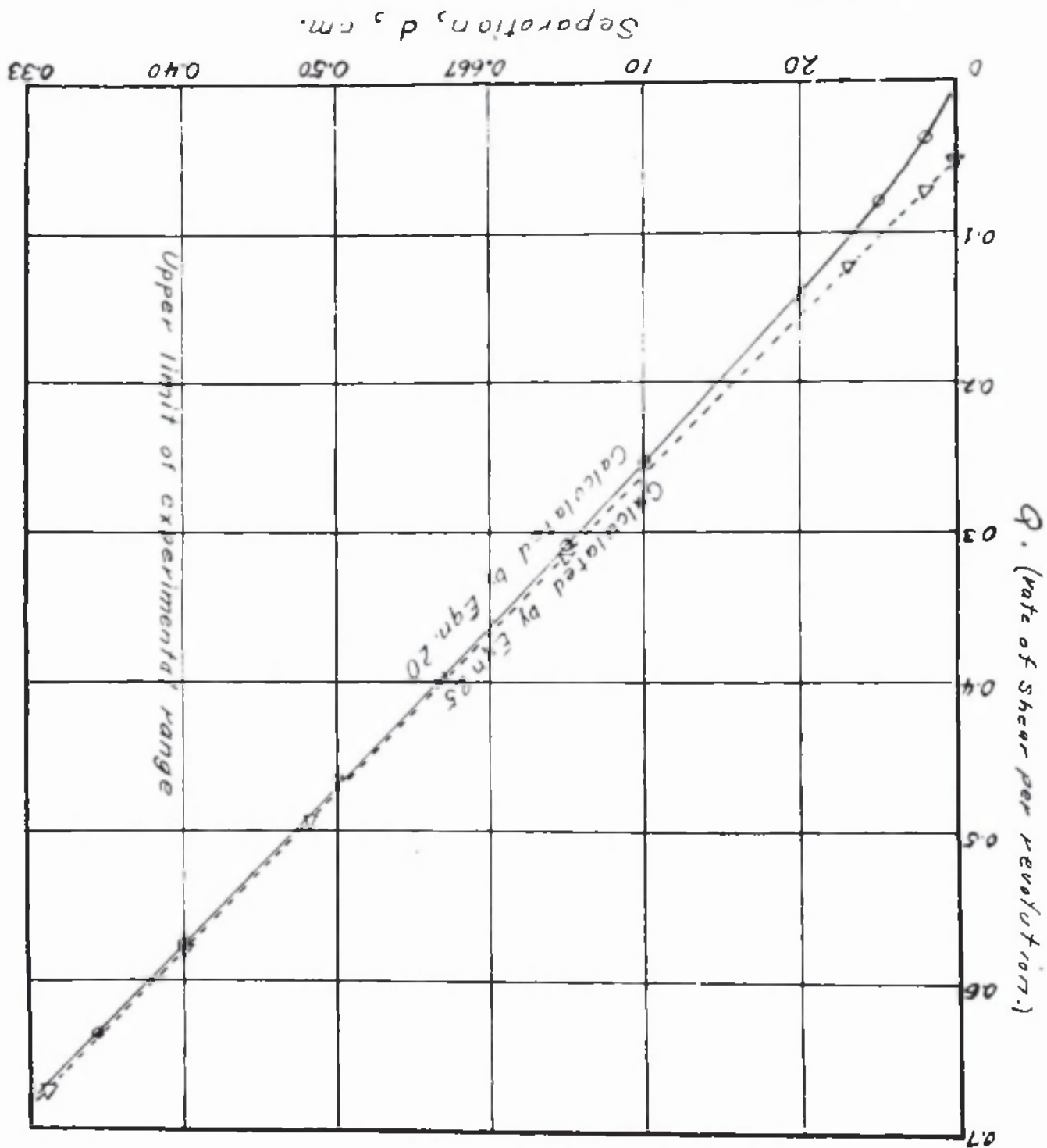
be independent of the speed when calculated to rate of shear, since compensatio is made by changing the separation between the shearing surfaces as the angular velocity is changed.

It would appear from the figures that some remaining or residual rate of shear exists independent of the separation and in some way is related to the speed of rotation. As noted above, the intercepts appear proportional to the speed of rotation.

It is of significance to note that the deflections are in linear proportion to the calculated rate of shear. This indicates t at the instrument is operating accordi g to the simple shearing action assumed in the Newtonian viscosity concept. A necessary corollary of Newtonian response (i. e. linear) to the sustained shearing process on liquids is that a zero deflection is obtained when the rate of shear decreases to zero. Therefore, it is concluded that e values of rate of shear indicated by the negative intercepts are actual existing rates of shear acti o the fluids and must be added to t e rate of shear calculated by Equati n 25 in order to obtain the total rate of shear generated by the rotating cup-cone system. Thus the expression giving the total rate of shear $\sigma$, acting upon the fluid contained in the annular space would be given by this equation

$$\sigma = \frac{2\pi}{60} \ \Omega \left[ \frac{R_E + \frac{1}{2}d}{d} \right] + \sigma_\hbar \tag{29}$$

where: $\sigma_\hbar$ = A constant representing the rate of shear indicated by the intercept.

If the separation between the walls of the cup and cone system is imagined to be made very large, say 1000 cm, it becomes easier to picture the origin of the constant value that is acting on the oil. With this large separation, the value of the rate of shear acting between the walls would be vanishingly small, yet it does not seem reasonable for the inner cone suspended in the center of a large cup filled with a viscous liquid and turning at a constant speed, to show a vanishingly small deflection. Conversely, it does not seem probable that the inner cone could exert any considerable retardation on the liquid nearer the outer wall. It also seems reasonable that, as the cup turns, the liquid would tend to turn with it, carried by its own momentum, until as the center is approached, the retarding action of the inner cone will set up sufficient shearing action to cause the liquid to form its own wall and cause the equivalent deflection on the torsion suspension. If now the outer wall is moved in to some point inside of the distance at which the liquid wall effect is set up, a rate of shear of its equivalence is set up and superimposed upon the other and is calculable according to Equation 25. Thus it is assumed that the "inertial wall effect" is always present, is independent of the separation and is directly proportional to the speed of revolution.

The following experiment was conducted to test this interpretation. A special cup was constructed from tin-plate which would fit friction tight into the cone A shown in Figure 5. This cup was much larger than the one normally

used and is shown by Figure 4c. By means of a hard wood
plug inserted in the micrometer column N, the vertical range
of the head settings was extended from 50 mm. to 100 mm. This
gave a separation with the special cup ranging from 0.8 to
2.7 cm.,corresponding to rates of shear from 2.61 to 6.36 sec.$^{-1}$
at a speed of 20 r.p.m.

Suitable oils were placed in the cup, with the head set-
ting at the greatest separation with the plug in position.
The motor was started and after the deflection was steady
it was read successively as the inner cone was lowered in 5 mm.
steps. Each time the oil was removed from the recess on the
top of the inner cone by means of the suction flask to a level
below the rim to minimize the end effects. It was necessary
to remove the plug when the head setting of 52.5 mm. was reached
and continue with the normal arrangement. This gave an overlap
of 6 - 7 readings, the pairs of which did not differ by more
than a few tenths of a degree. The data taken by this experi-
ment is recorded in Table 4, with the speed of rotation, the
head setting, the separation and the corresponding calculated
rate of shear. Deflections were obtained for oils F and E5
with torsion wire number 2 and for oil F with torsion wire
number MO.

Table **4**

Data of the Calibrating Oils in the Oversize Cup.

| Speed r.p.m. | Head Setting mm. | Separa-tion cm. | Rate of Shear sec.$^{-1}$ | Deflection, $\delta$. | | |
|---|---|---|---|---|---|---|
| | | | | Oil F Wire #2 | Oil B5 Wire #2 | Oil F Wire MO. |
| 20 | 97.5 | 2.7 | 2.61 | 12.6 | 46.7 | 22.9 |
| | 92.5 | 2.6 | 2.66 | 12.6 | 46.7 | 22.9 |
| | 87.5 | 2.5 | 2.74 | 12.6 | 46.5 | 22.9 |
| | 82.5 | 2.4 | 2.81 | 12.5 | 46.7 | 22.9 |
| | 77.5 | 2.3 | 2.89 | 12.6 | 46.8 | 22.9 |
| | 72.5 | 2.2 | 2.97 | 12.6 | 46.9 | 23.2 |
| | 67.5 | 2.1 | 3.07 | 12.6 | 47.0 | 23.3 |
| | 62.5 | 2.0 | 3.17 | 12.6 | 47.7 | 23.5 |
| | 57.5 | 1.9 | 3.28 | 12.6 | 48.5 | 23.6 |
| | 52.5 | 1.8 | 3.41 | 12.9* | 48.9* | 23.8* |
| | 47.5 | 1.7 | 3.54 | 13.0* | 49.4* | 24.2* |
| | 42.5 | 1.6 | 3.70 | 13.3* | 50.7* | 24.5* |
| | 37.5 | 1.5 | 3.87 | 13.5* | 51.4* | 25.0* |
| | 32.5 | 1.4 | 4.08 | 13.7* | 52.5* | 25.5* |
| | 27.5 | 1.3 | 4.30 | 14.2* | 53.6* | 25.9* |
| | 22.5 | 1.2 | 4.58 | 14.5* | 55.4* | 26.5 |
| | 17.5 | 1.1 | 4.90 | 14.6 | 57.4 | 27.3 |
| | 12.5 | 1.0 | 5.28 | 15.4 | 59.4 | 28.4 |
| | 7.5 | .9 | 5.76 | 16.0 | 62.5 | 29.8 |
| | 2.5 | .8 | 6.36 | 17.4 | 67.8 | 32.3 |

* These values are the average of deflections obtained
with the plug in place in the suspension assembly and
the normal arrangement, a range where an overlap exists.

Figure 13 shows the deflection from columns 5, 6 and 7 of Table 4 plotted against the rates of shear. The right hand portion of the curves are linear. The slopes over the straight line portion of the curves for the two different wires MO and 2 with the same oils are approximately the same indicating a partial obedience to Equation 26. However, as the rate of shear decreases towards the left end of the curves, it is seen that the deflection becomes constant and remains unchanged as the rate of shear is decreased to the limit of the cup-cone system. This fact is shown in another manner by Figure 14 in which the deflections are plotted against the separation. It is seen in Figure 14 that as the separation is made small from its maximum limit, the deflections remain constant until a critical separation is reached at about 2.1-2.2cm whence they commence to increase as the separation becomes smaller and smaller. At the smallest separation the inner cone is nearest the bottom of the cup and apparently is acted upon somewhat, by the shear existing between the bottom of the cup and the bottom of the inner cone, thus giving a slight increase in deflection which has raised the last points off the straight lines of Figure 13.

As a result of these experiments with conditions of large separations, the conclusion is forced that no matter how large the separation is made, a zero shearing action is never attained. This possibly is because the fluid itself, tends to set up its own outer wall and exert a shearing force that is dependent only upon the speed of revolution and its
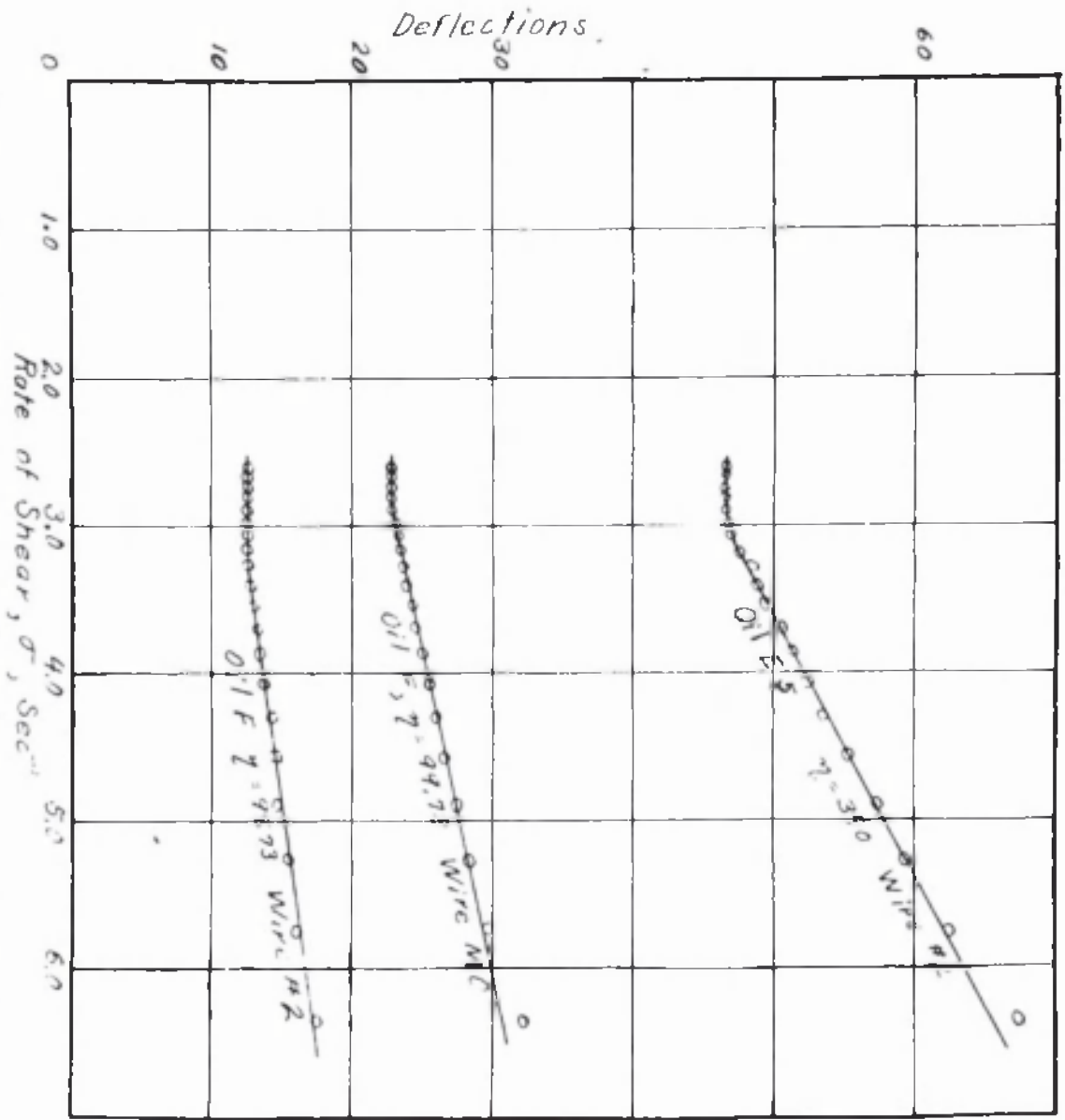
Figure 13. Graph Showing Deflections vs. Rates of
Shear at Large Separations Using the Oversize Cup.
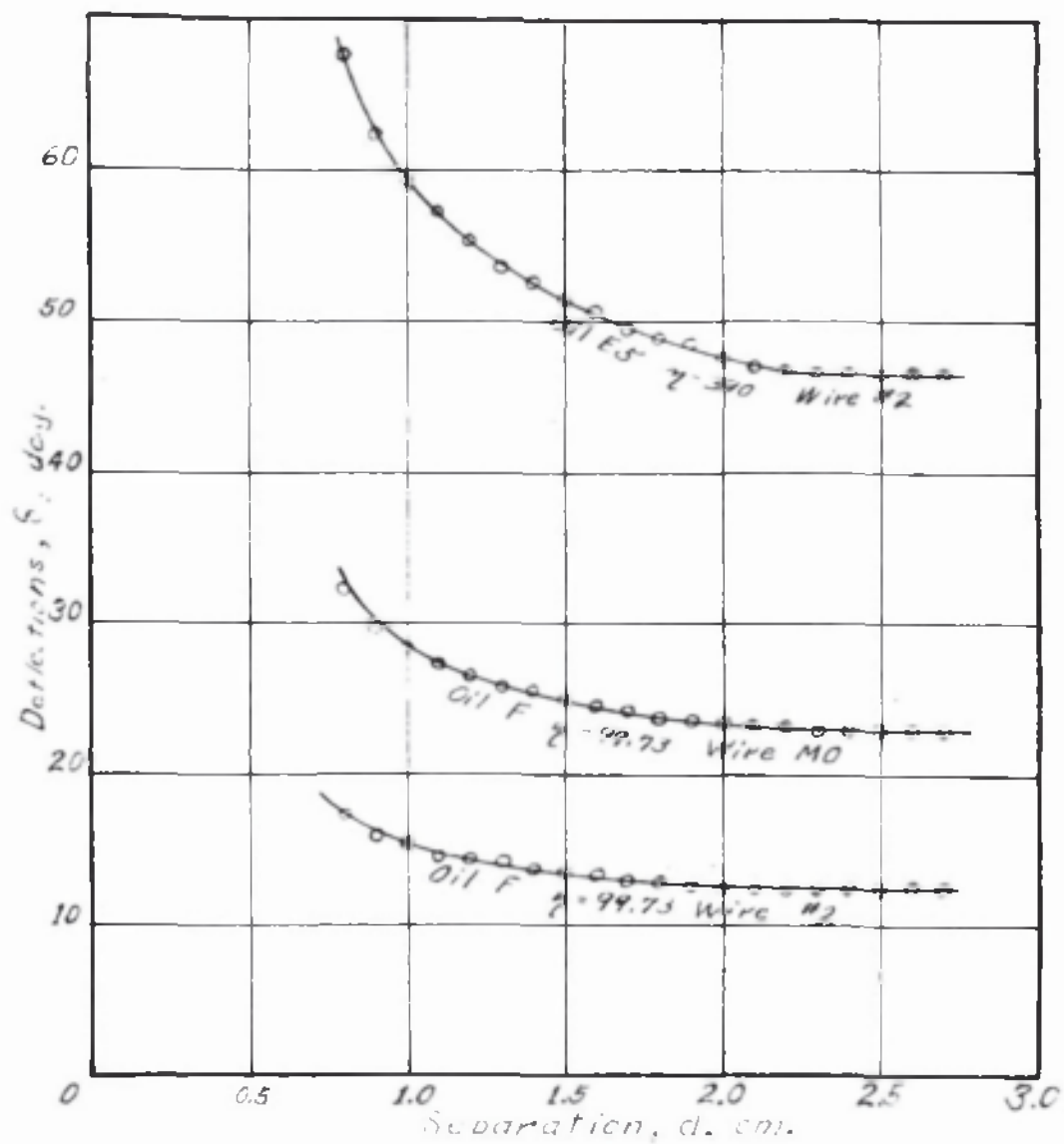
Figure 14. Graph Showing Deflections vs. Separations
Obtained with the Oversize Cup.

coefficient of internal friction (i. e. viscosity). This
residual shearing force exists, no matter how small the
separation is made and is additive to the shearing force
developed by the relative motion of the cup-cone system.
Consequently, Equation 29 represents the total rate of shear
that is acting on the fluid contained in the annular space
of the above cup-cone system. It remains now to evaluate $\sigma_z$
in Equation 29.

The evaluation of the residual rate of shear $\sigma_z$ was
accomplished graphically by determining accurately the values
of the intercepts on the rate of shear axis as shown by
Figures 11a, 11b, 11c. The calibration data of Table 3 was
plotted on large graph paper using a scale of one inch equals
ten reciprocal seconds rate of shear and ten degrees of de-
flection. By means of a steel straight edge lines were drawn
through the points, averaging by visual examination the best
straight line for the data. In the same fashion, the best
average value for the intercept was chosen from the conjunc-
tion of the lines on the rate of shear axis. These values
are given in Table 5.

Table 5

Intercept Values for the Residual Rate of Shear, $\sigma_z$.

| Speed of Revolution r. p. m. | 5 | 20 | 40 | 80 |
|---|---|---|---|---|
| $\sigma_z$, sec.$^{-1}$ | 0.95 | 3.8 | 7.4 | 16.3 |

The values of total rate of shear were calculated by adding the value of the intercept values of the residual rate of shear from Table 5 to the values of rate of shear given in Table 2, which in effect, is the complete evaluation of Equation 29 to obtain the rate of shear.

The total value of the rate of shear obtained for any given head setting and speed of revolution, is given in Table 6.

When the deflections obtained for the standard oils in the calibration experiments, are plotted with the values of total rate of shear according to Equation 29, the intercepts disappear and the family of curves for different speeds with the same oil, reduce to a single straight line rising from the origin with a constant slope. This is shown by Figures 15a, 15b, 15c, for wires 1, 2, and 3 respectively. The excellence of the straight line obedience to the Newtonian concept is strikingly brought out by these figures. The points all lie with a reasonable random distribution near the straight line that was drawn by the visual estimation of its most appropriate position among the points.

The equation of the straight lines appearing in Figures 15a, 15b, 15c can be written as follows

$$\delta = m\,\sigma$$

(30)

where:   $m$ = slope of the straight line.
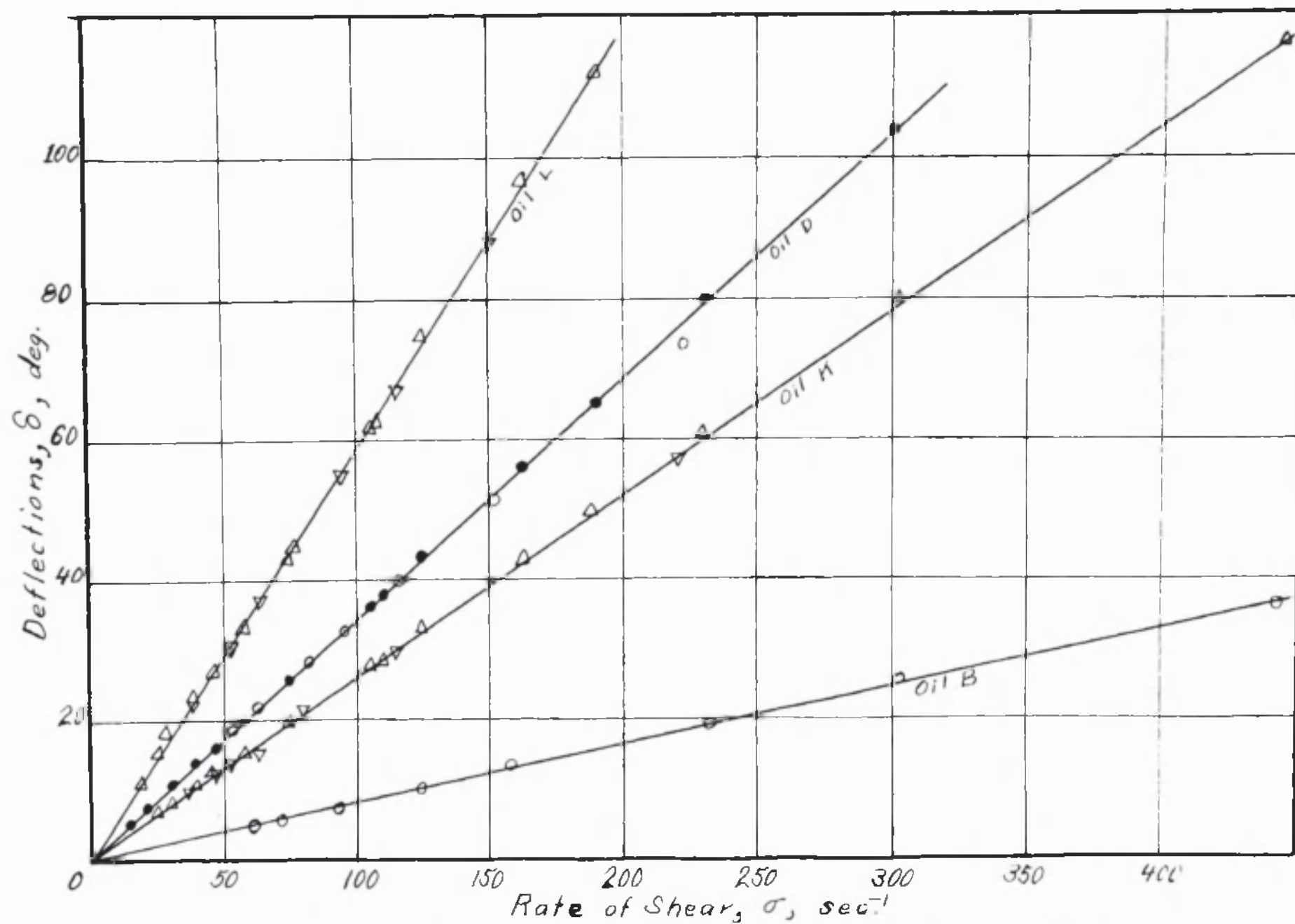
Figure 15a. Graph of the Calibration Data Using the Total Rate of Shear. Wire No. 1.
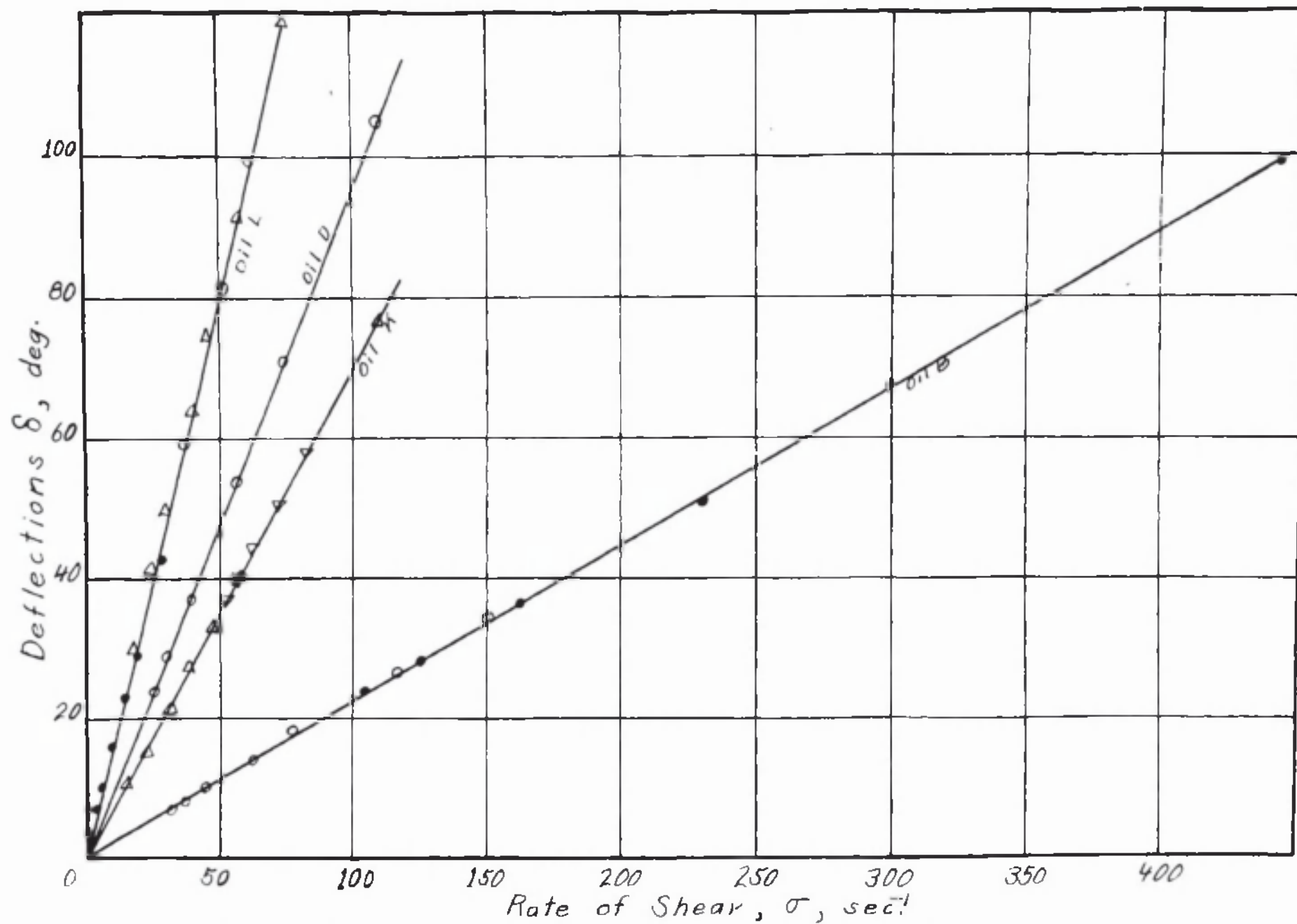
Figure 15 b. Graph of the Calibration Data Using the
Total Rate of Shear. Wire No. 2.
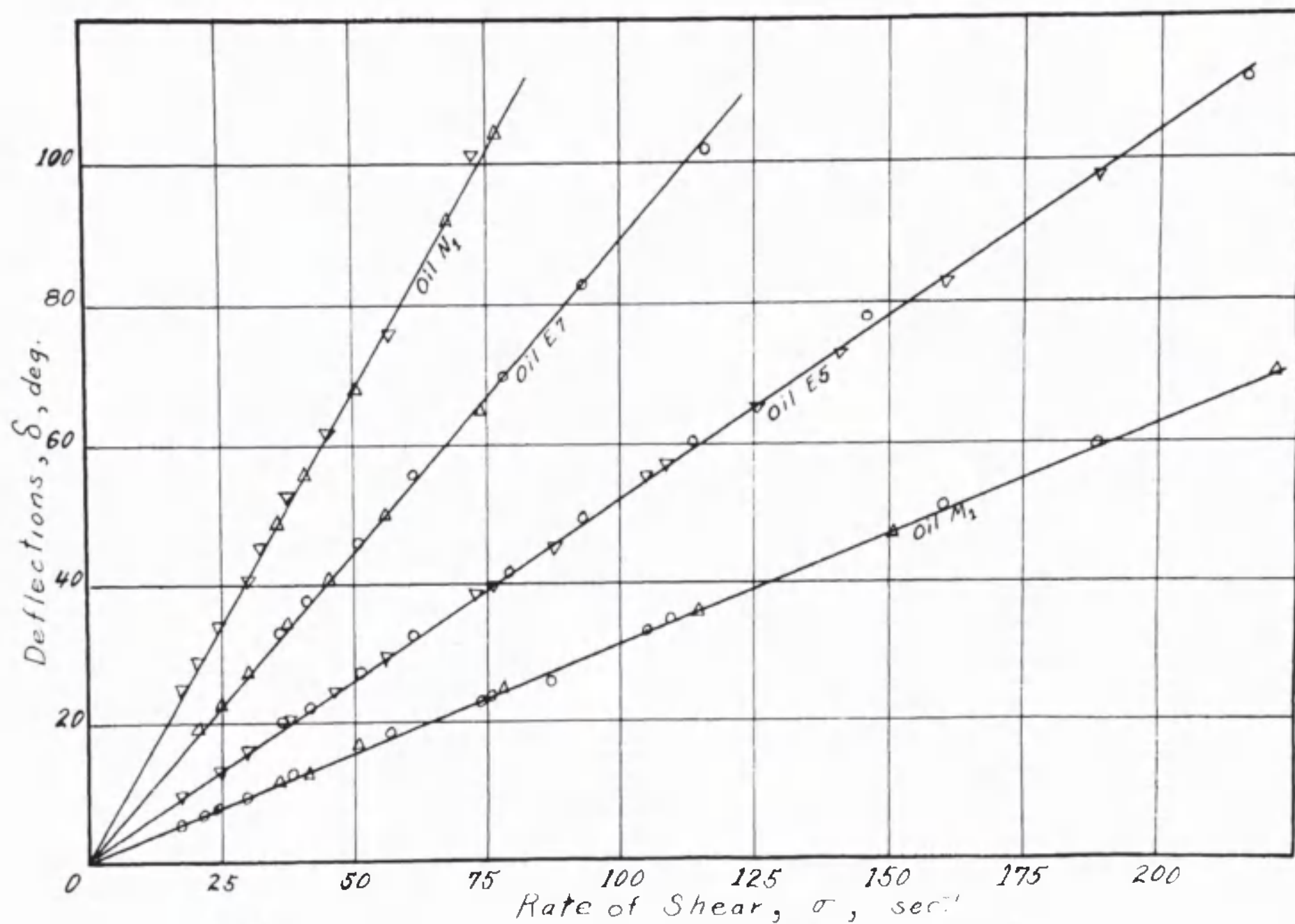
Figure 15c. Graph of the Calibration Data Using the Total Rate of Shear. Wire No. 3.

Table 6.

Total Rates of Shear for Various Indicated
Head Settings and Speeds of Rotation.

| Head Setting mm. | Total Rate of Shear $\sigma$, sec$^{-1}$ | | | |
|---|---|---|---|---|
| | 5 R.P.M. $\sigma$ | 20 R.P.M. $\sigma$ | 40 R.P.M. $\sigma$ | 80 R.P.M. $\sigma$ |
| 40 | 2.53 | 10.14 | 20.1 | 41.7 |
| 38 | 2.60 | 10.42 | 20.6 | 42.8 |
| 36 | 2.68 | 10.73 | 21.3 | 44.0 |
| 34 | 2.77 | 11.08 | 22.0 | 45.4 |
| 32 | 2.86 | 11.36 | 22.5 | 46.5 |
| 30 | 2.97 | 11.90 | 23.6 | 48.7 |
| 28 | 3.10 | 12.41 | 24.6 | 50.7 |
| 26 | 3.25 | 12.99 | 25.8 | 53.1 |
| 24 | 3.42 | 13.68 | 27.2 | 55.8 |
| 22 | 3.62 | 14.47 | 28.7 | 59.0 |
| 20 | 3.86 | 15.42 | 30.6 | 62.8 |
| 19 | 4.00 | 16.02 | 31.8 | 65.2 |
| 18 | 4.15 | 16.63 | 33.1 | 67.6 |
| 17 | 4.33 | 17.51 | 34.4 | 70.3 |
| 16 | 4.52 | 18.08 | 36.0 | 73.4 |
| 15 | 4.74 | 18.95 | 37.7 | 76.9 |
| 14 | 4.99 | 20.07 | 39.9 | 81.4 |
| 13 | 5.28 | 21.13 | 42.1 | 85.6 |
| 12 | 5.62 | 22.5 | 44.8 | 91.0 |
| 11 | 6.02 | 24.4 | 48.6 | 98.7 |
| 10 | 6.60 | 26.0 | 51.8 | 105.1 |
| 9 | 7.09 | 28.4 | 56.5 | 114.6 |
| 8 | 7.82 | 31.3 | 62.4 | 126.3 |
| 7 | 8.77 | 35.4 | 70.6 | 142.7 |
| 6 | 10.03 | 40.4 | 80.7 | 162.9 |
| 5.5 | 10.83 | 43.3 | 86.4 | 174.3 |
| 5 | 11.78 | 47.2 | 94.1 | 190 |
| 4.5 | 12.97 | 51.9 | 103.5 | 209 |
| 4 | 14.43 | 57.8 | 115.4 | 232 |
| 3.5 | 16.32 | 65.3 | 130.4 | 262 |
| 3 | 18.84 | 75.4 | 150.6 | 303 |
| 2.5 | 22.37 | 89.5 | 178.8 | 359 |
| 2 | 27.65 | 110.6 | 221 | 444 |

The slopes have been determined from a large sized plot similar to the ones used for the determination of the intercepts and have been recorded in table 7.

Combining Equation 28 with Equation 30 results in Equation 31 which allows the instrument constant k, to be calculated from the slope of the lines of Figures 15a, 15b, 15c.

$$k = \frac{n}{m}$$

(31)

where: $k$ = the wire constant which converts degrees of deflection to shearing stress.

Table 7 shows the complete data necessary for the calculation of the wire constants k, according to Equation 31. Column 5 shows the values of the constant k obtained for the wires and the various oils used for the calibration. It is seen that the individual values do not vary greatly from the average. The average values from column 6 when inserted in Equation 28 allow the calculation of the coefficient of viscosity for the material yielding the given deflection under the influence of the particular total rate of shear.

Table 7.

Constants Obtained from the Calibration Data.

| 1 | 2 | 3 | 4 | 5 | 6 |
|---|---|---|---|---|---|
| | Oil | | | | |
| Wire | Number | Viscosity $c.p.$ | Slope $m$ | $k$ | $k$ |
| 1 | R | 10.27 | 0.083 | 124.0 | |
| | K | 32.23 | 0.261 | 123.3 | |
| | D | 41.95 | 0.341 | 123.2 | |
| | | | | Ave. | 123.5 |
| 2 | B | 10.27 | 0.223 | 46.2 | |
| | K | 32.23 | 0.700 | 46.0 | |
| | D | 41.95 | 0.930 | 45.2 | |
| | | | | Ave. | 45.8 |
| 3 | F | 99.75 | 0.1305 | 764 | |
| | M | 239.7 | 0.313 | 763 | |
| | E5 | 390 | 0.517 | 769 | |
| | E7 | 664 | 0.867 | 767 | |
| | N | 976.5 | 1.308 | 74 | |
| | | | | Ave. | 762 |

Calculation of the Instrument Constant.

Further confirmation of the validity of assuming the existance of the residual rate of shear is obtained by the calculation of the viscosity of the oils used for calibration from the dimensions of the instrument, the speed of revolution and viscous moment registered by the torsion wire. As will be shown below, excellent checks have been obtained by calculation for the values of the coefficients of viscosity for the oils from the National Bureau of Standards and the Texas Oil Company.

According to the equation:

$$\tau = \frac{\delta T}{2\pi \ell R_e^2}$$ (21)

the shearing stress causing the deflection $\delta$, can be calculated from the measurements of the inner cone provided the value of T, the torsional constant, is known. The torsional constant was evaluated in the following manner.

When a disk at the end of a torsion wire is allowed to oscillate freely about an axis normal to its plane and coinciding with the torsion wire, the period of its oscillation is given by

$$\theta = 2\pi \sqrt{\frac{I}{C}}$$ (32)

where: $\theta$ = period of oscillation, seconds.

$I$ = moment of inertia of disk, $\frac{1}{2}$ MR.

$C$ = restoring couple per radian of angular displacement from rest position, ergs per radian.

Substituting the value for the moment of inertia of a

flat cyclindrical plate or disk and solving for the term    ,
Equation 32 becomes,

$$C = \frac{2 \pi^2 M R^2}{\Theta^2} \qquad (33)$$

where:   $M$ = mass of the disk, gms.

   $R$ = radius of the disk, cm.

Equation 33 affords a simple method for determining the
value of the torsional constants for the different wires used
in the experimental work.

Two disks, 6 and 10 inches in diameter, respectively,
were carefully prepared, each fitted with a small brass hub,
accurately centered and just sufficient to carry a set screw
by which the torsion wires could be clamped into the disks.
The disks were carefully measured and weighed.

The upper end of the torsion wire was clamped in a chuck
just high enough to raise the disk, fastened on the lower end
of the wire, clear of the table top.  An index mark was made
on the disk with a crayon or wax pencil.  A similar mark was
also made upon a piece of white paper lying partially under
the disk which could be moved to the mid-point of the os-
cillations after the motion had been started.  Oscillations
were started by displacing the disk through about 30° with
the thumb and forefinger of each hand and gently releasing
it.  A stop-watch, measuring tenths of a second was started,
when the index mark on the disk passed through the midpoint
of the oscillations, or when it reached the end of an os-
cillation.  The time for ten oscillations was measured and

the average taken. Several series were run from which a
grand average was taken to give the time for the period of
one complete oscillation. The data thus obtained substi-
tuted into Equation 33 with the values for the weight of the
disk and its radius allowed the calculation of the torsional
constant of the wire used. Using this procedure the tor-
sional constants were determined for the wires furnished
with the instrument and two additional wires prepared in this
laboratory. The complete data thus obtained is summarized
in the following Table 8.

Table 8

Data for the Torsional Constants of the Wires.

| | 1 | 2 | 3 | 4 | 5 | 6 | 7 | 8 |
|---|---|---|---|---|---|---|---|---|
| Wire | Disk | M | R | $\Theta$ | C | T | | K |
| | | gms. | cm. | sec. | ergs/rad. | ergs/d. | Calc. | Obs. |
| M-0 | 6 in. | 201.6 | 7.55 | 14.65 | 1057 ) | 18.06) | 0.269 | 0.258* |
| | 10 in. | 533.0 | 12.68 | 40.86 | 1013 ) | ) | | |
| #2 | 6 in. | 201.6 | 7.55 | 10.87 | 1870 ) | 32.37 | 0.4822 | 0.458 |
| | 10 in. | 533.0 | 12.68 | 30.56 | 1840 ) | | | |
| #1 | 6 in. | 201.6 | 7.55 | 6.63 | 5026 ) | 87.09 | 1.298 | 1.235 |
| | 10 in. | 533.0 | 12.68 | 18.63 | 4952 ) | | | |
| M-7 | 6 in. | 201.6 | 7.55 | 3.62 | 16970 ) | 290.0 | 4.41 | 4.11* |
| | 10 in. | 533.0 | 12.68 | 10.20 | 16260 ) | | | |
| #3 | 6 in. | 201.6 | 7.55 | 2.666 | 31080 ) | 537.74 | 8.93 | 7.62 |
| | 10 in. | 533.0 | 12.68 | 7.50 | 30550 ) | | | |

* Calculated from the ratio between the torsion constant
T and the value of k for wires 1, 2, and 3. (see below)

Column 5 gives the values of the torsional constants ex-
pressed as ergs per radian, while column 6 gives the average
of the values for the 6 and 10 disks expressed as ergs per de-
gree of twist. The latter is the more useful form since the

deflection reading is taken in degrees.

In columns 7 and 8 are given the values of the constants k as obtained by calculation and by direct calibration with the standard viscosity oils. These constants are used appropriately in Equation 28 to determine the viscosity of a material being sheared in the cup-cone system. The calculated values of the wire constants are based upon Equation 21 in the following manner.

$$\tau = \frac{\delta T}{2\pi l R_E^2} = k\delta \tag{21a}$$

whence:

$$k = \frac{T}{2\pi l R_E^2} \tag{34}$$

By measuring the inner cone with a vernier caliper it was determined that the slope length was 2.62 cm. and the effective radius, (1% longer than the mean radius) was 2.02 cm. Substituting these values in Equation 34 gives:

$$k = \frac{T}{67.16} \tag{35}$$

The values of the torsion constant T given in column 6 of Table 8, divided by 67.16 give the values of the wire constants shown in column 7. It follows from Equation 28 that the product of the constant k and the deflection is the shearing stress acting upon the surface of the inner cone. This is confirmed by the close agreement between the calculated values of k and the values obtained by direct calibration with the standard oils as is shown in the columns 7 and 8

of Table 8. The product of the calculated values of k and
the various slopes listed in column 4 of Table 7, gives the
coefficient of viscosity for the particular oil used for
the calibration measurements. Thus, the coefficient of vis-
cosity has been determined, by measurements of mass, time,
and length. This has been done for torsion wires 1, 2, and
3 and the results listed in column 5 of Table 9. Appearing
also in column 6 are the certified values of the viscosity
coefficient furnished with the standard oils.

Table 9.

Comparison of Calculated Value of the Coefficient
of Viscosity and the Certified Value for the Stan-
dard Oils.

| Wire | Oil | Slope* m | Calculated Const. k | Viscosity, c.p. Calc. | Certified | Per Cent Diff. |
|---|---|---|---|---|---|---|
| 1 | B | 0.083 | 129.8 | 10.77 | 10.27 | +4.9 |
| | K | 0.261 | 129.8 | 33.8 | 32.23 | +4.9 |
| | D | 0.341 | 129.8 | 44.2 | 41.95 | +5.5 |
| 2 | B | 0.223 | 48.2 | 10.72 | 10.27 | +4.4 |
| | K | 0.700 | 48.2 | 33.7 | 32.23 | +4.7 |
| | D | 0.930 | 48.2 | 44.8 | 41.95 | +6.9 |
| 3 | F | 0.1305 | 80. | 104.9 | 99.75 | +5.1 |
| | M | 0.313 | 80. | 252 | 239.7 | +5.0 |
| | E-5 | 0.517 | 80. | 416 | 390 | +6.7 |
| | E7 | 0.867 | 80. | 695 | 664 | +4.7 |
| | U | 1.308 | 80. | 1050 | 976.5 | +7.6 |
| | | | | | Average | +5.5 |

* From column 4 of Table 7.

The percentage difference is listed in column 7, from
which it is seen that the viscosity as determined by the Good-
eve instrument averages 5.5% greater than the true value.

This is in the direction expected, since incomplete correction of the end effects would cause a greater drag or deflection and a resulting greater viscosity would be indicated. However, it is interesting to note that the agreement is good over a wide range of viscosity and with two different torsion wires used with the same oils. The constants determined by the direct calibration method correct for the incomplete elimination of end effects and therefore are used in all subsequent measurements.

In order to cover more adequately the range of viscosities that were encountered in the experimental work with this instrument, two additional torsion wires were prepared and calibrated. These wires were prepared from Numbers 6, and 7 music wire and designated as M6 and M7 wires respectively. The residual twist caused by the spooling of the wire during manufacture and packaging was removed by connecting it in series with a suitable rheostat and passing an electric current until the wire turned slightly more than a faint yellow, while under moderate tension. This procedure removed the residual tendency to coil and did not seem to destroy to any great extent the tensile strength as indicated by kinking the wire before and after the straightening operation. Several pieces, 4-5 feet long were straightened, and from these the best section suitable for the desired torsion wire was selected. Brass ferrules were carefully soldered to each end, avoiding heating the wire more than necessary to melt the solder. The torsional constants of the wires were then de-

termined as described above.

The constant k for these wires was calculated from the ratio between the torsional constants C and the constant k obtained from the calibration of wires 1, 2, and 3 by means of the standard oils. The ratio for wire #1 is 1.417; for wire #2, 1.413; and for wire #3, 1.416; or an average of 1.415. Thus, the product of this ratio and the torsional constant of any newly prepared wire gives its value for the constant k.

As a result of the above calibration experiments, it has been demonstrated that the useful form of the Couette equation applying to the Goodeve viscosimeter is as follows:

$$\frac{\delta T}{2\pi \ell R_E^2} = \eta \left[ \frac{2\pi}{60} \Omega \left( \frac{R_E + \frac{1}{2}d}{d} \right) + \sigma_n \right] \tag{26a}$$

whence:

$$\delta k = \tau = \eta \sigma \tag{28a}$$

Thus it is assured, that a material placed in the cup of the instrument can be sheared at a known and constant rate. This constant rate of shear can be determined by Equation 29 or by using the listed values given in Table 6. The shearing stress that results from the constant rate of shear can be calculated by the product of the constant "k" and the observed deflection of the inner cone. Several different torsion wires have been calibrated, giving a wide range of usefulness to the instrument.

# CHAPTER VI.

## THE APPLICATION OF THE SHEARING ACTION OF THE GOODEVE INSTRUMENT TO BENTONITE SUSPENSIONS.

The bentonite used in these experiments was a typical Wyoming bentonite.*  It was practically all less than 325 mesh.  A small amount of grosser material, probably quartz, upon standing tended to settle from the more dilute suspensions.  The bentonite conforms in general to a sodium bentonite and had the following analysis.

| | |
|---|---|
| $SiO_2$ | 62.2% |
| $Al_2O_3$ | 21.2 |
| $Fe_2O_3$ | 3.98 |
| MgO | 2.75 |
| CaO | 1.25 |
| $K_2O$ | 0.24 |
| $Na_2O$ | 2.39 |
| $CO_2$ | 0.32 |
| Ig. Loss | 5.88 |
| $TiO_2$ | 0.06 |

It is well known that clay suspensions tend to change their colloidal characteristics over a period of many days after they have been prepared, therefore, the suspensions used in this work were allowed to age for a minimum of 45 days before being used.  For each concentration, an individual

---

\* American Colloid Company, B. C. Volclay, Micron grade. Chicago, Illinois.

suspension was prepared, in order to avoid disturbing any equilibrium of ionic balances or dispersive forces by dilution of a concentrated stock solution. No ions or electrolytes were added to the suspension. A total of eight individual suspensions were prepared from the air-dried bentonite ranging from 1 to 8 per cent bentonite by weight in steps of 1%.

The ability of the suspensions to form a gel was quite pronounced in the case of 6, 7 and 8 per cent suspensions, increasing in rigidity for a given time of setting as the concentration of bentonite increased from the 6 to the 8 per cent suspension . The formation of a rigid gel, as arbitrarily determined by the resistance of the material to an inversion of the container, was not so pronounced with the suspensions of bentonite concentrations less than 6%. However, it could definitely be observed qualitatively that the suspensions containing 3, 4, and 5 per cent bentonite seemed to thicken and become more viscous upon standing, the effect being less as the concentration becomes less. The 1 and 2 per cent suspensions did not seem to show this effect.

The ability of the bentonite suspensions to thicken and form rigid gels has been noted by many and several theories have been advanced to account for the phenomena. The adequacy of the several theories for gel formation is discussed by Goodeve[14] who concludes that only a scaffolding type of

---

[14] C. F. Goodeve, Trans. Faraday Soc. 35:344-7 (1939)

structure is capable of explaining all the experimental observations. The mechanistic picture of gelation and gels need not be concerned here beyond the recognition that structure, in the sense that the bentonite particles are held to fixed positions, is present when the sols change to gels.

The first series of experiments on the bentonite sols were undertaken with a viewpoint of following a procedure that would be practical for commercial use as a means of assessing the fluid condition of such materials similar to bentonite sols, i. e. oil-well drilling fluids, paints, printing inks, etc.

Since it was recognized from preliminary observations that considerable time was necessary for the attainment of equilibrium between the tendency of the sols to form gel structure and the disruptive action of the shearing forces, a rigorously defined program was used. This program introduced in the following tests an arbitrariness that is justified because it yields information in the space of a few minutes that otherwise would take many hours to ascertain with the more rigorous procedure outlined below. These first tests, while not entirely satisfactory in their experimental arrangements, were of value in gaining experience with the apparatus and magnitude of the quantities involved. Considerable more data than is presented here was taken. That which

is given, is typical of all, and from it certain indications can be obtained concerning the absence of slip at the wall and the relation of coagulation to viscosity.

The procedure used for the tests of Series I was as follows.

The cup-and-cone system was thoroughly washed with soap and water and then rinsed several times with absolute methyl alcohol. The use of the methyl alcohol was important, because it left the metal surface in a condition that allowed it to be completely wetted by the suspension. It also offered the additional advantage of allowing the cup and cone to be cleaned without removing them from the instrument. This was done by rinsing with water while scrubbing the surfaces with a camel hair brush, the rinsings being removed by one of the suction flasks. After the final rinsing with the methyl alcohol, the cup and cone were quickly dried by means of a gentle stream of air from the compressed-air line.

After the appropriate torsion wire was fitted, centered, and set to zero in the manner described above, the zero deflection reading was noted and recorded. The head setting was adjusted to the reading corresponding to the lowest rate of shear to be used with the given wire. The torsion wire assembly was then raised and turned to the right thus clearing the cup so that the sample can be easily poured into it. The stop watch and speed gears were checked for proper working order, and if necessary the temperature of the cone and water bath was adjusted.

When the instrument was ready, the sample was given the desired treatment in the structure breaker and immediately poured into the cup. A few seconds were allowed for air bubbles to rise to the surface; then the core was lowered into the sample. At the instant the sample was poured into the cup the stop watch was started. This was taken to correspond to the cessation of the stirring action of the structure breaker, i. e. as zero time. After the elapse of one minute, during which the sample had been placed in the cup and the cone lowered, the motor was switched on and the excess material removed from the recess on the top of the cone by means of the suction flask. A glance at the stroboscopic speed-check disk indicated whether or not the motor was turning at the correct speed. Any deviations were quickly corrected, by means of the variable resistor connected across the motor brushes. After the elapse of the second minute the deflection reading was noted through the telescope, and then immediately the cone was lowered to the next position. The reading was then recorded and the top of the inner cone checked to see if the level of the fluid in the upper recess was below the rim, thus standardizing the end effects. When necessary, the excess was removed by means of the suction flask. After the lapse of the third minute the second reading was taken and so on successively, until the entire range of rates of shear desired for the wire had been covered. The schedule of settings for the rates of shears at which the measurements were to be taken,

was prepared beforehand and covered a range of rates of shear from 5 to 444 sec.$^{-1}$ in about 25 successive values.

It was necessary to use three different speeds of rotation to cover this range in accordance with Table 6. The highest rate of shear, 444 sec.$^{-1}$ was obtained with the speed of 80 r.p.m. and a head setting of 2 mm.;while the lowest rate of shear obtainable at this speed was 105.1 sec.$^{-1}$. The next speed of rotation used was 20 r.p.m. which allowed rates of shear ranging from 110.6 to 26.0 sec.$^{-1}$, while the lowest rates of shear were obtained at 5.0 r.p.m. ranging from 27.6 to 5 sec.$^{-1}$. It was evident that sufficient overlap of the rates of shear obtained with the different speeds of rotation had been allowed. The significance of this overlap will be discussed below in relation to slipping at the wall and dependability of the results.

Some trouble was experienced at times with the inner cone going off center at the speed of 80 r.p.m. This occurrence happened more frequently at the greater separations and usually disappeared when the smaller separations were used. Unless the effect was excessive, in which case the experiment was repeated, the reading was taken as the visually-estimated mean of the vibration observed in the telescope.

This procedure was applied to each of the suspensions using different amounts of treatment in the structure breaker as measured by the number of strokes applied downwards with the piston. These were accurately counted for each particular test. The data thus accumulated is given in Tables 10 to 14

inclusive. Since much of this data is repetitious the tables give only the values of rate of shear and shearing stress. The shearing stress was, of course, obtained by the product of the wire constant and the deflection as indicated by Equation 21. The data obtained using the above procedure has been plotted on rheological diagrams shown by Figures 16a, b, c, d, e.

Figure 16a shows the rheological diagram for the suspension containing 1% bentonite which was obtained by plotting the data of Table 10. The points seem to indicate a straight line except for the portion determined at 80 r.p.m. wherein turbulence occurred. The viscosity coefficient as indicated by the slope is 1.4 cp. and the material can be classed as a Newtonian fluid. This material had been given no treatment in the structure breaker, the bottle being inverted several times to mix a small amount of settled material. Apparently little structure existed in this sol for a check test at 80 r.p.m. in which the material was given 100 strokes in the structure breaker, no significant difference was obtained in the deflection readings.

Figure 16b is the graph of the shearing stress-rate of shear data for the 2% suspension given in Table 11. In this case the points taken at 80 r.p.m. did not show turbulence as indicated by the minimum obtained in the case of the 1% suspension. Apparently, the viscosity is sufficiently great

Table 10.

Series I Tests.  Rate of Shear  - Shearing
Stress Data.  1% Bentonite Suspensions.

| Temperature 25°C | | Wire MO | |
|---|---|---|---|
| | | Shearing Stress, dynes/sq.cm. | |
| Speed of Rotation r.p.m. | Rate of Shear sec.$^{-1}$ | no agitation | 100 strokes |
| 80 | 62.8 | 1.59 | 1.54 |
| | 73.4 | 1.46 | 1.48 |
| | 85.6 | 1.51 | 1.41 |
| | 105.1 | 1.61 | 1.67 |
| | 114.6 | 1.71 | 1.74 |
| | 126.3 | 1.84 | 1.87 |
| | 142.7 | 2.02 | 2.05 |
| | 162.9 | 2.30 | 2.35 |
| | 174.3 | 2.43 | - |
| | 190 | 2.66 | 2.71 |
| | 209 | 2.92 | 2.97 |
| | 232 | 3.22 | 3.25 |
| | 262 | 3.63 | 3.65 |
| | 303 | 4.14 | 4.07 |
| | 359 | 4.93 | 4.98 |
| | 444 | 6.03 | 6.08 |
| 20 | 26.0 | 0.41 | |
| | 35.4 | 0.51 | |
| | 47.2 | 0.72 | |
| | 57.8 | 0.92 | |
| | 75.4 | 1.10 | |
| | 89.5 | 1.23 | |
| | 110.6 | 1.54 | |
| 5 | 5.0 | 0.12 | |
| | 10.0 | 0.20 | |
| | 16.3 | 0.28 | |
| | 22.4 | 0.38 | |
| | 27.6 | 0.44 | |

Table 11.

Series I Tests; Rate of Shear – Shearing Stress Data.
2% Bentonite Suspension.

**Temperature 25°C**  Wire MQ

| Speed of Rotation r.p.m | Rate of Shear sec.⁻¹ | Shearing Stress, dynes/sq. cm. | |
| | | Slightly Agitated | 100 Strokes |
|---|---|---|---|
| 80 | 105.1 | 2.53 | 2.46 |
| | 126.3 | 2.77 | 2.87 |
| | 142.7 | 3.41 | 3.10 |
| | 162.9 | 3.79 | 3.61 |
| | 174.3 | 4.10 | 3.89 |
| | 190 | 4.48 | 4.20 |
| | 209 | 4.84 | 4.61 |
| | 232 | 5.46 | 5.12 |
| | 262 | 6.04 | 5.79 |
| | 303 | 6.97 | 6.42 |
| | 359 | 8.09 | 7.78 |
| | 444 | 9.91 | 9.61 |
| 20 | 26 | 0.67 | 0.61 |
| | 35.4 | 0.82 | 0.78 |
| | 47.2 | 1.18 | 1.13 |
| | 57.8 | 1.36 | 1.38 |
| | 75.4 | 1.74 | 1.61 |
| | 89.5 | 2.02 | 1.99 |
| | 110.6 | 2.51 | 2.46 |
| 5 | 5 | | 0.13 |
| | 10 | | 0.20 |
| | 16.3 | | 0.38 |
| | 22.4 | | 0.51 |
| | 27.6 | | 0.58 |

## Table 12

### Series I Tests.  Rate of Shear – Shearing stress Data.
### 4% Bentonite Suspension.

| Temperature 25°C | | Wire MO | | | |
| | | Shearing Stress, dynes/sq. cm. | | | |
| Speed of Rotation r.p.m. | Rate of Shear sec.⁻¹ | Slightly Agitated (1) | Slightly Agitated (2) | 20 Strokes | 200 Strokes |
| --- | --- | --- | --- | --- | --- |
| 80 | 105.1 | 29.8 | 22.5 | 11.9 | 8.9 |
| | 126.3 | 31.6 | 24.8 | 14.5 | 10.4 |
| | 142.7 | 33.0 | 26.0 | 16.1 | 11.6 |
| | 162.9 | 35.0 | 28.3 | 18.1 | 13.1 |
| | 174.3 | 35.5 | 29.4 | 19.4 | 14.1 |
| | 190 | 36.8 | 30.9 | 20.8 | 15.2 |
| | 209 | 38.4 | 33.1 | 22.6 | 16.4 |
| | 232 | 40.7 | 35.4 | 24.8 | 18.1 |
| | 262 | 43.9 | 38.4 | 29.3 | 20.2 |
| | 303 | 47.3 | 42.7 | 30.8 | 22.9 |
| | 359 | 52.5 | 48.0 | 35.6 | 26.8 |
| | 444 | 59.3 | 56.0 | 42.7 | 32.3 |
| 20 | 26.0 | 11.0 | 7.0 | 3.5 | 2.5 |
| | 35.4 | 13.9 | 9.2 | 4.6 | 3.25 |
| | 47.2 | 16.7 | 11.6 | 6.0 | 4.25 |
| | 57.8 | 19.7 | 13.3 | 7.3 | 5.1 |
| | 75.4 | 23.2 | 16.0 | 9.1 | 6.4 |
| | 89.5 | 25.2 | 18.3 | 10.6 | 7.5 |
| | 110.6 | 28.3 | 21.5 | 12.8 | 9.0 |
| 5 | 5 | | 1.7 | | 0.46 |
| | 10 | | 3.1 | | 0.84 |
| | 16.3 | | 4.9 | | 1.35 |
| | 22.4 | | 6.0 | | 1.89 |
| | 27.6 | | 7.2 | | 2.2 |

## Table 13

Series I Tests.   Rate of Shear - Shearing Stress Data.
6% Bentonite Suspension.

Temperature 25°C

| Speed of Rotation r.p.m. | Rate of Shear sec.⁻¹ | Shearing Stress, dynes/sq.cm. Wire 1 | | | |
|---|---|---|---|---|---|
| | | Slightly Agitated | 50 Strokes | 100 Strokes | 200 Strokes |
| 80 | 105.1 | 112.2 | 45.3 | 32.1 | 34.7 |
| | 126.1 | 119.5 | 52.5 | 37.3 | 40.2 |
| | 142.7 | 120.5 | 56.9 | 40.8 | 43.2 |
| | 162.9 | 125.4 | 62.8 | 45.8 | 47.6 |
| | 174.3 | 124.5 | 66.5 | 48.9 | 50.3 |
| | 190 | 127.7 | 70.5 | 51.7 | 53.6 |
| | 209 | 131.5 | 75.4 | 56.1 | 57.3 |
| | 232 | 137.7 | 81.8 | 61.2 | 61.7 |
| | 262 | 146.7 | 89.2 | 67.4 | 67.8 |
| | 303 | 156.0 | 98.7 | 76.0 | 75.7 |
| | 359 | 168.8 | 111.8 | 86.9 | 86.3 |
| | 444 | 186.0 | 130.0 | 102.8 | 101.7 |
| 20 | 26.0 | 64.4 | 14.9 | 11.4 | 11.7 |
| | 35.4 | 75.1 | 19.7 | 14.5 | 14.6 |
| | 47.2 | 79.8 | 24.8 | 18.0 | 18.3 |
| | 57.8 | 82.8 | 28.7 | 21.3 | 21.4 |
| | 75.4 | 92.2 | 34.7 | 25.9 | 25.7 |
| | 89.5 | 96.0 | 39.5 | 29.3 | 28.8 |
| | 110.6 | 105.3 | 45.9 | 34.5 | 34.1 |
| 5 | 5 | 35.6 | 4.6 | 3.2 | 2.6 |
| | 10 | 44.4 | 8.3 | 5.6 | 5.2 |
| | 16.3 | 55.4 | 13.3 | 7.8 | 7.8 |
| | 22.4 | 59.3 | 16.4 | 10.1 | 10.5 |
| | 27.6 | 60.7 | 19.9 | 12.2 | 12.6 |

Table 14.

Series I Tests.    Rate of Shear - Shearing Stress Data.
8% Bentonite Suspension.

| Temperature 25°C | | Wire M7 | | |
|---|---|---|---|---|
| Speed of Rotation r.p.m. | Rate of Shear sec.⁻¹ | Shearing Stress | | |
| | | 10 Strokes | 100 Strokes | 200 Strokes |
| 80 | 105.1 | 280 | 179 | 158 |
| | 126.3 | 303 | 197 | 180 |
| | 143.7 | 309 | 206 | 189 |
| | 162.9 | 322 | 218 | 203 |
| | 174.3 | 321 | 225 | 212 |
| | 190 | 328 | 235 | 225 |
| | 209 | 336 | 246 | 238 |
| | 232 | 352 | 261 | 252 |
| | 262 | 369 | 280 | 269 |
| | 303 | 392 | 304 | 288 |
| | 359 | 419 | 335 | 317 |
| | 444 | 443 | 352 | 358 |
| 20 | 26.0 | 172 | 78 | 66 |
| | 35.4 | 187 | 94 | 82 |
| | 47.2 | 213 | 114 | 102 |
| | 57.8 | 248 | 127 | 115 |
| | 75.4 | 254 | 149 | 135 |
| | 89.5 | 265 | 166 | 151 |
| | 110.6 | 283 | 183 | 171 |
| 5 | 5 | 76 | 36 | 27 |
| | 10 | 103 | 49 | 42 |
| | 16.3 | 130 | 62 | 58 |
| | 22.4 | 152 | 81 | 77 |
| | 27.6 | 168 | 97 | 91 |
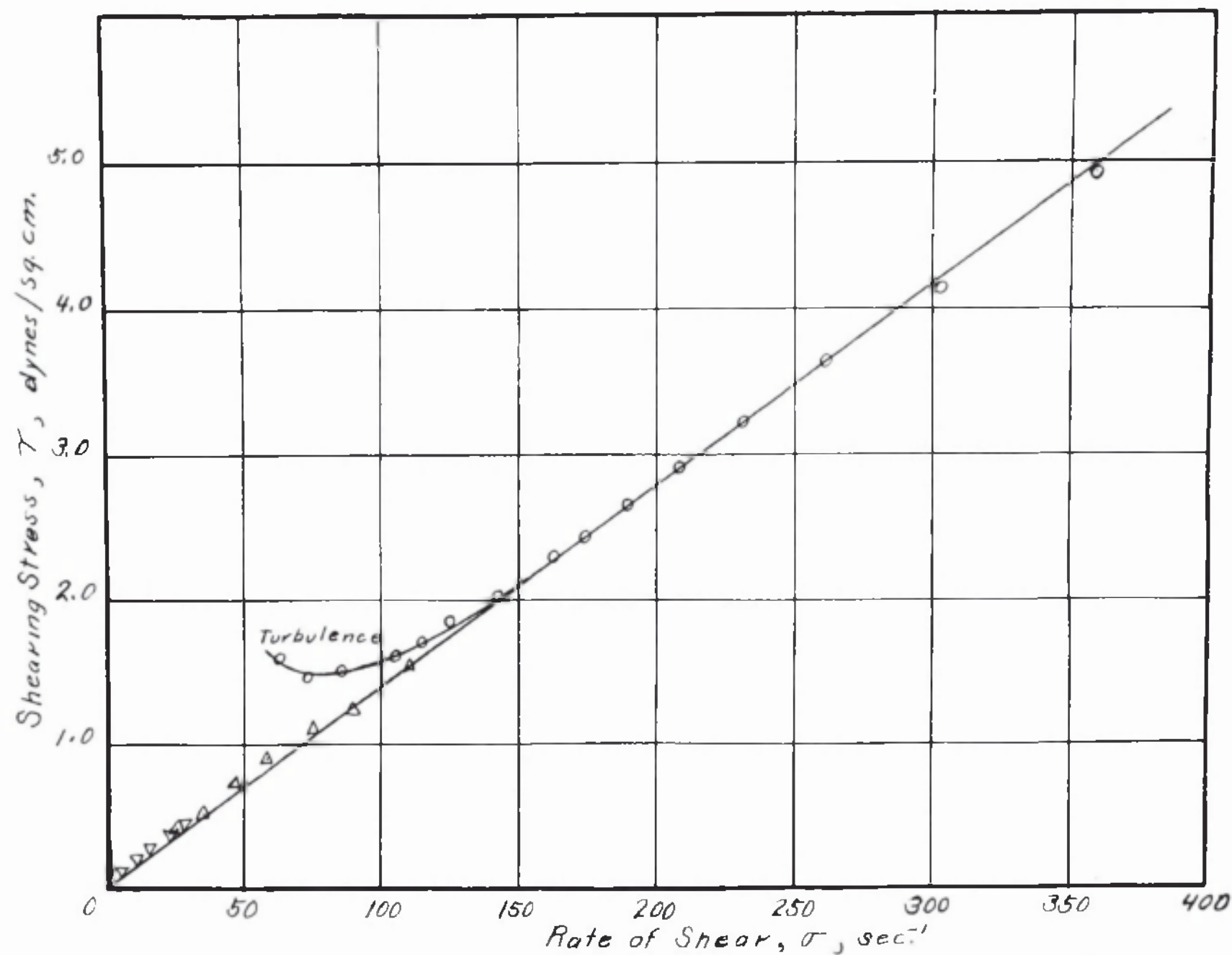
Figure 16a. Series I Tests. Rheological Diagram for the 1% Suspension.
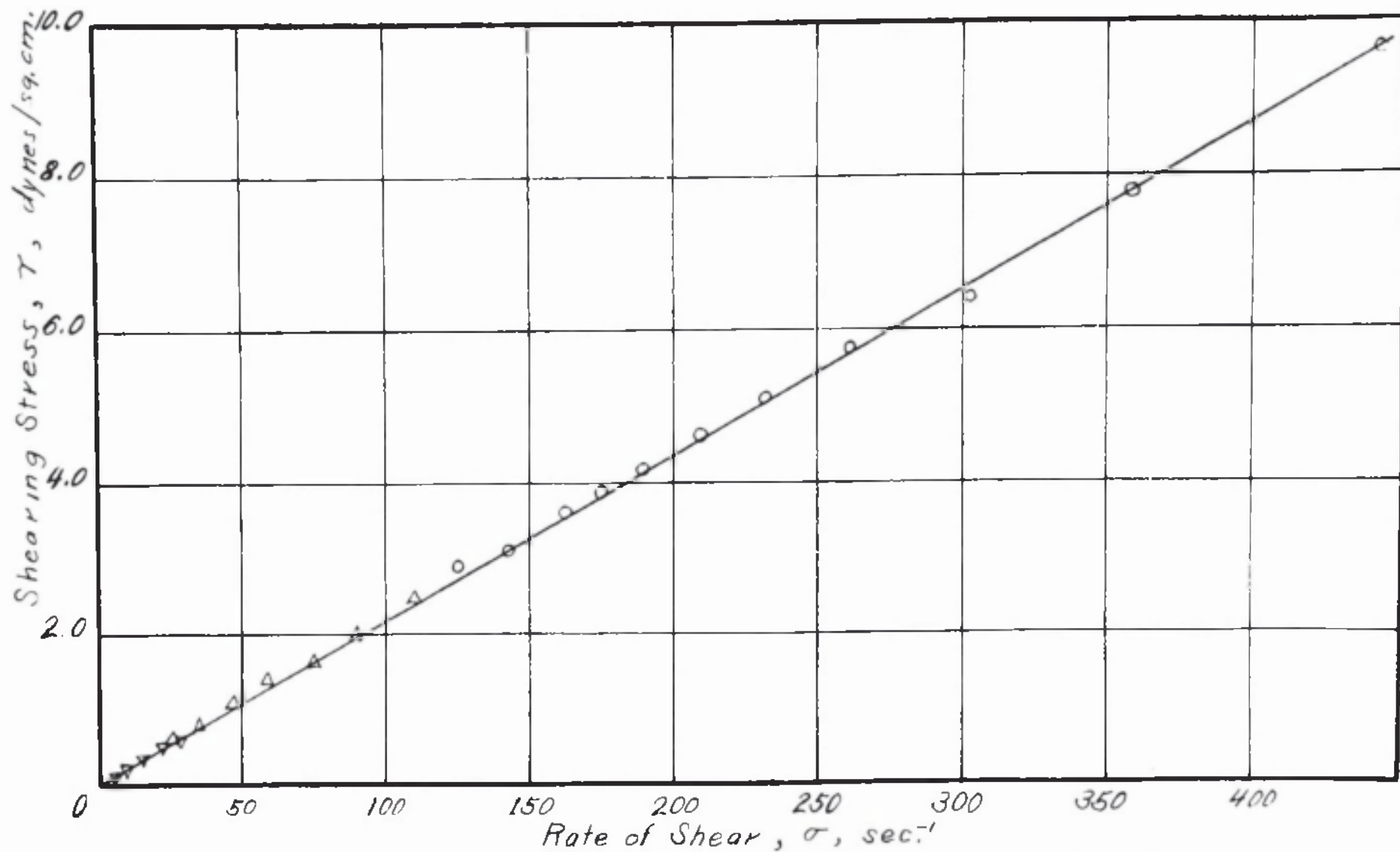
Figure 16b. Series I Tests. Rheological Diagram for the 2% Suspension.
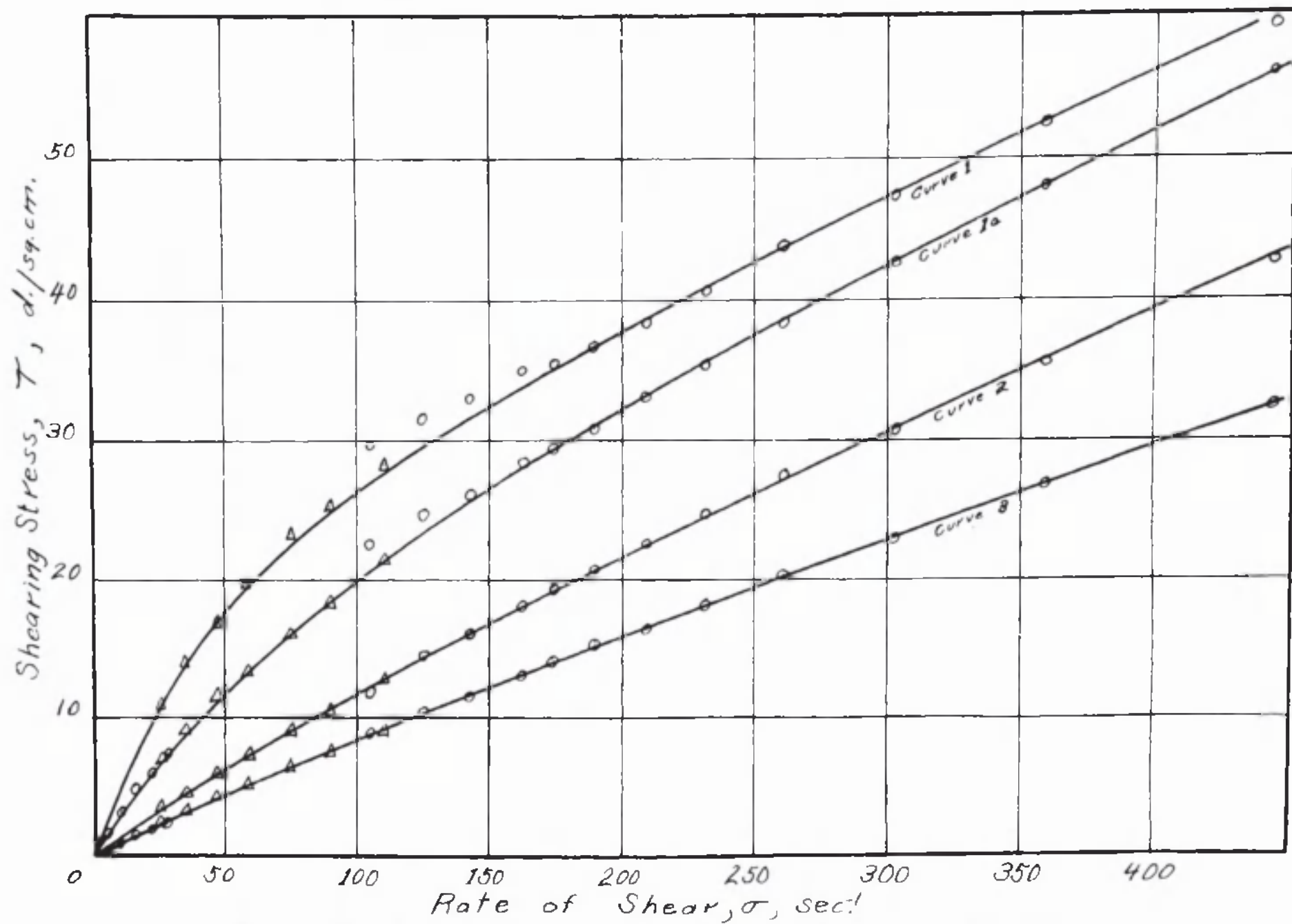
Figure 16c. Series I Tests. Rheologial Diagram for the 4% Suspension.
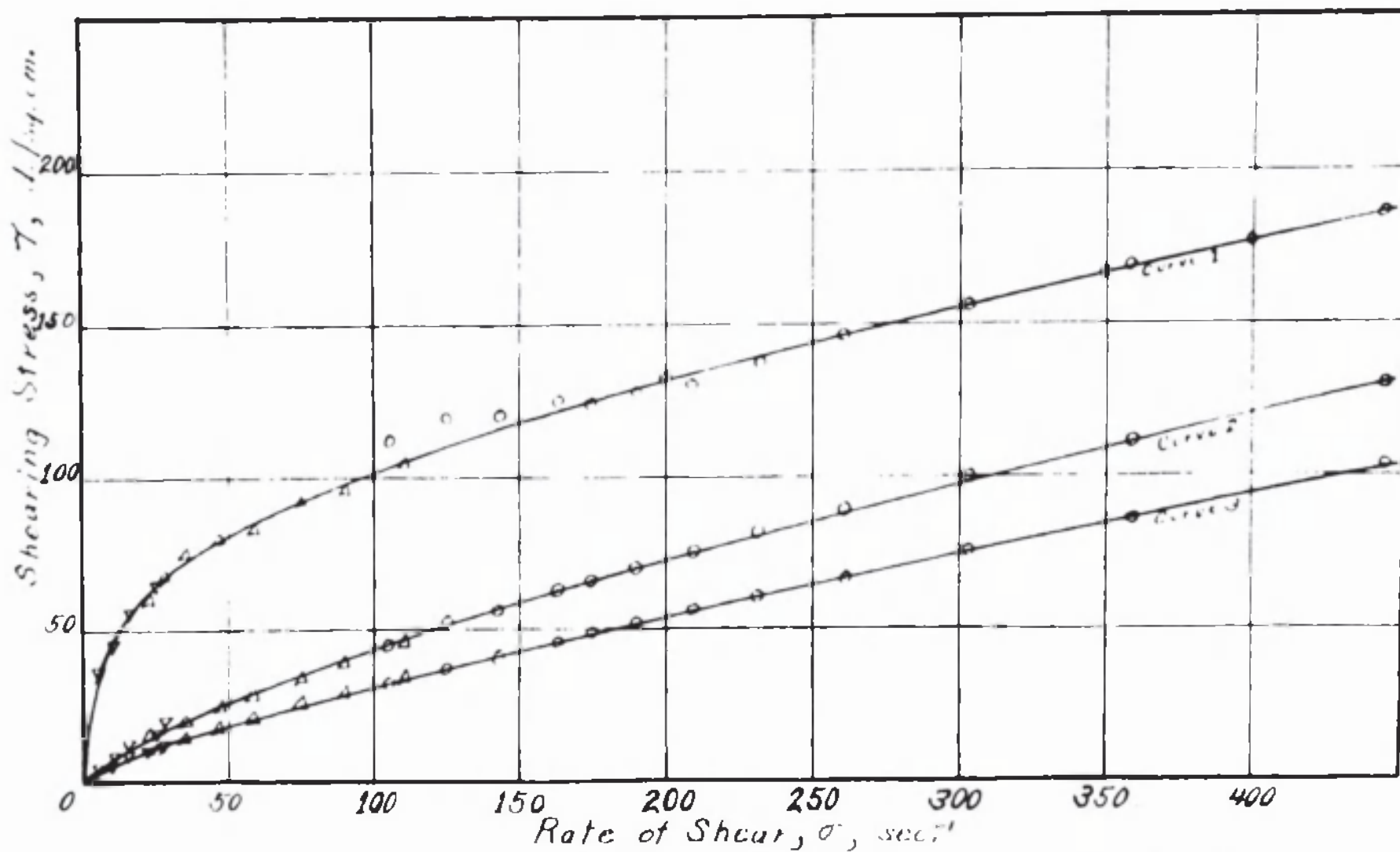
Figure 16 d. Series I Tests. Rheological Diagram for the
6 % Suspension.
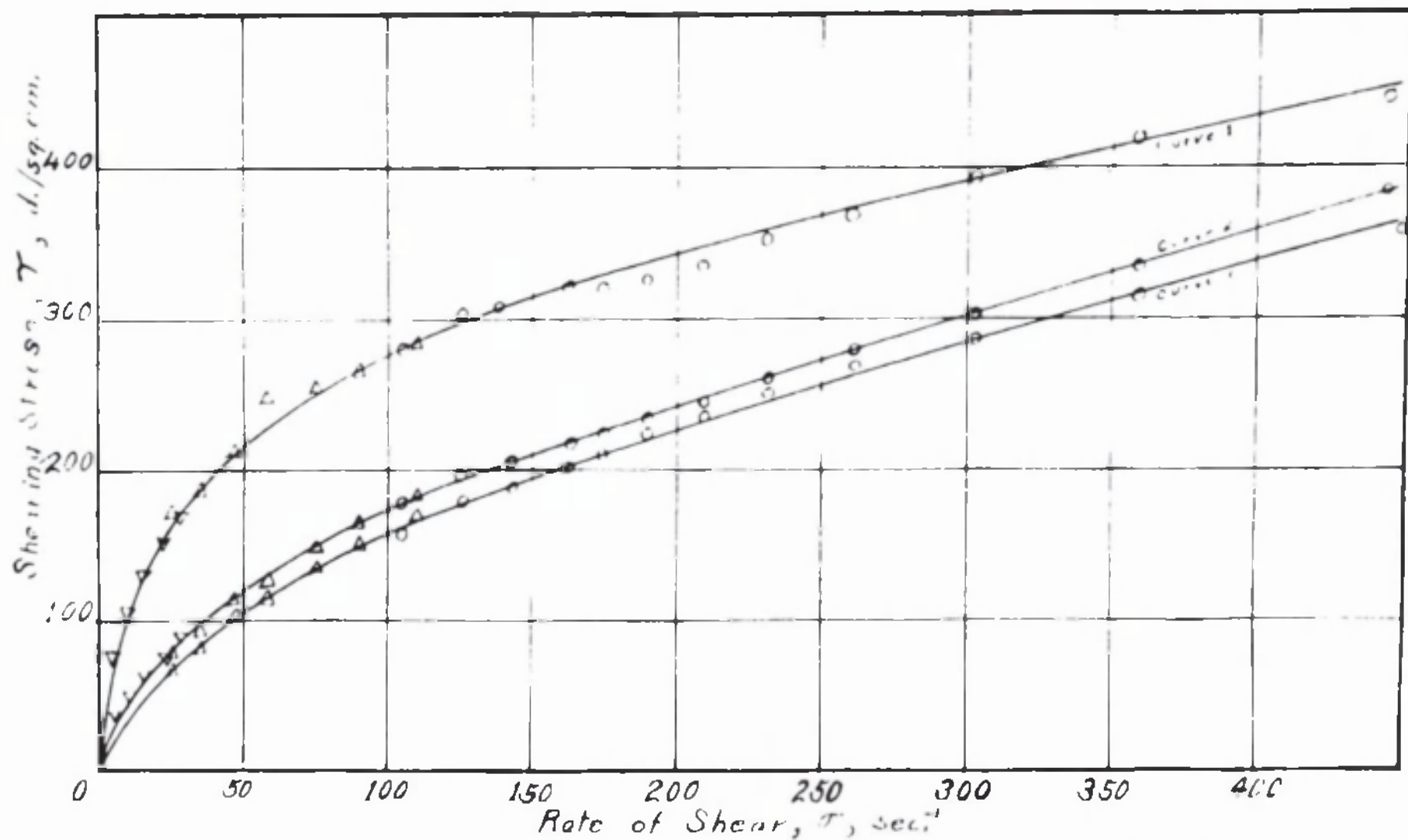
Figure 16e. Series I Tests. Rheological Diagram for the 8% Suspension.

to suppress the occurrence of turbulence. The slope of
the straight line indicates a viscosity coefficient of 2.4
cp. The material in this case had been given a small amount
of agitation in the bottle before the test in the same man-
ner as the 1% suspension. However, when the material was
given 100 strokes in the structure breaker, a slight lower-
ing of the viscosity was noted, which was insufficient to
allow plotting without undue enlargement of the shearing
stress scale used in Figure 16b.

The data obtained for the shearing stress-rate of shear
observations on the 4% sol are recorded in Table 12. The
rheological diagram of these data is shown by Figure 16c
which indicates that the concentration of bentonite is suf-
ficient to cause the effects of "structural viscosity" to be
quite noticeable. Four curves are shown in Figure 16c each
one representing different degrees of mechanical working be-
fore testing in the viscometer. Curves 1 and 1a were ob-
tained by the same procedure that was used for the previous
suspensions, that is, the bottle containing the sample was
inverted sufficiently to mix its contents and eliminate any
settling and segregation that may have taken place. The ma-
terial had been standing quiescent in the bottle for approxi-
mately 24 hours before the test was started. Apparently, the
gentle mixing was a little more vigorous with curve 1a than
with curve 1 since the two curves do not coincide. Curves
2 and 3 represent the same material as curves 1 and 1a, but
were given 20 and 200 strokes respectively in the structure

breaker before placing in the testing cup. The apparent
viscosity as represented by the quotient of the total shear-
ing stress by the total rate of shear was taken for each
curve at the abscissa of 300 sec.$^{-1}$ and recorded in Table 15.
For comparison, the differential viscosity as represented
by the slope of the curve at the abscissa of 300 sec.$^{-1}$ was
determined also and recorded in Table 15. The significance
of the comparison between the apparent viscosity and the
differential viscosity will be discussed below.

Figure 16d shows the rheological diagram obtained by
plotting the results with the 6% suspension, which is re-
corded in Table 13. Curve 1 represents the condition after
the mild mechanical disturbance of mixing by inverting the
container several times. Curve 2 represents the condition
after the material has been given 50 strokes in the structure
breaker. Curve 3 is of special interest because it is plot-
ted from data taken in two tests, one after 100 strokes in
the structure breaker has been applied, the other after 200
strokes. Since the data all plot on the same line, it is
evident that for this suspension and the previous ones, 100
strokes in the structure breaker is sufficient to render
the material into the state of maximum fluidity. As before,
the apparent and differential viscosity was determined for
each curve at the rate of shear of 300 sec.$^{-1}$. These data are
also given in Table 15.

In the case of the 8% suspension, the concentration of
the bentonite is sufficient to cause the system to gel in

approximately 24 hours upon quiescent standing. In order to obtain uniform results the gelled material was given 10 strokes in the structure breaker instead of the usual mixing by inverting the container several times. Determinations were also made upon the material after it had been given 100, 200, and 300 strokes in the structure breaker. The data thus obtained appears in Table 14 and is plotted in the customary manner in Figure 16e. As before, the apparent and differential viscosities have been determined at the rate of shear of 300 sec.$^{-1}$ and are recorded in Table 15.

## Table 15

### Comparison of Apparent Viscosity with Differential Viscosity taken at a Rate of Shear of 300 sec.

### In Centipoises.

| Suspension | 4% | | 6% | | 8% | |
|---|---|---|---|---|---|---|
| | Apparent | Differential | Apparent | Differential | Apparent | Differential |
| Curve 1 | 15.7[a] | 9.23 | 52.3[d] | 22.0 | 131[b] | 45 |
| 2 | 14.1[a] | 9.98 | 32.6[d] | 24.0 | 101[e] | 58 |
| 3 | 10.2[c] | 8.85 | 25.0[e,f] | 19.5 | 95[f] | 55 |
| 4 | 7.6[f] | 6.83 | | | 85[g] | 55 |
| Average | | 9.35* | | 21.8 | | 53 |

* Omitting curve 4.
a. Suspension mixed by several inversions.
b. 10 strokes in structure breaker.
c. 20 strokes in structure breaker.
d. 50 strokes in structure breaker.
e. 100 strokes in the structure breaker.
f. 200 strokes in the structure breaker.
g. 300 strokes in the structure breaker.

Table 15 gives a summary of the apparent and differential viscosity measured at the rate of shear of 300 sec$^{-1}$. for the 2, 4, and 6% suspensions after different amounts of mechanical

treatment in the structure breaker. In general the amount
of agitation or structure breaking increases from top to
bottom of the table. It is seen that the apparent viscosity
suffers considerable decrease with increasing amount of me-
chanical stirring before the test, whereas the differential
viscosity remained relatively constant. This would seem to
indicate that the effects of structure between the particles
has its greatest influence when the rate of shear is small.
When the rate of shear is large as in the upper ranges of
the curves of Figures 16a, b, c, d, e, the presence of struc-
ture has little influence upon the coefficient of viscosity
as represented by the differential or instantaneous ratio of
shearing stress to rate of shear, but on the other hand causes
the material to transmit a relative large shearing stress.
This is further substantiated by the distinct tendency of
the curves to become parallel. It is dangerous, however,
to attempt to read from the rheological diagrams of the Series
I tests more concerning the internal structure than they can
give, because of the original arbitrary technique of experi-
mental procedure. It does seem indicated, however, that the
effects of coagulation tend to lift the whole curve upwards
on the shearing stress axis. It is shown in the Series II and
III tests below that this condition is transitory since the
rate of shear seems to replace the destructive action of the
structure breaker. However, the results are of interest when
one considers the analogous condition when such a suspension
is subjected to a short period of shearing by being pumped

through a relatively short pipe line, a case that is
frequently found in industrial operations.

### Turbulence.

The test using water to represent a suspension of zero concentration is of special significance. The data given in Table 16 was obtained using the same procedure as for the calibration oils. These data have been plotted in the rheological diagram shown by Figure 17. It is interesting to note that at the lower rates of shear and the speed of 80 r.p.m., the curve passes through a minimum. This occurs only at the speed of 80 r.p.m. and large separations. The minimum was also observed in a similar experiment using methly alcohol.

It is concluded that the hooked portion of the curve obtained at the higher speed of 80 r.p.m. is caused by turbulence replacing concentric flow. This is in accordance with the formula given by Hatschek[15] to calculate the Reynolds number for uniform concentric cylinders,

$$Re = \frac{\sigma d^2 \rho}{z} \tag{36}$$

where   $Re$ = Reynold's number.

$d$ = distance between concentric surfaces, cm.

$\rho$ = density of material, gm. per cc.

$z$ = coefficient of viscosity, poises.

Goodeve[13] indicates that the value of Reynold's number must exceed about 1900 before turbulence sets in but does

---

[15] E. Hatschek. op. cit. p. 50
[13] C. F Goodeve. J. Sci. Inst. 16:19(1939)
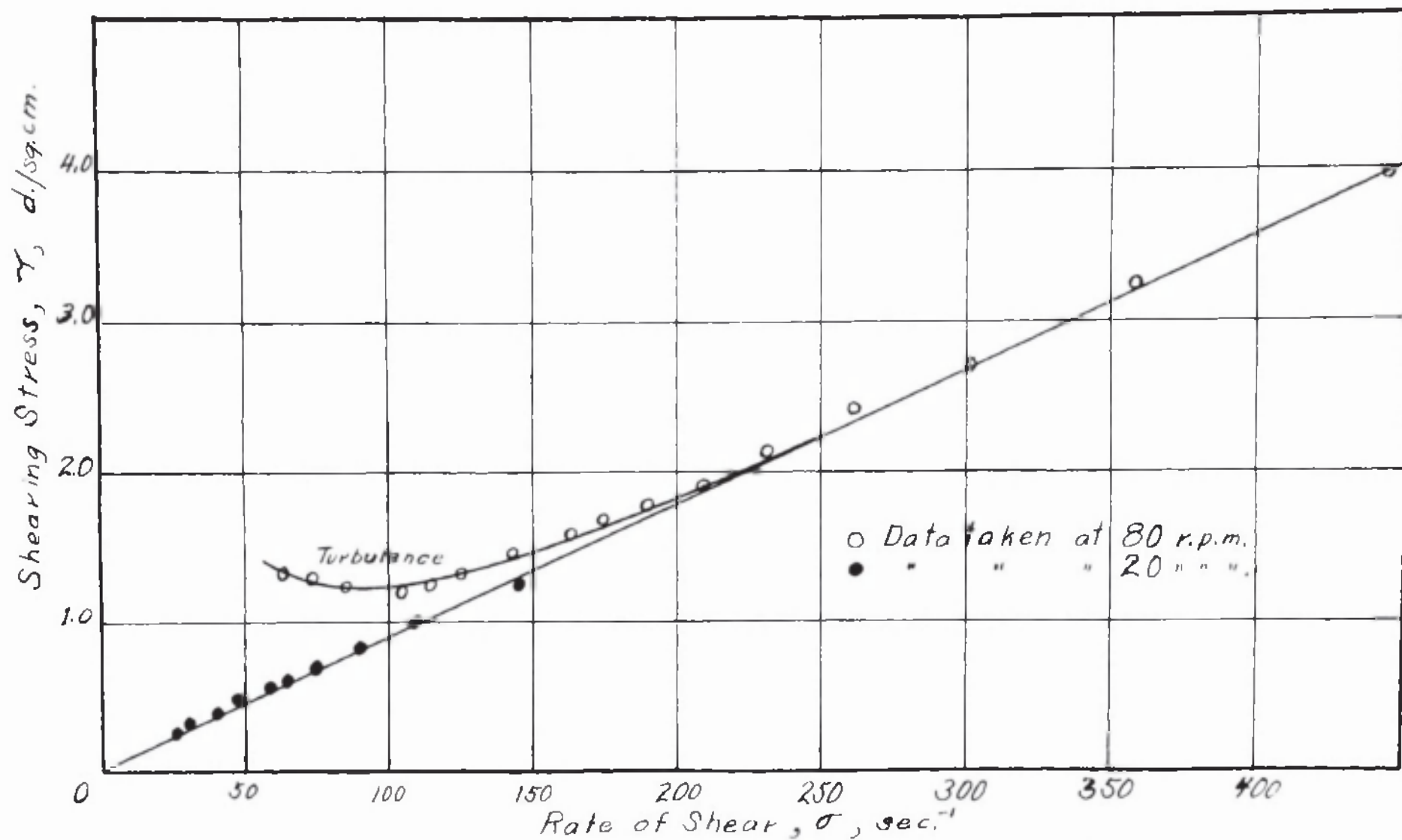
Figure 17. Series I Tests. Rheological Diagram for Water.

Table 16.

Series I tests. Rate of Shear – Shearing Stress Data.
Water (0% Bentonite Suspension)

| | | Wire MO |
| --- | --- | --- |
| Speed of Rotation r. p. m. | Rate of Shear sec.$^{-1}$ | Shearing Stress dynes/sq.cm. |
| 80.0 | 62.8 | 1.33 |
| | 73.4 | 1.30 |
| | 85.6 | 1.23 |
| | 105.1 | 1.20 |
| | 114.6 | 1.25 |
| | 126.3 | 1.33 |
| | 142.7 | 1.46 |
| | 162.9 | 1.59 |
| | 174.3 | 1.69 |
| | 190.6 | 1.79 |
| | 209 | 1.92 |
| | 232 | 2.15 |
| | 262 | 2.43 |
| | 302 | 2.71 |
| | 359 | 3.25 |
| | 444 | 3.96 |
| | 584 | 5.02 |
| | 867 | 7.15 |
| 20.0 | 26.0 | 0.25 |
| | 31.3 | 0.31 |
| | 40.4 | 0.38 |
| | 47.2 | 0.48 |
| | 57.8 | 0.56 |
| | 65.3 | 0.61 |
| | 75.4 | 0.69 |
| | 89.5 | 0.82 |
| | 110. | 1.00 |
| | 146 | 1.25 |
| | 216 | 1.79 |

not give any experimental evidence. This is the lower
figure customarily quoted for low in smooth pipes and it
does not necessarily apply to other systems. Table 17 shows
in the last column, the values of Reynold's number calculated
for some of the points of the curve of Figure 17. It is seen
that the value of Reynold's number decreases as the value of
the rate of shear increases, and the value of the separation
d, decreases. Estimating from Figure 17 that linearity ceases
at about the point where the rate of shear is 126.3 sec.$^{-1}$
(at 80 r.p.m.) the corresponding value of Reynold's number
is 360. This is considerably less than 1900. Barr[16] gives
a discussion concerning the occurrence of turbulence in con-
centric cylinder viscometers, from which it appears that
accuracy and rigidity of construction are important factors
in determining the onset of turbulent flow. According to the
work of Taylor[17] some doubt appears to exist that the values
of 1900 to 2100 can be used as a criterion, since he obtained
complete stability at values up to about 12,500. However, it
appears as a result of the experiments with water and methyl
alcohol, turbulence in the Goodeve instrument occurs at a
Reynold's-number value of about 350-450.

In the section on the calibration of the instrument, it
was pointed out that the practical upper limit of separation

---

[16]Guy Barr, op. cit. pp. 223-5
[17]Taylor, Phil. Trans. 223A, 289 (1922)

Table 17

Values of Reynolds Numbers

Calculated By: $Re = \dfrac{\sigma d^2 \rho}{\eta}$

| Material | Speed r.p.m. | $\sigma$ sec$^{-1}$ | $d$ cm. | $\eta$ poise | $\rho$ gms/cm | Re |
|---|---|---|---|---|---|---|
| Water | 80 | 62.8 | 0.40 | 0.00894 | 0.997 | 1135 |
| | 80 | 105.1 | 0.20 | 0.00894 | 0.997 | 470 |
| | 80 | 126.2 | 0.16 | 0.00894 | 0.997 | 360 |
| | 80 | 190 | 0.10 | 0.00894 | 0.997 | 212 |
| | 80 | 444 | 0.04 | 0.00894 | 0.997 | 79 |
| | 80 | 860 | 0.02 | 0.00894 | 0.997 | 39 |
| | 20 | 65.3 | 0.07 | 0.00894 | 0.997 | 36 |
| | 20 | 110.0 | 0.04 | 0.00894 | 0.997 | 20 |
| Me OH | 80 | 126.3 | 0.16 | 0.0055 | 0.79 | 454 |

was about 0.40 cm. and that 80 r.p.m. represented about
the fastest convenient speed of rotation that could be used
without appreciable centrifugal forces acting on the sample.
These are the extreme conditions under which a viscosity of
2.5 centipoises and unit density would be necessary to give
a Reynold's number of 400.  It was concluded that as long
as the measurements were made under conditions yielding a
Reynold's number less than 400 smooth concentric flow would
exist between the walls.

## Slip at the Walls.

Many investigators have given attention to the possibility of slip at the wall. The fundamental shearing arrangement which forms the basis of the viscosity concept of a necessity assumes its absence. Mooney[18] has developed a method which will demonstrate the absence or presence of slip at the walls. In general, his approach is to make several observations on the material with different combinations of radii and speeds of rotation so that the shearing stress is always the same. If slipping is absent, it will be found that the rates of shears necessary to generate the constant stress will be the same. Conversely, a constant rate of shear generated by different separations and speeds of rotation will give a constant shearing stress only if slipping is absent.

The absence of slip in the measurements taken with the bentonite sols has been many times demonstrated by the continuous lines obtained when the speed of rotation of the cup was changed. Figure 16e can be used as typical of all. At the rate of shear of 27.6 the separation between the cone and cup was as small as safely usable. In order to obtain higher rates of shear, the speed of rotation of the outer cups had to be raised from 5 r.p.m. to 20 r.p.m. At the same time,

---

[18]M. Mooney, J. Rheol. 2:210 (1931)

the inner cone was lifted to a separation that gave a rate
of shear of 26.0 sec.$^{-1}$ Lowering the inner cone at the 20
r.p.m. rotation speed gave successive rates of shear up to
110.6 sec.$^{-1}$ at which point the separation was again too small
to permit further observations. As before, the speed was in-
creased this time to 80 r.p.m. and the inner cone concomitantly
was raised to a separation giving a rate of shear of 105.1 sec.$^{-1}$
From this point, lowering the inner cone gives rates of shear
to 444 sec.$^{-1}$ at the upper limit. As is shown by Figure 16e
and the others, the shearing stresses observed in the regions
around 25 and 105 sec.$^{-1}$, where the speed overlap occurs, are
quite consistent with the smooth curve drawn through all the
points. Had slip been present the curves would have been dis-
continuous at the overlap points with those representing
higher rotation speeds being shifted below the preceding one,
it being reasonable to expect that a lowering of shearing
stress would be obtained when slipping is occurring. There-
fore it is concluded that slip is absent in the shearing
process which was applied to the bentonite sols by means of
the Goodeve apparatus. This is consistent with the results
found by Ambrose and Loomis[19] on bentonite sols using a
modified MacMichael viscometer in which two sets of radii
were used to show the absence of the slipping at the walls.

---

[19] H. A. Ambrose and A. G. Loomis. Physics 4:265-73 (1933)

CHAPTER VII

EFFECT OF CONSTANT SHEARING

In the preceding Chapter VI it has been pointed out that the sustained shearing process should result in attainment of an equilibrium between the structural forces and the shearing forces, provided a sufficient length of time is allowed. Since in the series I tests only 1 minute of sustained constant shearing was allowed before the rate of shear was increased to the next value it is possible that equilibrium conditions were not attained. In order to study the effect of continued shearing maintained constant for greater lengths of time, the following experiments were conducted.

### 1. Experimental Part, Series II Tests.

In these experiments, the tests were divided into two groups, one in which the sols had been allowed to stand quiescent in the viscometer cup for 18 hours before the shearing action was started; the other group in which no setting period was allowed. In both cases the effect of previous history was removed by the treatment in the structure breaker before the tests were commenced, thus affording a common starting point from which time could be measured. Two hundred strokes in the structure breaker were deemed sufficient to accomplish this reduction to a common starting point.

The procedure for a series of time-deflection observations

at a constant rate of shear was as follows:  The preliminary
adjustments of the instrument were made in the usual way for
the torsion wire selected as best suited for the particular
sample to be tested.  The micrometer screw on the head assembly
was set to give the desired rate of shear in combination with
the speed of rotation as determined from table 6.  Before the
sample was introduced the zero reading on the deflection drum
was noted, then the entire head assembly was placed in the
raised position thus lifting the inner cone out of the sample
cup.  The temperature of the water bath was checked and in the
case of the 18-hour tests, the thermostat was used to insure
a constant temperature over night.  When the apparatus was
in readiness, the sample was given the required number of
strokes in the structure breaker and immediately transferred
to the viscometer cup.  For the tests of the zero hours stand-
ing period, the inner cone was swung into position and the
excess material removed from the cup as quickly as possible
after the cessation of the treatment in the structure breaker.
As soon as possible thereafter, the motor was started while
the scale deflection was watched through the telescope.  A
stop-watch was started the instant the deflection has risen
to the maximum value after starting the motor.  Scale deflec-
tion readings were then taken every minute for the first 10
minutes, thence every 5 minutes up to 30 minutes and in some
cases longer.  In the case of the tests for the 18-hour stand-
ing period series, the procedure was the same except that the
time for the start of the setting period was noted at the instant

the head assembly and inner cone were lowered into position.
In this case the excess suspension above the inner cone was
not removed but left in the cup until just before the motor
was started at the end of the setting period. The sample cup
was closed during the setting period with a rather closely
fitting bakelite cover to prevent excessive evaporation.
A few minutes before the end of the 18-hour setting period
the cover on the sample cup was lifted off and the excess
sample on the top of the inner cone was removed by means of
the suction flask, extreme care being taken during these opera-
tions not to touch or disturb in any way the inner cone. Ex-
actly at the end of the 18-hour setting period the motor was
started and the stop-watch started as before when the deflec-
tion had risen to the maximum value. The maximum value of the
deflection was estimated as closely as possible for the read-
ing corresponding to zero time in the time-deflection readings.
This procedure was repeated for several different values of
rate of shear on the 2, 4, 6, and 8 per cent suspensions. The
data thus obtained are recorded in Table 18 for the zero-hour
setting period and in Table 19 for the 18-hour setting period.
The deflections of the inner cone were converted to shearing
stress by multiplying with the constant of the torsion wire.
The values of the shearing stress and time for the zero hour
setting period tests given in Table 18 have been plotted at
the various constant rates of shear in Figures 18, 19, 20 and
21 for the 2, 4, 6, and 8 per cent suspensions, respectively.
It is seen from these figures that the shearing stress is

Table 18

Series II Tests.   Time-Deflection Studies at Constant Rate
of Shear.
Zero Hour Setting Period
2% Bentonite Suspension.

Temperature 25°         Wire MO

| Time Minutes | σ = 10 δ | τ | σ = 51.9 δ | τ | σ = 105.1 δ | τ | σ = 142.7 δ | τ | σ = 190 δ | τ |
|---|---|---|---|---|---|---|---|---|---|---|
| 0 | 0.9 | 0.23 | 4.4 | 1.13 | 10.0 | 2.56 | 12.8 | 3.28 | 17.2 | 4.40 |
| 1 | 1.0 | 0.25 | 4.6 | 1.18 | 10.0 | 2.56 | 12.9 | 3.30 | 17.4 | 4.46 |
| 2 | 1.0 | 0.25 | 4.6 | 1.18 | 10.0 | 2.56 | 12.8 | 3.28 | 17.4 | 4.46 |
| 3 | 1.0 | 0.26 | 4.6 | 1.18 | 10.1 | 2.59 | 12.9 | 3.30 | 17.5 | 4.48 |
| 4 | 1.0 | 0.26 | 4.6 | 1.18 | 10.0 | 2.56 | 12.9 | 3.30 | 17.4 | 4.46 |
| 5 | 1.0 | 0.26 | 4.6 | 1.18 | 10.1 | 2.59 | 12.8 | 3.28 | 17.4 | 4.46 |
| 6 | 1.0 | 0.26 | 4.6 | 1.18 | 10.2 | 2.61 | 12.9 | 3.30 | 17.4 | 4.46 |
| 7 | 1.0 | 0.26 | 4.6 | 1.18 | 10.1 | 2.59 | 12.9 | 3.30 | 17.4 | 4.46 |
| 8 | 1.0 | 0.26 | 4.6 | 1.18 | 10.1 | 2.59 | 12.9 | 3.30 | 17.4 | 4.46 |
| 9 | 1.0 | 0.26 | 4.6 | 1.18 | 10.0 | 2.56 | 12.9 | 3.30 | 17.4 | 4.46 |
| 10 | 1.0 | 0.26 | 4.6 | 1.18 | 10.1 | 2.59 | 12.9 | 3.30 | 17.4 | 4.46 |
| 15 | 1.0 | 0.26 | 4.6 | 1.18 | 10.2 | 2.61 | 12.8 | 3.28 | 17.3 | 4.43 |
| 20 | 1.0 | 0.26 | 4.6 | 1.18 | 10.4 | 2.66 | 13.0 | 3.33 | 17.3 | 4.43 |
| 25 | 1.0 | 0.26 | 4.6 | 1.18 | 10.3 | 2.64 | 13.0 | 3.33 | 17.3 | 4.43 |
| 30 | 1.0 | 0.26 | 4.6 | 1.18 | 10.4 | 2.66 | 13.0 | 3.33 | 17.4 | 4.46 |
| 35 | 1.0 | 0.26 | 4.6 | 1.18 | | | | | | |

| Time Minutes | σ = 222 δ | τ | σ = 303 δ | τ | σ = 359 δ | τ | σ = 444 δ | τ |
|---|---|---|---|---|---|---|---|---|
| 0 | 20.9 | 5.35 | 26.2 | 6.71 | 30.8 | 7.88 | 35.7 | 9.14 |
| 1 | 20.9 | 5.35 | 26.2 | 6.71 | 30.5 | 7.81 | 35.7 | 9.14 |
| 2 | 21.0 | 5.38 | 26.2 | 6.71 | 30.4 | 7.78 | 35.9 | 9.20 |
| 3 | 21.0 | 5.38 | 26.1 | 6.68 | 30.4 | 7.78 | 35.6 | 9.12 |
| 4 | 21.0 | 5.38 | 25.8 | 6.61 | | | 36.2 | 9.28 |
| 5 | 21.0 | 5.38 | 26.1 | 6.68 | 30.5 | 7.81 | 36.3 | 9.30 |
| 6 | 21.0 | 5.38 | 26.1 | 6.68 | 30.6 | 7.83 | 36.3 | 9.30 |
| 7 | 21.0 | 5.38 | 26.1 | 6.68 | 30.5 | 7.81 | 36.2 | 9.28 |
| 8 | 21.0 | 5.38 | 26.2 | 6.71 | 30.4 | 7.78 | 36.3 | 9.30 |
| 9 | 21.0 | 5.38 | 26.2 | 6.71 | 30.4 | 7.78 | 36.6 | 9.37 |
| 10 | 21.0 | 5.38 | 26.1 | 6.68 | 30.5 | 7.81 | 36.7 | 9.40 |
| 15 | 21.0 | 5.38 | 26.1 | 6.68 | 30.7 | 7.86 | 36.7 | 9.40 |
| 20 | 21.0 | 5.38 | 25.7 | 6.58 | 30.7 | 7.86 | 36.9 | 9.45 |
| 25 | 21.0 | 5.38 | 25.1 | 6.32 | 31.0 | 7.94 | 36.9 | 9.45 |
| 30 | 21.0 | 5.38 | 25.4 | 6.51 | 31.2 | 7.99 | 37.0 | 9.47 |
| 35 | 21.0 | 5.38 | | | | | | |

## Table 18 Continued.

Zero Hour Setting Period.
4% Bentonite Suspension.

| Time | σ = 10 | | σ = 51.9 | | σ = 105.1 | | σ = 142.7 | | σ = 190 | Wire NO |
|---|---|---|---|---|---|---|---|---|---|---|
| Minutes | δ | γ | δ | γ | δ | γ | δ | γ | δ | γ |
| 0 | 3.6 | 0.92 | 17.4 | 4.46 | 33.0 | 8.45 | 43.8 | 11.22 | 52.0 | 13.32 |
| 1 | 3.6 | 0.92 | 17.7 | 4.53 | 33.2 | 8.50 | 44.1 | 11.29 | 52.1 | 13.33 |
| 2 | 3.6 | 0.92 | 17.7 | 4.53 | 33.2 | 8.50 | 44.1 | 11.29 | 52.6 | 13.46 |
| 3 | 3.7 | 0.95 | 17.8 | 4.61 | 33.4 | 8.56 | 44.2 | 11.32 | 52.8 | 13.52 |
| 4 | 3.7 | 0.95 | 17.9 | 4.58 | 33.5 | 8.58 | 44.3 | 11.34 | 53.0 | 13.57 |
| 5 | 3.8 | 0.97 | 17.9 | 4.58 | 33.5 | 8.58 | 44.3 | 11.34 | 53.2 | 13.63 |
| 6 | 3.8 | 0.97 | 17.9 | 4.58 | 33.7 | 8.63 | 44.4 | 11.38 | 53.3 | 13.65 |
| 7 | 3.8 | 0.97 | 17.9 | 4.58 | 33.7 | 8.63 | 44.5 | 11.39 | 53.4 | 13.68 |
| 8 | 3.8 | 0.97 | 18.0 | 4.61 | 33.7 | 8.63 | 44.5 | 11.39 | 53.5 | 13.70 |
| 9 | 3.8 | 0.97 | 18.2 | 4.66 | 33.7 | 8.63 | 44.6 | 11.41 | 53.7 | 13.73 |
| 10 | 3.8 | 0.97 | 18.2 | 4.66 | 33.7 | 8.63 | 44.7 | 11.43 | 53.5 | 13.70 |
| 15 | 3.9 | 1.00 | 18.3 | 4.68 | 34.2 | 8.76 | 44.8 | 11.47 | 54.1 | 13.84 |
| 20 | 4.0 | 1.02 | 18.4 | 4.71 | 34.3 | 8.78 | 45.1 | 11.53 | 54.3 | 13.90 |
| 25 | 4.1 | 1.05 | 18.5 | 4.73 | 34.7 | 8.89 | 45.1 | 11.53 | 54.5 | 13.96 |
| 30 | 4.1 | 1.05 | 18.4 | 4.71 | 34.8 | 8.91 | 45.2 | 11.57 | 54.7 | 14.00 |

| Time | σ = 225 | | σ = 303 | | σ = 359 | | σ = 444 | |
|---|---|---|---|---|---|---|---|---|
| Minutes | δ | γ | δ | γ | δ | γ | δ | γ |
| 0 | 61.5 | 15.75 | 83.8 | 21.4 | 100.4 | 25.7 | 110.6 | 28.3 |
| 1 | 61.6 | 15.77 | 83.6 | 21.4 | 100.6 | 25.7 | 108.4 | 27.8 |
| 2 | 61.6 | 15.77 | 83.5 | 21.4 | 100.9 | 25.8 | 107.8 | 27.6 |
| 3 | 61.7 | 15.80 | 83.4 | 21.4 | 101.0 | 25.9 | 107.6 | 27.6 |
| 4 | 61.6 | 15.77 | 83.4 | 21.4 | 101.5 | 26.0 | 107.6 | 27.6 |
| 5 | 61.6 | 15.77 | 83.6 | 21.4 | 101.5 | 26.0 | 108.3 | 27.7 |
| 6 | 61.6 | 15.77 | 83.6 | 21.4 | 101.7 | 26.0 | 108.5 | 27.8 |
| 7 | 61.7 | 15.80 | 83.8 | 21.4 | | | 108.7 | 27.8 |
| 8 | 61.7 | 15.80 | 83.8 | 21.4 | 102.0 | 26.1 | 108.7 | 27.9 |
| 9 | 61.8 | 15.83 | 83.9 | 21.5 | 102.2 | 26.2 | 109.3 | 28.0 |
| 10 | 61.9 | 15.86 | 84.0 | 21.5 | 102.5 | 26.2 | 109.6 | 28.1 |
| 15 | 62.5 | 16.00 | 84.0 | 21.5 | 102.8 | 26.3 | 110.9 | 28.4 |
| 20 | 62.8 | 16.10 | 85.1 | 21.8 | 103.4 | 26.4 | 112.5 | 28.8 |
| 25 | 63.3 | 16.20 | 85.3 | 21.8 | 103.7 | 26.5 | 113.6 | 29.0 |
| 30 | 63.6 | 16.29 | 86.0 | 22.0 | 104.3 | 26.7 | 114.8 | 29.4 |

## Table 18 Continued

Zero Hour Setting Period
6% Bentonite Suspension.

Temperature 25°    Wire #1

| Time Minutes | $\sigma=10$ δ | γ | $\sigma=51.9$ δ | γ | $\sigma=105.1$ δ | γ | $\sigma=142.7$ δ | γ | $\sigma=190$ δ | γ |
|---|---|---|---|---|---|---|---|---|---|---|
| 0 | 4.0 | 4.95 | 16.4 | 20.3 | 27.7 | 34.3 | 38.8 | 48.0 | 44.2 | 54.7 |
| 1 | 4.8 | 5.93 | 16.5 | 20.4 | 27.2 | 33.6 | 38.5 | 47.6 | 44.1 | 54.5 |
| 2 | 4.8 | 5.93 | 16.6 | 20.5 | 27.3 | 33.6 | 38.5 | 47.6 | 44.1 | 54.5 |
| 3 | 4.8 | 5.93 | 16.9 | 20.9 | 27.2 | 33.6 | 38.4 | 47.5 | 44.2 | 54.7 |
| 4 | 4.9 | 6.06 | 17.0 | 21.0 | 27.6 | 34.1 | 38.4 | 47.5 | 44.2 | 54.7 |
| 5 | 5.0 | 6.18 | 17.1 | 21.1 | 27.4 | 33.9 | 38.5 | 47.6 | 44.7 | 55.2 |
| 6 | 5.0 | 6.18 | 17.2 | 21.2 | 27.5 | 34.0 | 38.5 | 47.6 | 44.6 | 55.1 |
| 7 | 5.0 | 6.18 | 17.4 | 21.5 | 27.5 | 34.0 | 38.5 | 47.6 | 44.8 | 55.4 |
| 8 | 5.0 | 6.18 | 17.4 | 21.5 | 27.7 | 34.3 | 38.5 | 47.6 | 44.8 | 55.4 |
| 9 | 5.1 | 6.30 | 17.4 | 21.5 | 27.7 | 34.3 | 38.3 | 47.4 | 44.8 | 55.4 |
| 10 | 5.2 | 6.43 | 17.5 | 21.6 | 27.8 | 34.4 | 38.4 | 47.5 | 44.7 | 55.3 |
| 15 | 5.1 | 6.30 | 17.7 | 21.9 | 27.9 | 34.5 | 38.4 | 47.5 | 45.0 | 55.6 |
| 20 | 5.5 | 6.80 | 17.8 | 22.0 | 28.0 | 34.7 | 38.4 | 47.5 | 45.1 | 55.7 |
| 25 | 5.5 | 6.80 | 17.8 | 22.0 | 28.1 | 34.8 | 38.4 | 47.5 | 45.2 | 55.8 |
| 30 | 5.6 | 6.92 | 17.8 | 22.0 | 28.1 | 34.8 | 38.4 | 47.5 | 45.5 | 56.2 |
| 35 | 5.6 | 6.92 | | | | | | | | |
| 40 | 5.7 | 7.05 | | | | | | | | |

| Time Minutes | $\sigma=232$ δ | γ | $\sigma=303$ δ | γ | $\sigma=359$ δ | γ | $\sigma=444$ δ | γ |
|---|---|---|---|---|---|---|---|---|
| 0 | 50.8 | 62.8 | 63.5 | 78.5 | 73.3 | 90.0 | 89.3 | 110.4 |
| 1 | 50.4 | 62.5 | 62.0 | 76.6 | 71.4 | 88.3 | 87.1 | 107.8 |
| 2 | 50.5 | 62.4 | 61.6 | 76.2 | 71.0 | 87.8 | 87.0 | 107.6 |
| 3 | 50.7 | 62.6 | 61.7 | 76.3 | 70.7 | 87.4 | 86.5 | 106.9 |
| 4 | 50.5 | 62.4 | 61.7 | 76.3 | 70.8 | 87.5 | 86.3 | 106.7 |
| 5 | 50.5 | 62.4 | 61.6 | 76.2 | 70.7 | 87.4 | 86.2 | 106.5 |
| 6 | 50.6 | 62.5 | 61.7 | 76.3 | 70.6 | 87.2 | 85.9 | 106.2 |
| 7 | 50.5 | 62.4 | 61.5 | 76.0 | 70.6 | 87.2 | 85.7 | 105.8 |
| 8 | 50.5 | 62.4 | 61.4 | 75.9 | 70.6 | 87.2 | 85.4 | 105.6 |
| 9 | 5005 | 62.4 | 61.4 | 75.9 | 70.7 | 87.4 | 85.3 | 105.4 |
| 10 | 50.6 | 62.5 | 61.4 | 75.9 | 70.6 | 87.2 | 85.2 | 105.3 |
| 15 | 50.6 | 62.5 | 61.2 | 75.7 | 70.3 | 87.0 | 84.2 | 104.0 |
| 20 | 50.2 | 62.1 | 61.1 | 75.6 | 70.2 | 86.8 | 83.0 | 103.0 |
| 25 | 49.9 | 61.7 | 61.0 | 75.4 | 70.2 | 86.8 | 82.9 | 102.5 |
| 30 | 50.0 | 61.8 | 61.0 | 75.4 | 69.8 | 86.3 | 82.2 | 101.6 |

## Table 18 Continued.

### Zero Hour Setting Period.
### 8% Bentonite Suspension.

Temperature 25°                                             Wire 17

| Time Minutes | $\sigma=10$ $\delta$ | $r$ | $\sigma=26$ $\delta$ | $r$ | $\sigma=52$ $\delta$ | $r$ | $\sigma=105.1$ $\delta$ | $r$ |
|---|---|---|---|---|---|---|---|---|
| 0 | 14.6 | 60.0 | 19.3 | 79.2 | 23.8 | 97.6 | 40.5 | 166 |
| 1 | 9.6 | 39.4 | 18.4 | 75.4 | 21.6 | 88.7 | 35.8 | 147 |
| 2 | 9.6 | 39.4 | 18.5 | 76.8 | 21.6 | 88.7 | 35.8 | 147 |
| 3 | 9.7 | 39.8 | 18.8 | 77.0 | 21.8 | 89.4 | 35.9 | 147 |
| 4 | 9.7 | 39.8 | 19.0 | 77.9 | 21.8 | 89.4 | 36.1 | 148 |
| 5 | 9.8 | 40.3 | 19.1 | 78.3 | 21.8 | 89.4 | 36.2 | 148 |
| 6 | 9.8 | 40.3 | 19.2 | 78.7 | 21.8 | 89.4 | 36.2 | 148 |
| 7 | 9.8 | 40.3 | 19.3 | 79.2 | 21.9 | 89.8 | | |
| 8 | 9.9 | 40.6 | 19.4 | 79.5 | 22.0 | 90.1 | 36.2 | 148 |
| 9 | 9.9 | 40.6 | 19.4 | 79.5 | 22.1 | 90.6 | 36.3 | 149 |
| 10 | 9.9 | 40.7 | 19.5 | 80.0 | 22.0 | 90.1 | 36.3 | 149 |
| 15 | 10.0 | 41.1 | 19.6 | 80.3 | 22.4 | 91.8 | 36.5 | 150 |
| 20 | 10.1 | 41.4 | 19.6 | 80.3 | 22.5 | 92.3 | 36.5 | 150 |
| 25 | 10.1 | 41.4 | 19.6 | 80.3 | 22.6 | 92.6 | 36.6 | 150 |
| 30 | 10.2 | 41.8 | 19.7 | 80.9 | 22.9 | 94.1 | 36.7 | 151 |
| 35 | 10.3 | | | | | | 36.8 | |
| 40 | 10.4 | | | | | | | |

| Time Minutes | $\sigma=190$ $\delta$ | $r$ | $\sigma=303$ $\delta$ | $r$ | $\sigma=444$ $\delta$ | $r$ |
|---|---|---|---|---|---|---|
| 0 | 57.3 | 235 | 68.6 | 282 | 86.4 | 355 |
| 1 | 57.7 | 237 | 67.8 | 279 | 82.6 | 339 |
| 2 | 57.5 | 236 | 67.9 | 279 | 82.2 | 338 |
| 3 | 57.4 | 236 | 67.8 | 279 | 81.9 | 336 |
| 4 | 57.4 | 236 | 67.8 | 279 | 81.1 | 333 |
| 5 | 57.4 | 236 | 67.8 | 279 | 80.9 | 332 |
| 6 | 57.4 | 236 | 67.8 | 279 | 80.7 | 331 |
| 7 | 57.4 | 236 | 67.9 | 279 | 80.5 | 331 |
| 8 | 57.4 | 236 | 67.6 | 278 | 80.0 | 328 |
| 9 | 57.4 | 236 | 67.6 | 278 | 80.0 | 328 |
| 10 | 57.1 | 234 | 67.6 | 278 | 79.7 | 327 |
| 15 | 57.0 | 234 | 67.3 | 277 | 79.6 | 327 |
| 20 | 56.7 | 233 | 67.2 | 277 | | |
| 25 | 56.7 | 233 | 66.8 | 274 | 81.0 | 332 |
| 30 | 56.3 | 231 | 66.8 | 274 | 79.8 | 328 |
| 35 | 56.4 | | | | | |

## Table 19

Series II Tests.   Time Deflection Studies at Constant
Rate of Shear.
18 Hour Setting Period.
2% Bentonite Suspension

Temperature 25°                                                    Wire MO

| Time minutes | $\sigma = 10$ | | $\sigma = 105.1$ | | $\sigma = 190$ | | $\sigma = 303$ | | $\sigma = 444$ | |
|---|---|---|---|---|---|---|---|---|---|---|
| | $\delta$ | $\tau$ | $\delta$ | $\tau$ | $\delta$ | $\tau$ | $\delta$ | $\tau$ | $\delta$ | $\tau$ |
| 0 | 8.0 | 2.05 | 23.1 | 5.92 | 19.5 | 4.98 | 34.4 | 8.81 | 45.0 | 11.50 |
| ½ | 2.2 | 0.56 | 11.7 | 3.00 | 17.6 | 4.51 | 30.0 | 7.68 | 41.0 | 10.50 |
| 1 | 1.1 | 0.28 | 10.9 | 2.79 | 16.3 | 4.17 | 28.0 | 7.18 | 38.6 | 9.88 |
| 2 | 1.0 | 0.26 | 10.9 | 2.79 | 16.2 | 4.15 | 27.3 | 7.00 | 38.1 | 9.75 |
| 3 | 1.0 | 0.26 | 10.9 | 2.79 | 16.2 | 4.15 | 27.3 | 7.00 | 38.0 | 9.73 |
| 4 | 1.0 | 0.26 | 10.9 | 2.79 | 16.2 | 4.15 | 27.3 | 7.00 | 37.9 | 9.70 |
| 5 | 1.0 | 0.26 | 10.9 | 2.79 | 16.2 | 4.15 | 27.3 | 7.00 | 37.9 | 9.70 |
| 10 | 1.0 | 0.26 | 10.9 | 2.79 | 16.0 | 4.10 | 27.2 | 6.96 | 37.6 | 9.62 |
| 15 | 1.0 | 0.26 | 10.9 | 2.79 | 16.1 | 4.13 | 27.2 | 6.96 | 37.5 | 9.60 |
| 20 | 1.0 | 0.26 | 10.8 | 2.76 | 16.0 | 4.10 | 27.1 | 6.94 | 37.5 | 9.60 |
| 25 | 1.0 | 0.26 | 10.8 | 2.76 | 16.0 | 4.10 | 27.1 | 6.94 | 37.5 | 9.60 |
| 30 | 1.0 | 0.26 | 10.8 | 2.76 | 16.0 | 4.10 | 27.1 | 6.94 | 37.5 | 9.60 |

4% Bentonite Suspension.

Temperature 25°                                                    Wire MO

| Time minutes | $\sigma = 10$ | | $\sigma = 105.1$ | | $\sigma = 190$ | | $\sigma = 303$ | | $\sigma = 444$ | |
|---|---|---|---|---|---|---|---|---|---|---|
| | $\delta$ | $\tau$ | $\delta$ | $\tau$ | $\delta$ | $\tau$ | $\delta$ | $\tau$ | $\delta$ | $\tau$ |
| 0 | 8.6 | 2.2 | 54.1 | 13.9 | 79.1 | 20.3 | 100.9 | 25.8 | 153.4 | 39.3 |
| 1 | 7.6 | 1.95 | 48.8 | 12.5 | 70.9 | 18.1 | 94.1 | 24.1 | | |
| 2 | 7.4 | 1.90 | 47.4 | 12.2 | 69.1 | 17.7 | 93.2 | 23.8 | 128.9 | 33.0 |
| 3 | 7.2 | 1.84 | 46.8 | 12.0 | 68.3 | 17.5 | 91.7 | 23.5 | 127.9 | 32.7 |
| 4 | 7.2 | 1.84 | 46.4 | 11.9 | | | 90.9 | 23.3 | 127.5 | 32.6 |
| 5 | 7.0 | 1.80 | 45.9 | 11.7 | 68.0 | 17.4 | 90.7 | 23.2 | 127.4 | 32.6 |
| 6 | 6.9 | 1.77 | 45.5 | 11.6 | 68.0 | 17.4 | 90.5 | 23.2 | 127.2 | 32.6 |
| 7 | 6.9 | 1.77 | 45.3 | 11.6 | 68.0 | 17.4 | 90.3 | 23.1 | 126.6 | 32.4 |
| 8 | 6.9 | 1.77 | 45.2 | 11.6 | 68.1 | 17.4 | 90.1 | 23.1 | 126.5 | 32.4 |
| 9 | 6.9 | 1.77 | 44.9 | 11.5 | 68.2 | 17.5 | 90.2 | 23.1 | 126.1 | 32.3 |
| 10 | 6.9 | 1.77 | 44.7 | 11.4 | 68.3 | 17.5 | 90.0 | 23.1 | 126.1 | 32.3 |
| 15 | 6.8 | 1.74 | 44.2 | 11.3 | 67.1 | 17.2 | 90.6 | 23.2 | 126.8 | 32.5 |
| 20 | 6.6 | 1.69 | 43.9 | 11.2 | 66.9 | 17.1 | 91.0 | 23.3 | 127.5 | 32.7 |
| 25 | 6.5 | 1.67 | 43.2 | 11.1 | 66.9 | 17.1 | 91.5 | 23.4 | 127.7 | 32.7 |
| 30 | 6.5 | 1.67 | 43.0 | 11.0 | 66.8 | 17.1 | 92.1 | 23.6 | 128.4 | 32.9 |

Table 19 Continued.

18 Hour Setting Period
6% Bentonite Suspension.

Temperature 25° — Wire #1

| Time minutes | $\sigma = 40.4$ | | $\sigma = 90$ | | $\sigma = 190$ | | $\sigma = 303$ | |
|---|---|---|---|---|---|---|---|---|
| | $\delta$ | $\tau$ | $\delta$ | $\tau$ | $\delta$ | $\tau$ | $\delta$ | $\tau$ |
| 0 | 123 | 152 | 127 | 157 | 148 | 183 | 150 | 185 |
| 1 | 32.0 | 39.5 | 39.2 | 48.4 | 59.1 | 72.9 | 77.9 | 96.2 |
| 2 | 28.5 | 35.1 | 31.0 | 44.4 | 56.2 | 69.3 | 74.9 | 92.4 |
| 3 | 25.3 | 32.2 | 34.6 | 42.6 | 54.7 | 67.4 | 73.1 | 90.1 |
| 4 | 24.0 | 29.6 | 33.6 | 41.4 | 53.8 | 66.3 | 72.1 | 88.9 |
| 5 | 23.1 | 28.5 | 32.9 | 40.6 | 53.1 | 65.4 | 71.7 | 88.4 |
| 6 | 22.7 | 28.0 | 32.5 | 40.1 | 52.8 | 65.2 | 71.1 | 87.7 |
| 7 | 21.5 | 26.5 | 32.2 | 39.7 | 52.3 | 64.6 | 70.9 | 87.5 |
| 8 | 21.1 | 26.0 | 31.7 | 39.1 | 52.1 | 64.2 | 70.5 | 87.0 |
| 9 | 20.9 | 25.8 | 31.6 | 38.9 | 51.6 | 63.6 | 70.0 | 86.4 |
| 10 | 20.6 | 25.4 | 31.2 | 38.5 | 51.5 | 63.5 | 69.9 | 86.2 |
| 15 | 19.9 | 24.5 | 30.6 | 37.7 | 50.6 | 62.4 | 69.3 | 85.4 |
| 20 | 19.3 | 23.8 | 29.9 | 36.8 | 50.1 | 61.7 | 69.1 | 85.2 |
| 25 | 18.9 | 23.3 | 29.7 | 36.6 | 50.0 | 61.6 | 68.9 | 85.0 |
| 30 | 18.8 | 23.2 | 29.7 | 36.6 | 49.8 | 61.4 | 68.8 | 84.9 |

| Time minutes | $\sigma = 444$ | |
|---|---|---|
| | $\delta$ | $\tau$ |
| 0 | 162 | 200 |
| 0.5 | 102.4 | 126.4 |
| 1 | 98.4 | 121.5 |
| 2 | 95.0 | 117.1 |
| 3 | 93.7 | 115.4 |
| 4 | 92.2 | 113.7 |
| 5 | 91.7 | 113.0 |
| 6 | 91.2 | 112.4 |
| 7 | 90.6 | 111.7 |
| 8 | 90.1 | 111.2 |
| 9 | 89.9 | 111.1 |
| 10 | 89.7 | 110.5 |
| 15 | 88.4 | 109.0 |
| 20 | 87.5 | 107.8 |
| 25 | 87.0 | 107.4 |
| 30 | 86.5 | 106.8 |

## Table 19 Continued

18 Hour Setting Period
8% Bentonite Suspension.

Temperature 25°                                                                 Wire M7

| Time minutes | σ = 10 δ | τ | σ = 90 δ | τ | σ = 105.1 δ | τ | σ = 190 δ | τ | σ = 303 δ | τ |
|---|---|---|---|---|---|---|---|---|---|---|
| 0 | 105.8 | 434 | 177 | 726 | 58.8 | 242 | | | | |
| ½ | | | | | | | 71.7 | 295 | 87.5 | 359 |
| 1 | 38.3 | 157 | 45.9 | 188 | 53.0 | 218 | 66.5 | 273 | 84.2 | 346 |
| 2 | 26.8 | 110 | 42.0 | 173 | 45.0 | 197 | 62.9 | 258 | 81.5 | 335 |
| 3 | 23.5 | 96.3 | 40.4 | 166 | 46.0 | 189 | 60.4 | 248 | 80.3 | 330 |
| 4 | 22.6 | 92.7 | 39.2 | 161 | 44.9 | 184 | 59.9 | 246 | 80.1 | 329 |
| 5 | 21.4 | 87.8 | 38.3 | 157 | 44.5 | 183 | 59.4 | 244 | 79.5 | 327 |
| 6 | 20.4 | 83.7 | 38.0 | 156 | 44.0 | 181 | 59.0 | 242 | 79.1 | 325 |
| 7 | 20.0 | 82.0 | 37.6 | 154 | 43.5 | 179 | 58.8 | 242 | 78.3 | 322 |
| 8 | 19.1 | 78.3 | 37.2 | 153 | 43.1 | 177 | 58.5 | 241 | 78.0 | 321 |
| 9 | 18.1 | 74.2 | 37.0 | 152 | 42.8 | 176 | 58.3 | 240 | 77.1 | 317 |
| 10 | 16.5 | 67.7 | 36.7 | 151 | 42.6 | 175 | 58.1 | 239 | 77.1 | 317 |
| 15 | 12.8 | 52.5 | 35.7 | 147 | 41.9 | 172 | 57.4 | 236 | 75.8 | 312 |
| 20 | 11.7 | 48.0 | 35.4 | 145 | 41.4 | 170 | 56.7 | 233 | 75.0 | 308 |
| 25 | 11.6 | 47.6 | 35.0 | 143 | 41.3 | 170 | 56.6 | 233 | 74.5 | 306 |
| 30 | 11.3 | 46.4 | 35.0 | 143 | 41.3 | 170 | 56.4 | 232 | 73.7 | 303 |

| Time minutes | σ = 444 δ | τ |
|---|---|---|
| 0 | | |
| ½ | 99.6 | 409 |
| 1 | 95.7 | 393 |
| 2 | 91.5 | 375 |
| 3 | 89.5 | 367 |
| 4 | 88.3 | 362 |
| 5 | 87.8 | 361 |
| 6 | 87.0 | 357 |
| 7 | 86.7 | 356 |
| 8 | 86.5 | 355 |
| 9 | 86.1 | 353 |
| 10 | 86.0 | 353 |
| 15 | 83.8 | 345 |
| 20 | | |
| 25 | | |
| 30 | 81.8 | 336 |

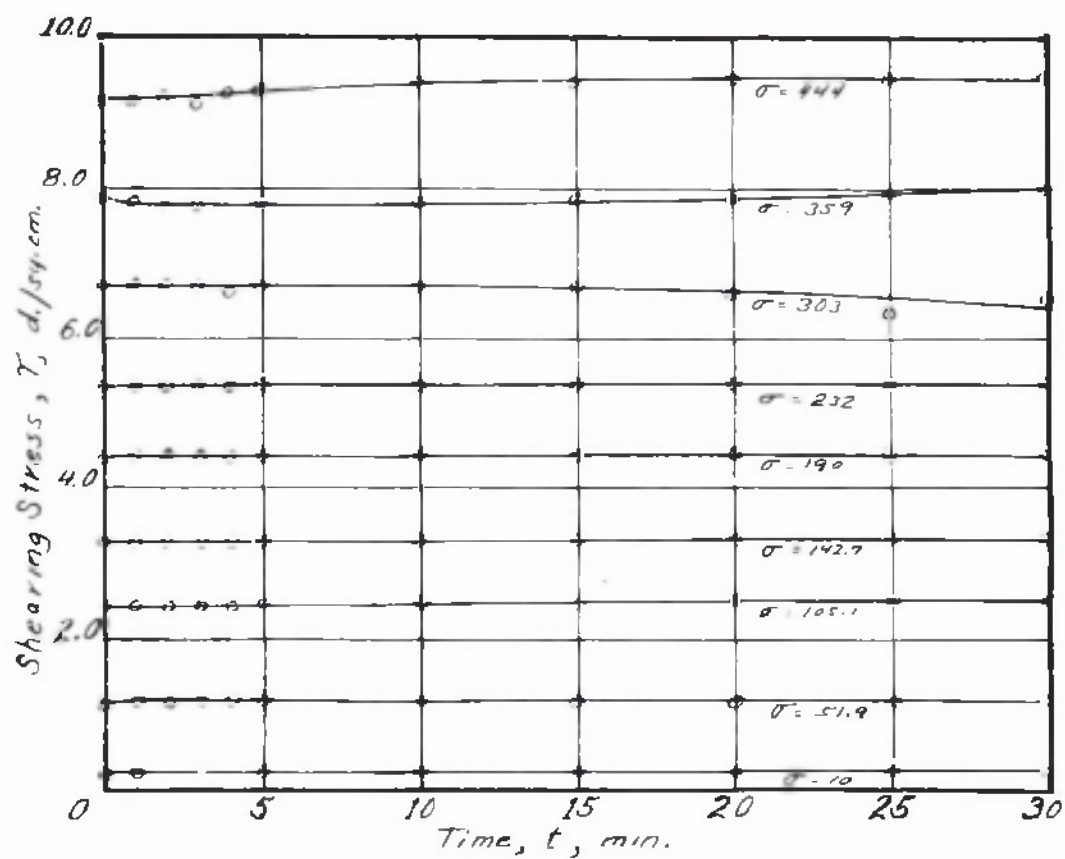Figure 18. Series II Tests. Time-Shearing
Stress Graph. 2% Bentonite Suspension
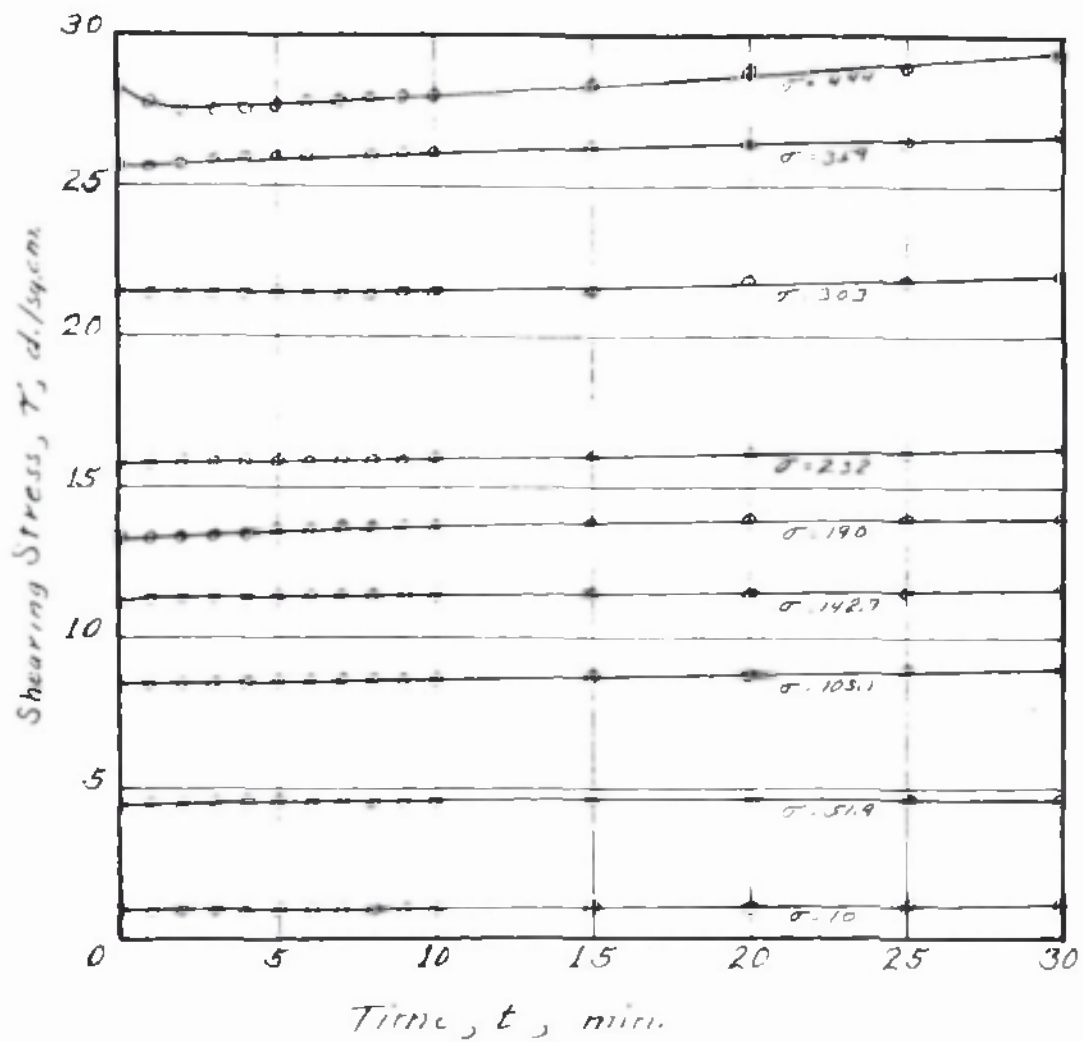Zero Setting Period

Figure 19. Series II Tests. Time - Shearing
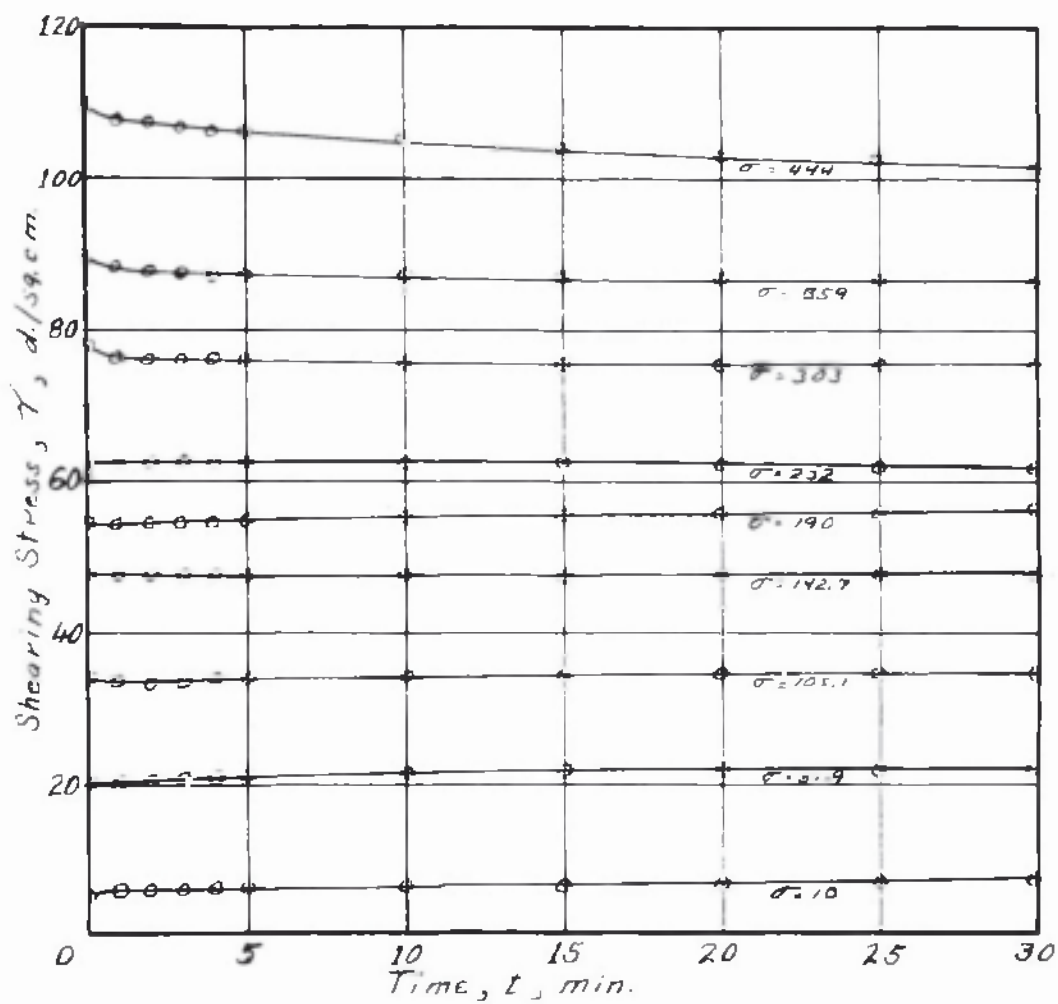Stress Graph 4% Bentonite Suspension.
Zero Setting Period

Figure 20. Series II Tests. Time-Shearing
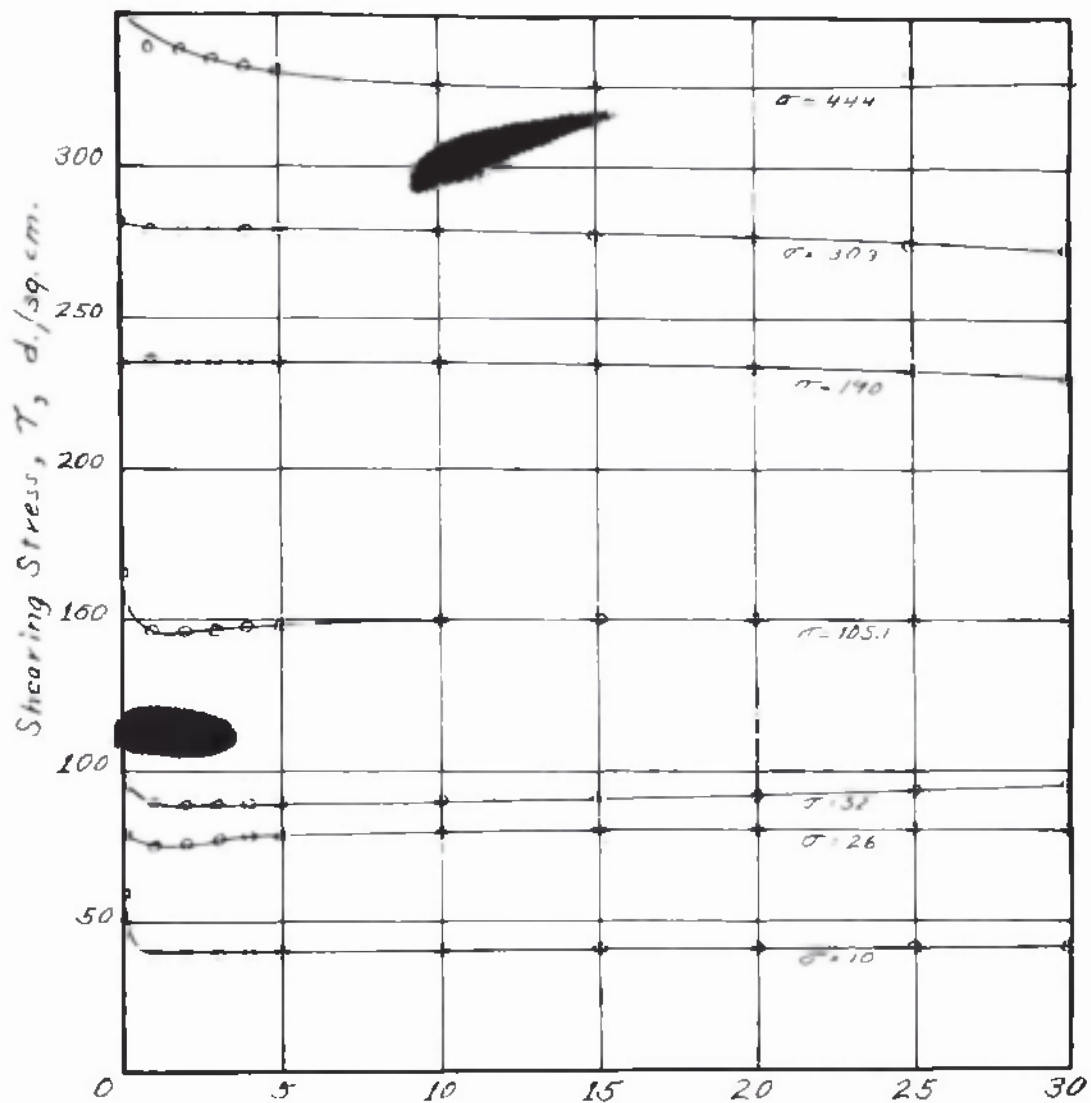Stress Graph. 6% Bentonite Suspension.
Zero Setting Period

Figure 21. Series II Tests. Time-Shearing Stress
Graph. 8% Bentonite Suspension
Zero Setting Period

essentially constant from the start to the end of the 30-minute
period during which the readings were taken.  In the 8% suspen-
sion a decreasing shearing stress is noted over the first two
or three minutes which in some cases passes through a slight
minimum.  This effect is found to a lesser degree in the 6,
4, and 2 per cent suspensions.  Since observations with New-
tonian fluids fail to show this effect, it is concluded that
a small amount of structure was able to form during the short
length of time from the cessation of the treatment in the
structure breaker until the shearing action was started by the
beginning of the rotation of the sample cup.  It is consistent
that this effect would be more noticeable with the higher con-
centrations of bentonite.

On the basis that the action of the structure breaker had
quantitatively destroyed all structure or bonding between the
particles in the suspensions, it was expected that the shear-
ing stress would rise from some lower value at the beginning
of the test to a higher and finally constant value toward
the conclusion of the test.  This behavior has been reported
by Broughton and Hand[20] for bentonite suspensions which they
ascribe to the formation of structure that offers increased
resistance to the shearing action.  The evidence of Figures
18, 19, 20 and 21 indicates that this behavior does not occur
with the bentonite solutions used here.  It is concluded that

---

[20] G. Broughton and S. Hand: Trans. Am. Inst. Min. & Met.
Engrs. T.P. 1002, 1936.

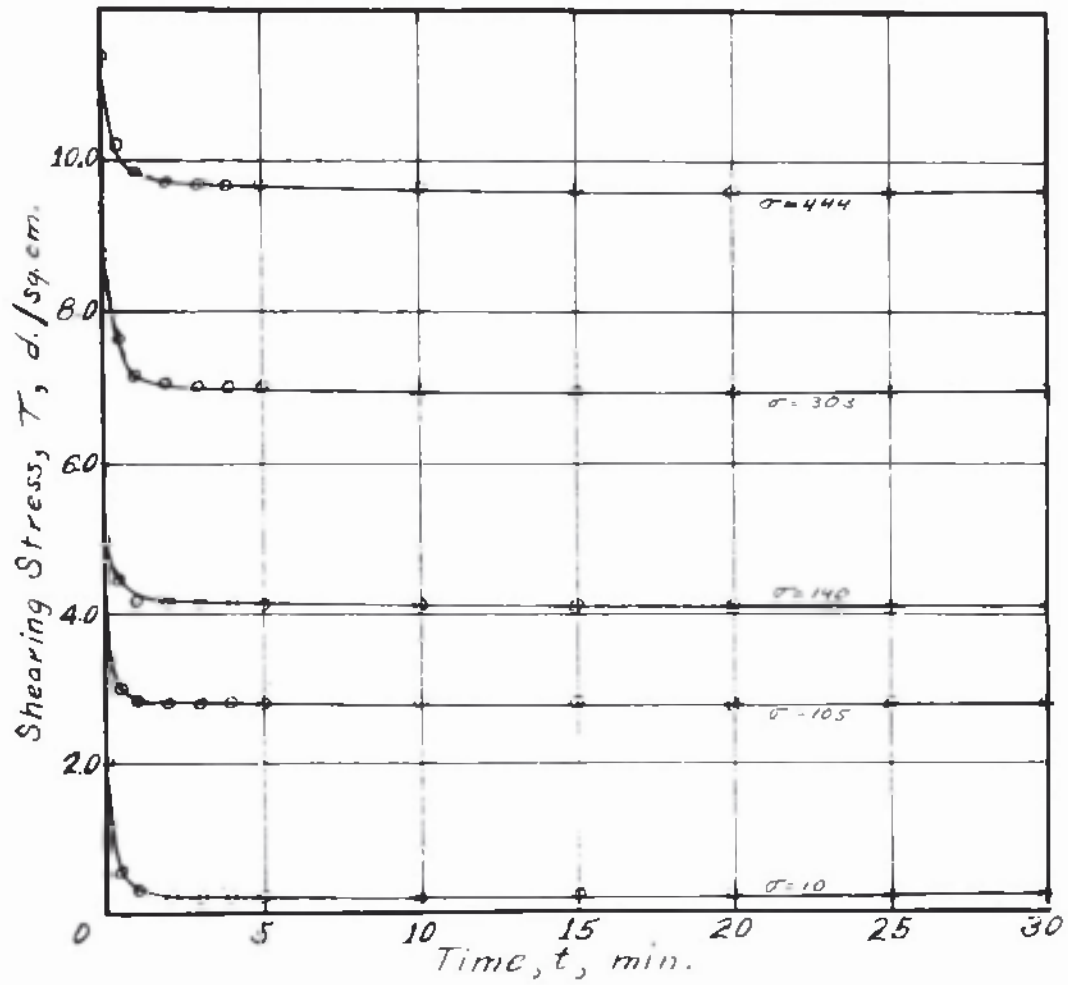Figure 22. Series II Tests Time—Shearing Stress
Graph 2 % Bentonite Suspension.
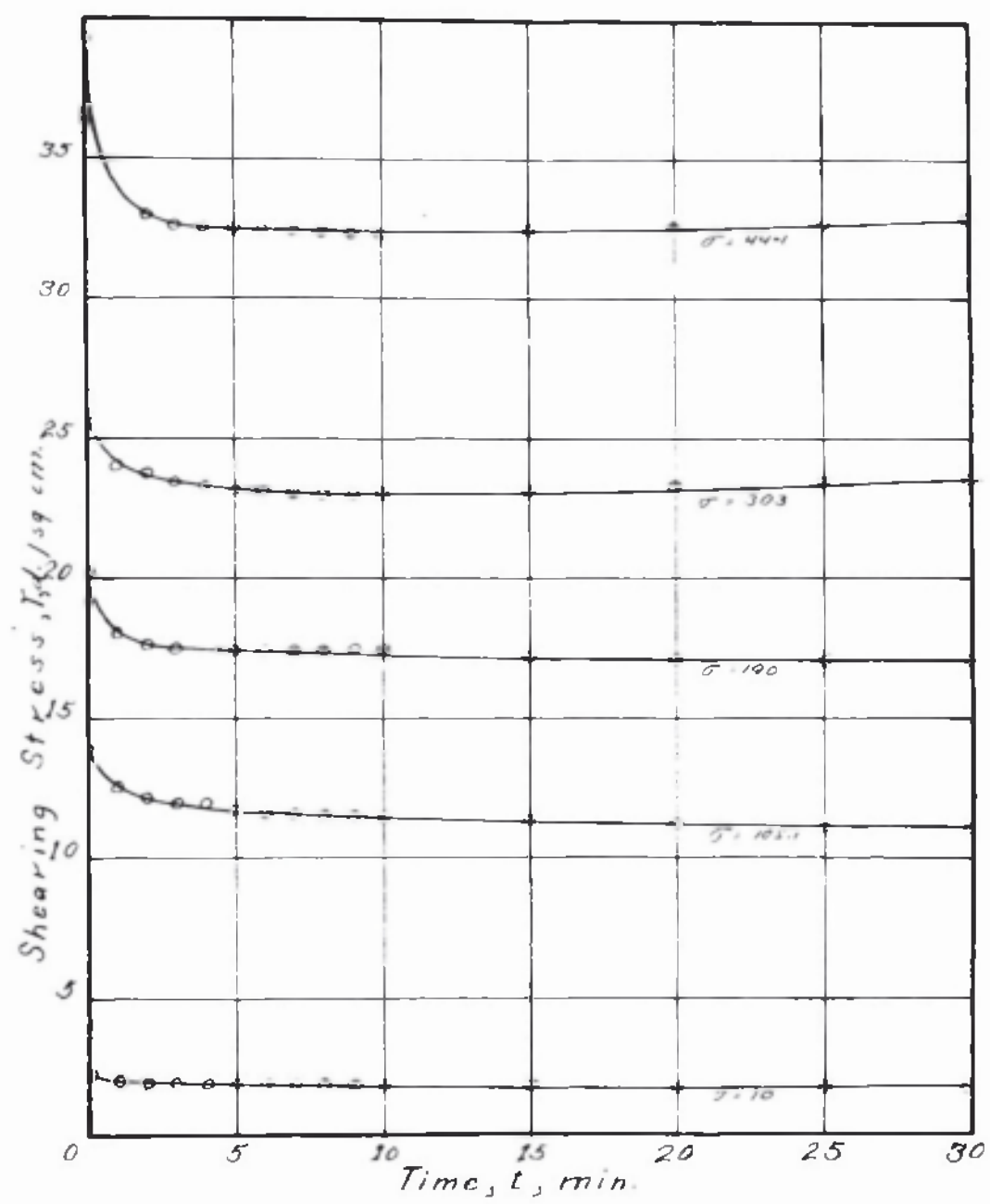18-Hour Setting Period

Figure 23. Series II Tests. Time – Shearing Stress
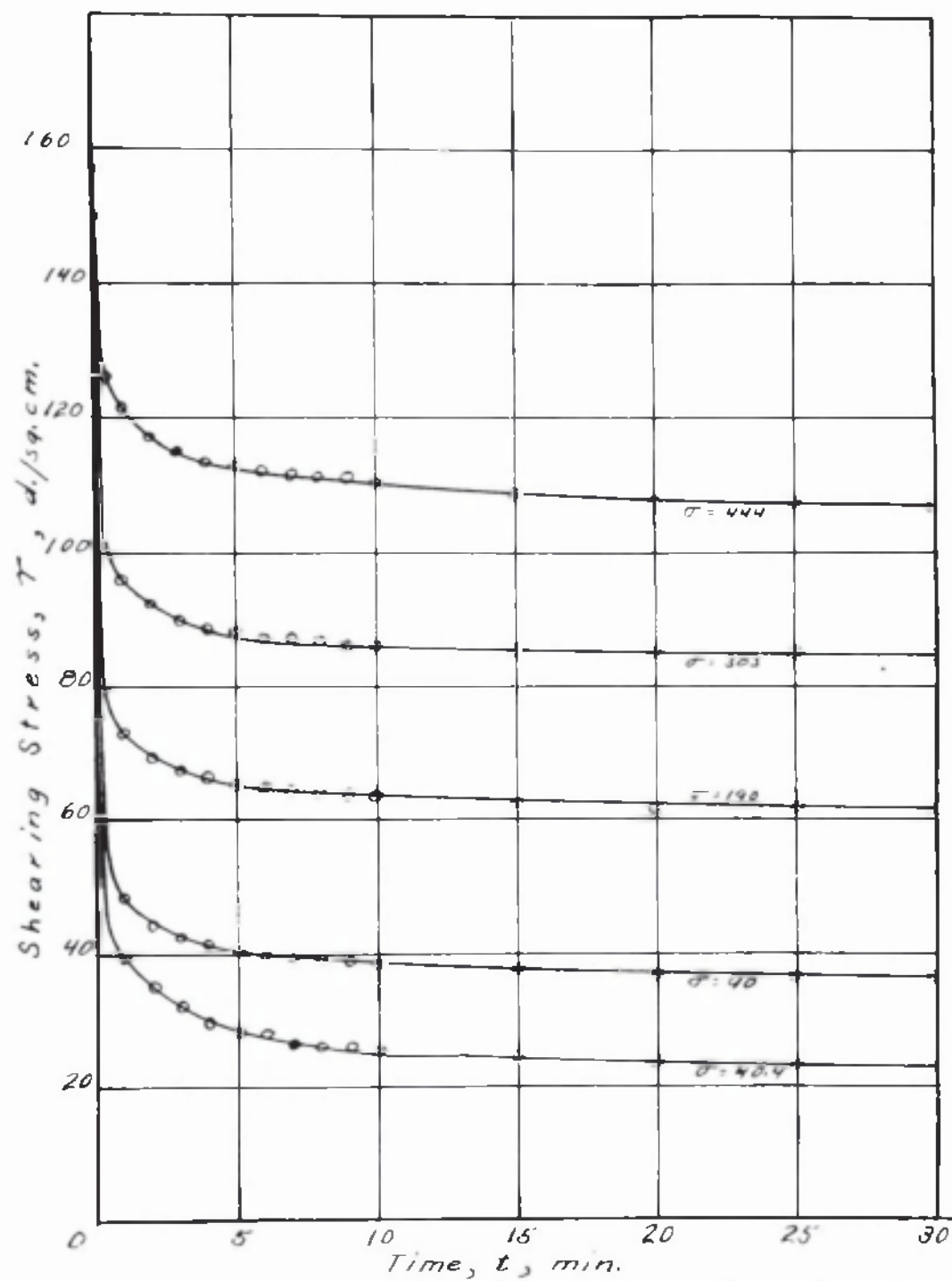Graph. 4 % Bentonite Suspension.
18-Hour Setting Period

Figure 24. Series II Tests. Time-Shearing Stress
Graph. 6% Suspension. 18-Hour Setting Period.
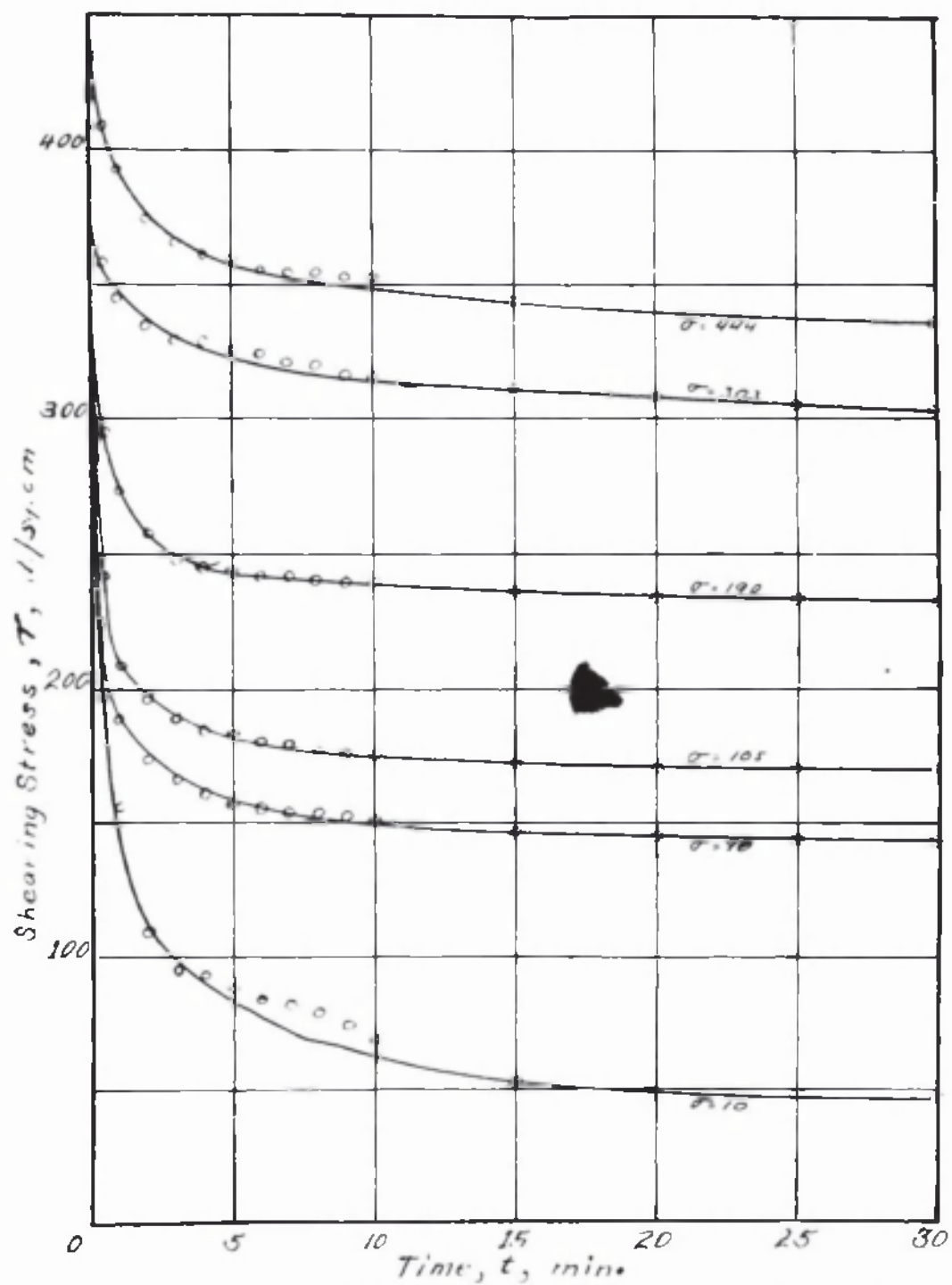
Figure 25. Series II Tests. Time-Shearing Stress Graph. 8% Suspension. 18-Hour Setting Period.

only negligible amounts of structure, if any, are able to form in the presence of the shearing action of the cup and cone system over periods of time up to 60 minutes.

The data of Table 19 for the 18-hour setting period are plotted in Figures 22, 23,24 and 25 for the 2, 4, 6, and 8 per cent suspensions, respectively. Inspection of these figures shows that the shearing stress rapidly decreases from some momentarily large value at the beginning of the shearing action, to a constant value after the shearing has been operating for a period of minutes. The 2% suspension showed only a small maximum shearing stress at the start in comparison with the 4, 6 and 8 per cent suspensions. In this case the shearing stress dropped to a constant value within 2-3 minutes of the constant shearing. Passing progressively to the 4, 6 and 8 per cent suspensions, it is seen that the decrease of the shearing stress takes place from higher and higher initial values and arrives at the constant value more and more slowly. This latter process takes approximately 10, 20 and 25 minutes for the 4, 6, and 8 per cent suspensions, respectively. These results would indicate that the structure formed in the suspensions during the 18-hour setting period was destroyed by the constant shearing action rather slowly in the case of the more concentrated 4, 6, and 8 per cent bentonite suspensions. The constant shearing stress can be regarded as an equilibrium or steady state in which the formation of structure is prevented or exactly counterbalanced by the disruptive action of the sustained shearing.

2. Rheological Diagram for the Equilibrium State.

The values of the shearing stress at equilibrium for the 2, 4, 6, and 8 per cent suspensions were taken from Figures 18 to 25 at the end of 10, 10, 20 and 30 minutes respectively, and plotted as a function of the rate of shear at which they were determined. This is shown by Figure 26, which is the rheological diagram of the suspensions at the equilibrium state. Theoretically, after equilibrium had been attained, the shearing stress should be the same regardless of whether the material originally possessed a great amount of structure or very little structure as obtained by the 18-hour setting period or the zero hour setting periods, respectively. Inspection of Figure 26 shows that a reasonable approach to this condition was obtained. In general, the equilibrium points obtained from the suspension which had set 18 hours before the test, lie above the corresponding points obtained from the suspension having zero setting period. However, the difference is not great when considered in relation to the range of shearing stress that is covered. The curvature of the lines decreases progressively from the 8% suspension to the 2% suspension, the latter showing practically no curvature, which is consistent with the results obtained in the Series I tests.

A plot of the data which determined the curves of Figure 26 is given on logarithmic coordinates in Figure 27. It is seen that straight lines are obtained for the shearing stress-rate of shear relationship. On the logarithmic basis the lines are represented by this equation.
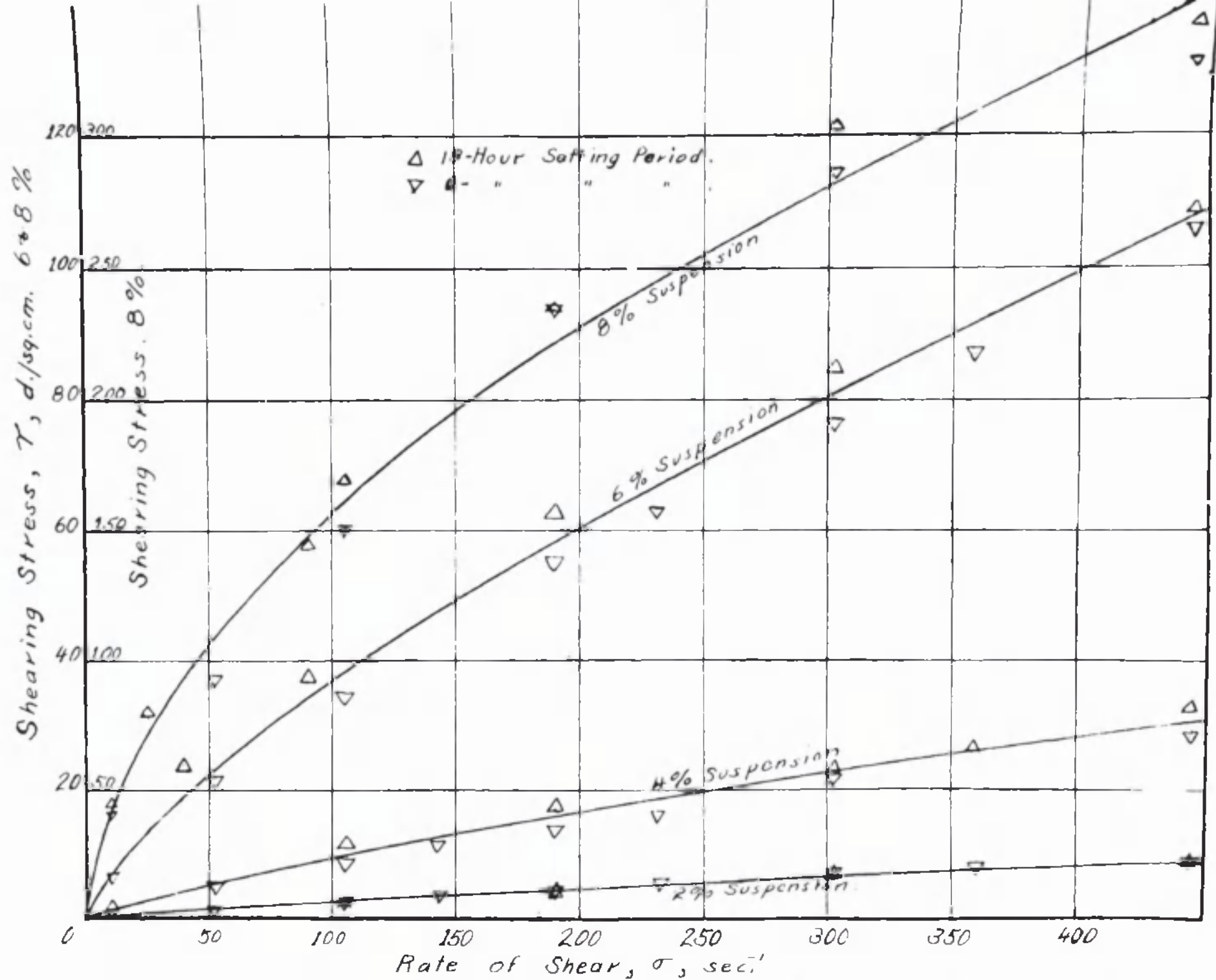
Figure 26. Rheological Diagram for the Bentonite Suspensions at the Equilibrium Condition.
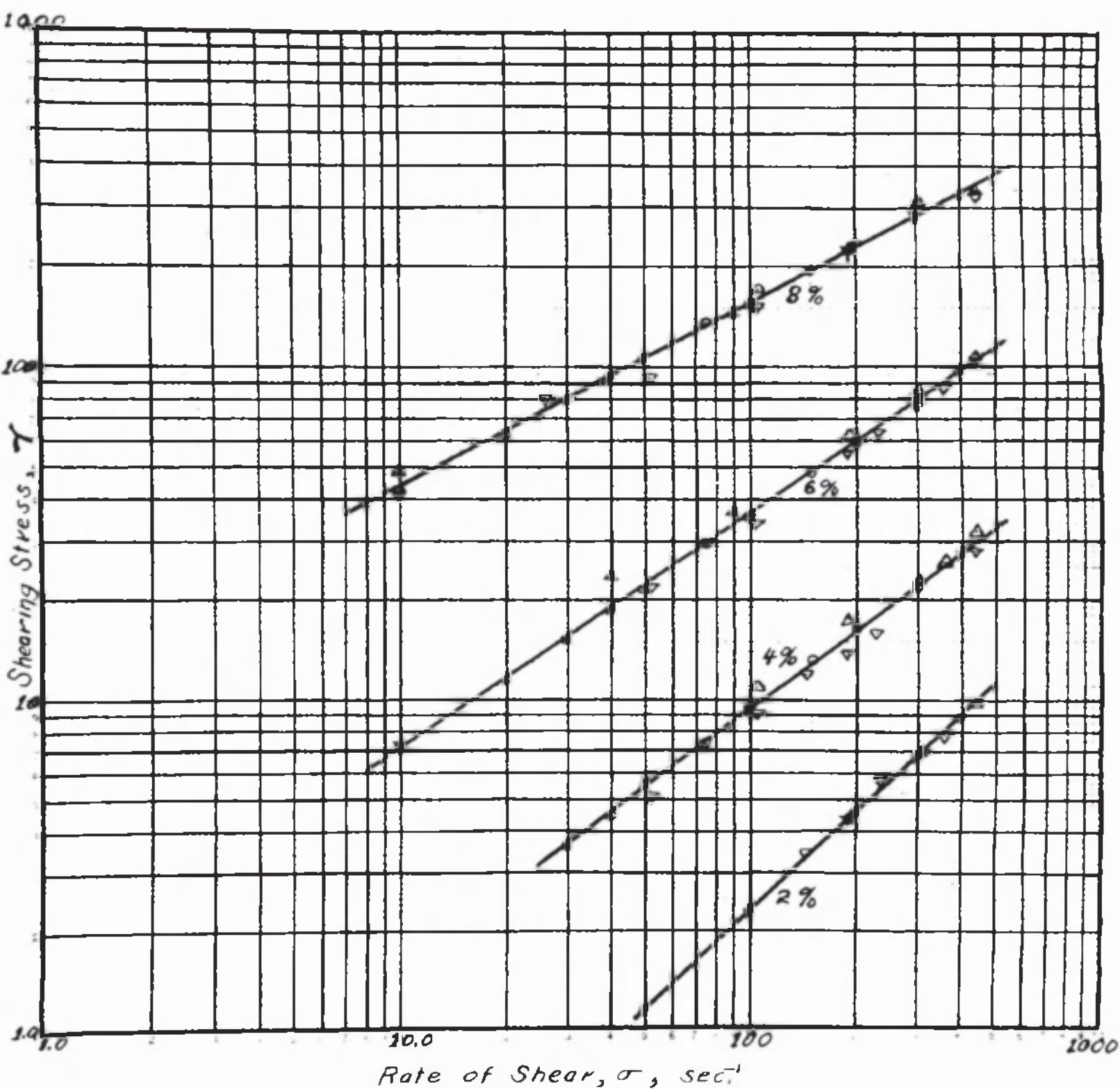
Figure 27. Logarithmic Plot of the Curves of Figure 26

$$\log \tau = \log b + n \log \sigma \qquad (37)$$

or

$$\tau = b \sigma^n \qquad (38)$$

In Table 20 are given the constants which have been determined from Figure 27 and when substituted in Equation 38 will reproduce the curves of Figure 26. The exponent n, is almost unity for the 2% suspension and decreases in value with the increasing concentration of bentonite in the 4, 6, and 8 per cent suspensions. When the exponent is unity, the Equation 38 reduces to the Newtonian relationship and the term b, takes on the dimensions of viscosity.

Table 20.

Values of the Constants for the Ostwald Equation (Eq.38)

| Constant | Bentonite Suspension. | | | |
|---|---|---|---|---|
| | 2% | 4% | 6% | 8% |
| n | 0.98 | 0.774 | 0.708 | 0.550 |
| b | 0.023 | 0.269 | 1.41 | 12.5 |

3. Interpretations Based on the Parabolic Equation.

According to Kruyt[21] a gel is made up of a network of solid particles or filaments that holds enclosed within its mass a large amount of liquid medium. Hauser and Reed[22] have given evidence that the bentonite solutions develop structure by the formation of chains or fibrils of the bentonite particles. The chain of fibrilar appearance has been reported[23] to be quite visible under the microscope when the bentonite sols are allowed to slowly dry and form paper-like films.

Under the action of a sustained shearing force, it is considered that the network breaks into numerous gel fragments or secondary particles; and as suggested by Kraemer and Williamson[24] "permeated in gel-like fashion with the liquid medium." These gel fragments cause the non-Newtonian behavior by releasing liquid under the influence of the sustained shearing. This conversion of trammeled liquid to untrammeled liquid causes an increase in the fluidity of the suspension. The process is prevented from going to completion for a given rate of shear by the dynamic conditions that continually bring the free particles to the boundaries of the fragments where, if the relative translational velocity between the fragment and free particle is low and the orientation proper, bonding can take place and the gel fragment tends to grow in size.

[21] H R Kruyt. Chimie & Industrie 42: 587-608 (1939)
[22] E. A. Hauser and C. E. Reed, J. Am. Chem. Soc. 58:1822(1936).
[23] E. A. Hauser & O. S. Le Bean. J. Phys. Chem. 43: ;037-48(1939)
[24] E. O. Kraemer and R. V. Williamson. J. Rheology, 1:76 (1929)

As a result of these two effects the gel fragment attains an average equilibrium size that is consistent with the rate of shear it is suffering.

It seems probable that this process operates according to the parabolic form of equation shown above. However, there are certain limiting conditions that must be satisfied. When the rate of shear becomes quite large the gel fragments are reduced in size and ultimately become either nonexistent or remain at a constant size. In this condition the sol behaves as a Newtonian fluid and its coefficient of viscosity is only somewhat greater than that of the fluid medium.

By dividing both sides of Equation 38 by the rate of shear as follows:

$$\frac{\tau}{\sigma} = \frac{b\sigma^n}{\sigma} = b\sigma^{n-1} \tag{39}$$

and since $\eta = \frac{\tau}{\sigma}$

$$\eta = \frac{b}{\sigma^{1-n}} \tag{40}$$

Equation 40 is obtained which gives the value of the coefficient of viscosity at any given value of the rate of shear. Equation 38 shows that as the rate of shear becomes zero, the value of the shearing stress becomes zero, which is consistent with the observations shown above. Since it is shown in Table 20 that the exponents $n$, are all less than 1, Equation 40 indicates that the viscosity of the **bentonite** suspensions becomes infinite at zero rate of shear, which is the equivalent of standing quiescent. In other words, the parabolic equatio seems to be
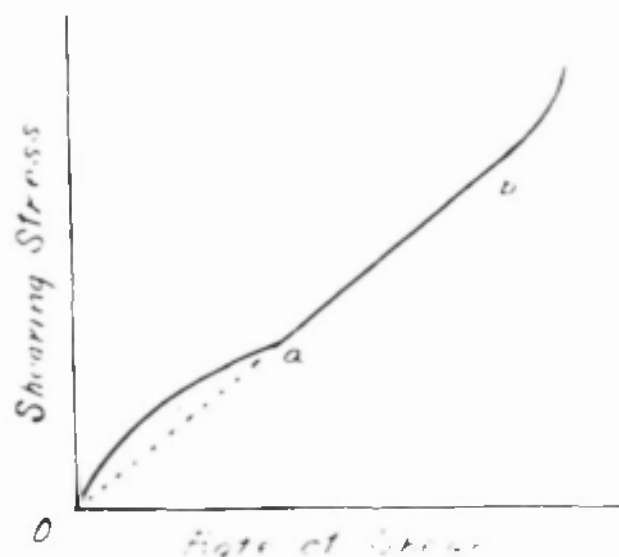
**Figure 28.** Diagrammetic Representation of the
Rheological Curve According to Ostwald.
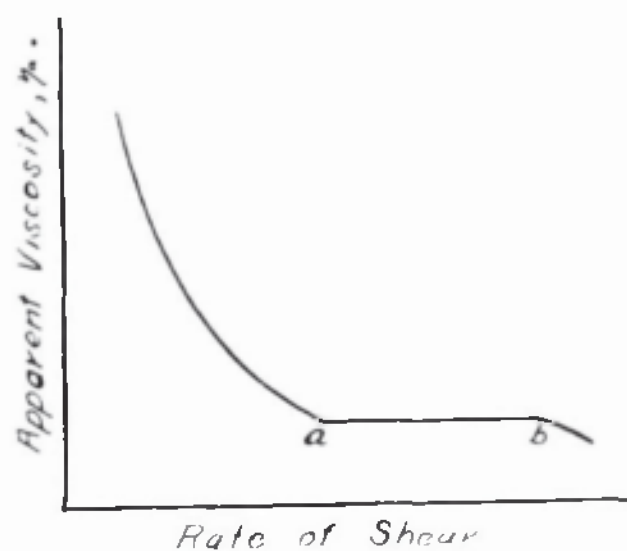


**Figure 29.** Diagrammetic Representation of the Apparent
Viscosity vs. Rate of Shear According to the Ostwald
Concept.

consistent with the experimental facts in regard to the limiting condition for which the rate of shear approaches zero.

However, when the rate of shear approaches a very large or infinite value not only does the parabolic equation require that the shearing stress become very large or infinite, but also that the viscosity become a very low value and even less than that of the fluid medium itself. This latter requirement of Equation 40 has been a serious criticism by those who have felt that the whole course of the flow curve should be a smooth curve at low values of rate of shear and resolve into a straight line at high values of rate of shear.[25, 26] However, according to the conception of Ostwald and Auerback[27] which is supported by the experiments of Porter and Rao[28] Farrow, Lowe,[29] and de Waele,[30] the process of disaggregation may be complete or reach a constant condition at high rates of shear wherein the parabolic relationship will no longer influence the rheological curve and the Newtonian fluid behavior governs. Diagrammetrically this process is shown by Figure 28 which has been offered by Ostwald[31] as descriptive of the flow behavior of many different sols. The shearing process represented by the section from 0

[25] C. N. van Nieuwenburg. First Report on Viscosity and Plasticity. loc. cit. p.167
[26] R. V. Williamson. Ind. & Eng. Chem. 21: 1108 (1929).
[27] Wo. Ostwald. Koll. Z. 47:176 (1929)
[28] Porter and Rao. Trans. Farad Soc. 23:311 (1927).
[29] Farrow, Lowe. J. Text. Inst. 14:T414 (1923)
[30] A. de Waele, Koll. Z. 38:27 (1926)
[31] Wo. Ostwald. Koll. Zeits. 43:190 (1927) and ibid possim.

to a, corresponds to the parabolic relationship and represents the process of disaggregation of the gel fragment. At point a, the disaggregation is either complete or has reached a condition where no further increase in the rate of shear will cause the release of more trammeled liquid. Hence, in the section from a to b the flow curve is Newtonian and its coefficient is governed by the volumetric effect of the particles or gel fragments as indicated by the Einstein Equations.[32]

$$\eta = \eta_0 \left( 1 + 2.5 \varphi \right)$$

(41)

where  $\eta$  = effective coefficient of viscosity of the material

$\eta_0$ = coefficient of viscosity of the fluid medium .

$\varphi$ = fraction of the volume occupied by solid particles, (or gel fragments).

Furthermore, since the influence of the parabolic section is gone, the straight portion between a to b extrapolates backward through the origin and the apparent viscosity becomes constant. At the point b, the onset of turbulence is encountered which Ostwal considers is hastened by the presence of the solid particles and structure. In many cases as shown by Ostwald and others[33] the transition at a is quite smooth and regular although there is no reason to believe it cannot be quite abrupt. This apparently is the reason Ostwald hesitates to write a complete rheological equation as a sum of the parabolic and Einstein equations.

---

[32] A. Einstein. Ann. Phys. 19:289 (1906) ibid. 34:591 (1911).
[33] M. Reiner and R. Schoenfeld-Reiner. Koll. Z. 65:44 (1933).

Since the Ostwald interpretation allows the parabolic relationship and provides for a change in flow conditions when disaggregation is complete or becomes constant, it is felt that the behavior of the bentonite suspensions indicate a reasonable conformation to this concept. A further test would be obtained by plotting the values of the apparent viscosity $\eta_a$, against the rate of shear for which they were obtained. A plot of this type would show the apparent viscosity decreasing as a regular hyperbola as the rate of shear increases until the point a, in Figure 28 was reached, whereupon it would become a straight horizontal line. This has been shown diagrammetrically by Figure 29.

A search for this type of behavior was applied to the data of the Series I tests on the 2 and 3 per cent suspension since it was obvious that the equilibrium curves for the 4, 6, and 8 per cent suspensions in Figure 26 had not been carried to rates of shear sufficiently high to show the linear section that extrapolates back to the origin. The expectation for the sigmoid effect would be greatest with the 2 and 3 per cent suspensions, near the beginning of the rheological curves. Since the time-shearing stress diagrams on Figures 19 and 23 have indicated that equilibrium was attained in approximately 4 minutes for the 4% suspension, it is considered that the Series I tests for the 2 and 3 per cent suspensions were conducted at practically equilibrium conditions. The data for the 2% suspension of the Series I tests are given in the Table 21 and in addition the data for the 3% suspension which has not

### Table 21

Values of Apparent Viscosity for the 2 and 3
per cent Suspensions for Various Shearing
Stresses and Rates of Shear.

| Rate of Shear sec$^{-1}$ | 2% | | 3% | |
|---|---|---|---|---|
| | $\gamma$ d./sq.cm. | $\eta_a$ c.p. | $\gamma$ d./sq.cm. | $\eta_a$ c.p. |
| 5 | 0.128 | 2.56 | 0.205 | 4.10 |
| 10 | 0.256 | 2.56 | 0.486 | 4.86 |
| 16.0 | 0.384 | 2.36 | 0.666 | 4.08 |
| 22.4 | 0.512 | 2.28 | 0.896 | 4.00 |
| 27.6 | 0.589 | 2.13 | 1.153 | 4.17 |
| 26.0 | 0.614 | 2.36 | 1.128 | 4.33 |
| 35.4 | 0.768 | 2.17 | 1.510 | 4.27 |
| 47.2 | 1.128 | 2.39 | 1.97 | 4.18 |
| 57.8 | 1.382 | 2.39 | 2.43 | 4.20 |
| 75.4 | 1.613 | 2.14 | 3.07 | 4.08 |
| 89.5 | 1.99 | 2.23 | 3.60 | 4.02 |
| 110.6 | 2.46 | 2.23 | 4.38 | 3.96 |
| 105.1 | 2.46 | 2.34 | 4.41 | 4.18 |
| 126.3 | 2.87 | 2.29 | 4.98 | 3.96 |
| 142.7 | 3.10 | 2.17 | 5.77 | 4.04 |
| 162.9 | 3.61 | 2.22 | 6.58 | 4.04 |
| 174.3 | 3.89 | 2.23 | 7.20 | 4.13 |
| 190. | 4.20 | 2.21 | 7.58 | 3.99 |
| 209 | 4.61 | 2.20 | 8.27 | 3.96 |
| 232 | 5.12 | 2.20 | 9.14 | 3.94 |
| 262 | 5.77 | 2.20 | 10.16 | 3.88 |
| 303 | 6.42 | 2.12 | 11.74 | 3.87 |
| 359 | 7.78 | 2.17 | 13.77 | 3.82 |
| 444 | 9.61 | 2.16 | 16.85 | 3.78 |

appeared before. The apparent viscosity has been calculated by dividing the shearing stress by the rate of shear for each observation, and is expressed as centipoises. The values of the apparent viscosity from Table 21 have been plotted against the corresponding values of the rate of shear in Figure 30. It is seen that a constant value seems to be indicated at the higher rates of shear, while at the lowest rates of shear the uncertainty of the data is greater, but it does seem to be evident that a decrease of the apparent viscosity results as the rates of shear increases at the beginning. This would indicate at least that it is possible for the Ostwald type of flow to be present, but not sufficient enough to be demonstrated clearly by the relatively insensitive method used.

Two other formulas have been suggested to describe the shearing stress-rate of shear behavior of materials similar to bentonite suspensions. They will be considered briefly in relation to their suitability for explaining the behavior of bentonite suspensions.

Williamson[26] has proposed the following equation for materials like dry suspensions, paint, pitchs, etc. that show a viscosity curve rising from the origin.

$$\tau = \frac{f\sigma}{s+\sigma} + \eta_\infty \sigma \quad or \quad \eta_a = \frac{\tau}{\sigma} = \frac{f}{s+\sigma} + \eta_\infty \qquad (42)$$

where $\eta_\infty$ = the coefficient of viscosity at infinite rate of shear.

$f$ = a constant determined by the intercept of the asymptote on the stress axis.

$s$ = a constant.

[26] R.V. Williamson. Ind. & Eng. Chem. 21:1108 (1929)
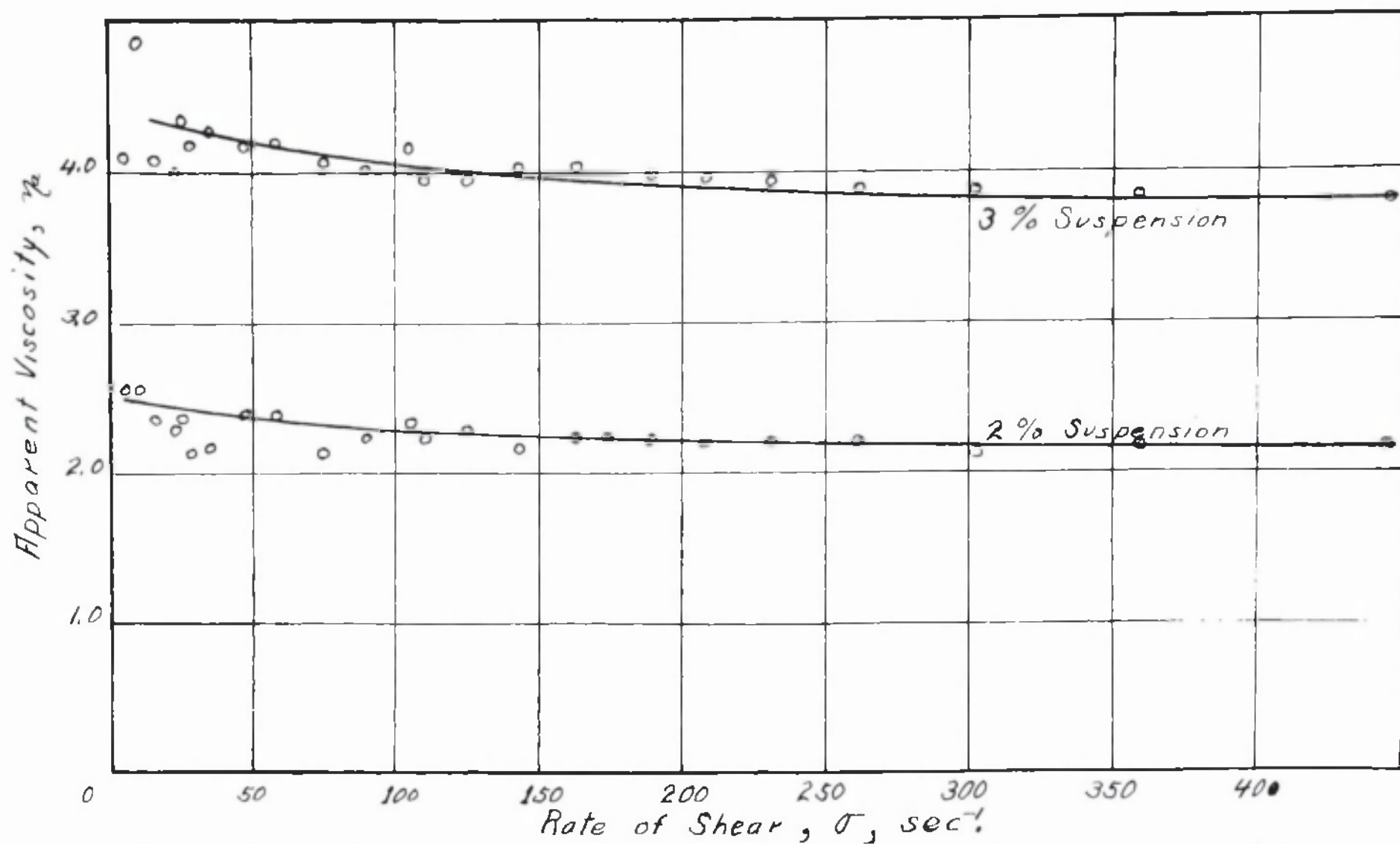
Figure 30. Plot of Experimentally Determined Apparent Viscosities versus Rate of Shear

In the above equation, when $\sigma$ approaches zero, the shearing stress approaches zero and the viscosity becomes a constant value. It is felt that the viscosity of the bentonite suspensions must become infinite at zero rate of shear, therefore the Williamson equation cannot apply. Furthermore, a test of the curves of Figure 26 does not indicate a hyperbolic character as is demended by the first term of the Williamson equation.

The equation recommended by Goodeve for the measurement of thixotropy is also a dual membered equation for the relation between shearing stress and rate of shear. It is as follows:

$$\tau = \sigma \eta_\infty + f \qquad \text{or} \qquad \eta_a = \frac{\tau}{\sigma} = \eta_\infty + \frac{f}{\sigma} \tag{43}$$

where $\eta_\infty$ = the coefficient of viscosity at infinite rate of shear.

$f$ = the coefficient of thixotropy, a constant having the dimensions of dynes/sq.cm. but not considered a yield value.

As before when the limiting conditions of this equation are examined it is seen that as $\sigma$ approaches zero, the viscosity becomes infinite, but the shearing stress becomes constant at some finite value that is related to $f$. This behavior of the bentonite suspensions has not been indicated by the rheological diagrams plotted in the Series I tests, nor by Figure 26 of the Series II tests, therefore, this equation was not considered applicable.

## 4. Résumé and Conclusions.

The parabolic equation has been found adequate to describe the relationship between the shearing stress and rate of shear for the bentonite sols at equilibrium conditions. However, since the constants elude exact physical description, the equation is only empirical. Consideration of the limiting conditions has led to the rejection of the equations proposed by Williamson and Goodeve and most logically indicate the behavior suggested by Ostwald. A search at the higher rates of shear gave only cursory indications of the Ostwald behavior, hence it is felt that a more sensitive and precise experimental arrangement is necessary. It has been shown that the equilibrium condition for the growth of structure and its destruction by a sustained rate of shear is attained from initial conditions of great fluidity and no fluidity (i.e. the gelled condition).

# CHAPTER VIII

## INFLUENCE OF THIXOTROPY.

### 1. General Considerations Concerning Thixotropy.

In the previous sections no discussion of thixotropy or
of its influence upon the fluid properties of the bentonite
sols was presented.  This omission has been made advisedly,
in order to avoid diversion from the basic question under con-
sideration in this investigation, namely, what is the result
obtained when the shearing stresses of many sustained and con-
stant rates of shears are applied to bentonite sols.  By this
postponment, we now are in a position to understand more clearly
the relation of thixotropy to the fluid properties of bentonite
suspensions and similar materials.

Freundlich[35] introduced the term thixotropy to describe
the reversible, isothermal sol to gel transformation of cer-
tain colloid systems by alternate shaking and subsequent rest.
The correlation of this phenomena with fluid properties has
resulted in much confusion.  Pryce-Jones[36] considers it in
relation to the fluid properties of paints and similar colloid
systems.  He points out that for thixotropic materials different
paths would be transversed by the curves for the relationship
between shearing stress and rate of shear when a cyclic increase
and decrease of the variables is determined.  This hysteresis

[35]H. Freundlich, Thixotropy.  (Hermann and Co. Paris. 1935)
[36]J. Pryce-Jones, J. Oil and Color Chemists Association. 19:
295-337 (1936)

behavior has been discussed by Reiner[37] as being indicative of the nature of the forces operating between the particles, and suggests its use as a means of ascertaining the type of micellar interaction.  However, these authors treat the subject from a qualitative standpoint and do not offer any data taken from actual experiment.  Ambrose & Loomis[19] give a diagram for a 5% bentonite sol showing the torque measured as degrees twist of a torsion wire, that is developed by increasing and decreasing the speed of revolution of a concentric cylinder viscometer. Their curves show an open loop, greater torque being obtained as the speed of rotation was increased by increments to the maximum value, than the corresponding points obtained as the speed of rotation was decreased by increments to the original value.  The previous condition of the bentonite sol was not described by the authors, however, it is probable that the sol had been subjected to little or no agitation before the shearing action was started.  Bingham[38] has stated that in his earlier work duplicate values were obtained from either direction of increasing or decreasing shearing stresses.  Scott-Blair and Crowther[39] also indicate in some of their experiments that it makes no difference on the results obtained how many times their clay pastes were pushed through the capillaries at a given rate. This would seem to indicate that the two latter investigators were

[37] M. Reiner, Physics, 5:340 (1934)
[38] E. C. Bingham. J. Rheology 3:194 (1932).
[39] J. W. Scott Blair and E. M. Crowther, J. Phys. Chem. 33:321 (1929)

working with nonthixotropic materials.

The indication is that two kinds of behavior may be recognized. One, in which the equilibrium or steady state is reached quickly after a given shearing stress or rate of shear is applied, the second in which equilibrium is attained only slowly. Since the difference is only a matter of degree, systems intermediate will occasionally be found to add to the confusion. The former condition has been called false body by Pryce-Jones,[36] the latter as the influence of thixotropy. Kruyt[40] points out that the false-body type of gel formation may be due to contacts between particles of any orientation resulting in bonds forming, while in the slower process of thixotropy only preferred orientation result in bonding of particles. This picture seems reasonable and consistent with the known experimental facts.

In the ultimate analysis, the determination of a hysteresis curve for a system can indicate (as suggested by Reiner) that orientation of the particle is necessary before a structure can form and that a time lag will exist in the attainment of equilibrium when a constant rate of shear or shearing stress is applied to the system that possesses structure.

Experimentally, the determination of a hysteresis curve is difficult and becomes empirical since it must be decided how long the material is to be sheared at any one given rate.

---

[40]H. R. Kruyt, loc. cit.

Extended shearing at a constant rate approaches the equilibrium state at which no hysteresis could be demonstrated. The other extreme offers little more since it implies the condition of uniformly increasing rate of shear with the observations taken as an instantaneous reading. In comparison with the information gained by the time studies at constant rates of shear, of the Series II experiments, hysteresis curves have little to offer of fundamental nature. However, despite the attendant empiricism, a hysteresis determination was made upon the 5% bentonite sol so as to present actual data illustrating the hysteresis effect in terms of the fundamental rheological units, shearing stress and rate of shear.

## 2. Experimental Technique.

The hysteresis curves were determined, Series III tests, for the 5% bentonite suspension after 0- and 18-hours setting time. The 0-hours setting time was obtained by means of the usual 200 strokes in the structure breaker just before the sol was poured into the viscometer cup. During the 18-hour setting time, the cup was covered with a reasonably tight-fitting cover to prevent excessive evaporation. Before the sample was introduced, the instrument was cleaned, adjusted and fitted with the proper torsion wire. The cup was filled to approximately 1 cm above the upper edge of the inner cone; the excess above the upper edge of the inner cone was not removed as in the previous experiments. This was necessary because the inner cone descended and returned several times during one series of observations. When all was in readiness, with the inner cone at the highest position corresponding to the lowest rate of shear, the motor was started. After the lapse of one minute as determined by a stop-watch starting with the motor, the deflection reading was taken and the cone immediately lowered to the next position. Deflection readings were taken successively at rates of shear according to the schedule used in the Series I tests for one minute intervals, until the cone had been lowered to its lowest position corresponding to the highest rate of shear. After the reading had been taken for the one minute of shearing at the maximum rate, an additional reading was taken after the elapse of a second minute, whereupon the rate of shear was then decreased to the first value

on the descending series. Readings then were taken at one
minute intervals in the descending series for the same values
of rate of shear as before, until the lowest value was again
reached. Here, as before, a second reading was taken after
the elapse of a second minute at the terminal point and then
the increasing series was again started. This cyclic process
was repeated several times for the speeds of rotation of 20
and 80 r.p.m. The data so obtained with the 5% suspension
are given in Table 22 and have been plotted in Figure 31. The
deflections obtained in degrees were converted to shearing
stress by multiplying by the wire constant, disregarding the
lack of end corrections.

## Table 22

Series III Tests. Shearing Stress - Rate of
Shear Data Showing Hysteresis Effect
Zero-Hour Setting Period
5% Bentonite Suspension.

Temperature 25°                                                                          Wire #2

| Speed r.p.m. | Head Setting mm. | Rate of Shear sec.⁻¹ | Shearing Stress | | | |
| | | | Cycle 1 | | Cycle 2 | |
| | | | increasing | decreasing | increasing | decreasing |
|---|---|---|---|---|---|---|
| 80 | 10 | 105.1 | 19.4 | 21.4 | 21.4 | 21.8 |
| | 8 | 126.3 | 23.1 | 24.7 | 24.8 | 25.1 |
| | 7 | 142.7 | 25.5 | 26.8 | 27.1 | 27.3 |
| | 6 | 162.9 | 28.7 | 29.6 | 30.0 | 30.2 |
| | 5.5 | 174.3 | 30.5 | 31.4 | 31.8 | 31.9 |
| | 5 | 190 | 32.7 | 33.5 | 33.9 | 34.1 |
| | 4.5 | 209 | 35.3 | 36.0 | 36.4 | 36.6 |
| | 4 | 232 | 38.7 | 39.1 | 39.6 | 39.8 |
| | 3.5 | 262 | 42.5 | 43.1 | 43.5 | 43.7 |
| | 3 | 302 | 47.7 | 48.0 | 48.7 | 48.8 |
| | 2.5 | 359 | 54.6 | 54.8 | 55.8 | 55.7 |
| | 2 | 444 | 64.9 | 64.7 | 66.0 | 65.5 |
| 20 | 10 | 26 | 5.77 | 6.88 | 6.78 | 7.24 |
| | 7 | 35.4 | 7.52 | 8.43 | 8.03 | 8.85 |
| | 5 | 47.2 | 9.66 | 10.32 | 10.61 | 10.78 |
| | 4 | 57.8 | 11.36 | 11.93 | 12.23 | 12.38 |
| | 3 | 75.4 | 14.03 | 14.43 | 15.05 | 15.05 |
| | 2.5 | 89.5 | 16.12 | 16.4 | 16.97 | 16.93 |
| | 2 | 110.6 | 19.1 | 19.1 | 20.0 | 19.75 |

Table 22 Continued
18-Hour Setting Period
5% Bentonite Suspension

Temperature 25°                                                                 Wire #2

| Speed | Head Setting (mm) | Rate of Shear (sec⁻¹) | Shearing Stress, dynes/sq. cm. | | | | | | | | | |
|---|---|---|---|---|---|---|---|---|---|---|---|---|
| | | | Cycle 1 | | Cycle 2 | | Cycle 3 | | Cycle 4 | | Cycle 5 | |
| | | | in-creasing | de-creasing | in-creasing | de-creasing | in-creasing | de-creasing | in-creasing | de-creasing | in-creasing | de-creasing |
| 80 | 10 | 105.1 | 96.2 | 68.2 | 67.1 | 63.0 | 61.9 | 57.8 | 56.4 | 53.9 | 53.8 | 51.1 |
| | 8 | 126.3 | 96.8 | 72.9 | 71.0 | 67.2 | 65.6 | 61.3 | 60.5 | 58.7 | 57.7 | 56.6 |
| | 7 | 142.7 | 95.8 | 76.4 | 73.7 | 71.2 | 66.6 | 65.1 | 63.5 | 62.2 | 61.2 | 60.0 |
| | 6 | 162.9 | 97.7 | 79.3 | 77.9 | 75.3 | 72.8 | 69.4 | 67.9 | 66.3 | 65.6 | 64.6 |
| | 5.5 | 174.3 | 96.4 | 82.7 | 79.9 | | 74.3 | 72.4 | 70.4 | 69.1 | 68.0 | 67.4 |
| | 5 | 190. | 97.5 | 86.6 | 82.7 | 80.1 | 77.7 | 75.8 | 73.3 | 72.3 | 71.1 | 70.8 |
| | 4.5 | 209 | 99.6 | 89.7 | 86.0 | 83.5 | 81.3 | 79.4 | 77.1 | 76.5 | 74.8 | 74.7 |
| | 4 | 232 | 103.3 | 95.2 | 90.7 | 87.9 | 85.7 | 84.5 | 81.7 | 81.3 | 79.5 | 79.6 |
| | 3.5 | 262 | 107.5 | 100.7 | 96.4 | 93.3 | 91.4 | 90.2 | 87.5 | 87.1 | 85.3 | 85.3 |
| | 3 | 302 | 113.4 | 106.7 | 103.4 | 100.0 | 98.8 | 97.2 | 95.0 | 93.9 | 92.8 | 92.7 |
| | 2.5 | 359 | 121.0 | 114.5 | 112.0 | 107.1 | 107.7 | 104.8 | 104.7 | 101.8 | 102.3 | 100.7 |
| | 2 | 444 | 131.7 | 123.0 | 124.0 | 117.3 | 121.0 | 114.5 | 117.4 | 112.4 | 115.4 | 110.6 |
| 20 | 10 | 26.0 | 55.7 | 45.5 | 43.1 | 40.8 | 39.3 | 37.4 | 36.5 | 35.1 | 34.6 | 33.3 |
| | 7 | 35.4 | 59.4 | 51.2 | 46.0 | 46.3 | 42.5 | 43.7 | 40.8 | 40.8 | 38.4 | 39.0 |
| | 5 | 47.2 | 64.3 | 55.7 | 52.2 | 51.4 | 44.4 | 48.9 | 47.1 | 47.3 | 45.1 | 45.2 |
| | 4 | 57.8 | 65.6 | 60.3 | 57.0 | 56.2 | 53.6 | 54.3 | 51.3 | 52.5 | 50.0 | 50.2 |
| | 3 | 75.4 | 71.2 | 63.7 | 64.4 | 60.6 | 61.2 | 58.7 | 59.4 | 57.2 | 57.4 | 55.6 |
| | 2.5 | 89.5 | 72.3 | 67.1 | 67.2 | 64.9 | 64.8 | 61.8 | 61.8 | 60.6 | 61.3 | 59.3 |
| | 2 | 110.6 | 75.7 | 70.8 | 73.4 | 69.9 | 70.8 | 67.4 | 69.8 | 64.9 | 68.0 | 63.8 |

3. Interpretation and Conclusions Regarding Thixotropy.

Inspection of the data given in Table 22 and Figure 31 shows, for the suspension which had set for 18 hours before the test, the fluidity increased at a somewhat lesser rate towards the end of the test, but did not even remotely approach the fluidity of the suspension that had not been allowed to set before the test, i. e. the zero-hour setting period. The time during which the material had been sheared, was considerably longer than the time necessary to reach the equilibrium state as indicated by the time studies of the Series II tests. These tests indicated that the equilibrium state was attained for the 6% suspension after 20 minutes of constant shearing, hence it must be concluded that the 5% suspension in this case has had ample time to arrive at the equilibrium state. The cyclic curves for the suspension which was not allowed to set before the test was started showed only a very slight increase in consistency, as though the fluidity of the material was greater than the equilibrium value at the start of the test. However, the increase is slight and can hardly be noticed in comparison to the increase of fluidity of the 18 hours setting tests when both are plotted on the same scale of Figure 31. From the indications of the Series II tests, it is suggested that the lower curve represents approximately the equilibrium state to which the upper curves should have degenerated. The tests taken at the speed of rotation of 80 r.p.m. lasted 60 minutes which is 3 times as long as was shown by the Series II tests to be necessary for the viscosity to decrease to that of

Figure 31. Cyclic Increase and Decrease of the Shearing Stress - Rate of Shear with the 5% Bentonite Suspension

the equilibrium state. This seeming reluctance of the material to break down is probably due to the fact that the greater portion of it occupied the spaces above and below the inner cylinder and in reality was sheared for only the fraction of the time of the experiment when it was passed through the annular space from the top to the bottom or vice versa.

These effects are undoubtedly due to the fact that not all of the material was being sheared at the same time. As the inner cylinder descended into the cup during the increasing series of rate of shear, fresh material was forced into the annular space from the bottom of the cup. This would have the effect of raising the shearing stresses to a higher value than would have been obtained had all the material been sheared to the same extent. As the core ascended for the decreasing series of rates of shear, the material flowed back through the annular space to the space below the inner cone. The net result was that a portion of the material was sheared at the high rates for only a very short time as compared to the rest of the material. It is possible, that gentle parasitic shearing between the end of the cone and the bottom of the cup could have hastened the setting tendency of the sol during the period it was occupying the lower space. This effect has been reported by other investigators[41] for bentonite sols, and would cause

---

[41] E. A. Houser and C. E. Reed. J. A. C. S. 40:1169 (1930).
J. Phys. Chem. 41:911 (1937).

the higher readings of shearing stress at the higher rates of shears with the successive cycles.

In conclusion, the cyclic tests are not of considerable value because the determination is fraught with empiricism. As mentioned above, Reiner indicates that a hysteresis loop shows that only ordered positions of the particles results in bonds being formed, while its absence means that all positions will be tenable for a bond to form between particles. The former is associated with the thixotropy which is the concern of Freundlich's definition, whereas the latter is the concern of those who recognize "false-body". The same information can be obtained by the time study experiments of the Series II tests, and are much more sound in the basic arrangement of the shearing action applied to the material being studied. The author prefers to consider thixotropy and false body as one because the borderline or intermediate cases will probably be encountered frequently. Obviously the sols used in this investigation are thixotropic because the shearing stress decreased rather slowly under a constant and sustained rate of shear as shown in the Series II tests. A false-bodied material would have approached the equilibrium state very quickly after the shearing was started, but would differ from the Newtonian material by giving a non-linear rheological diagram.

CHAPTER IX

THE RELATION OF YIELD VALUE TO THE FLUID STATE.

One of the most outstanding characteristics of a bentonite suspension is its ability to develop sufficient structure to sustain a load, i. e. possess a yield value,[42] which is generally considered as the critical minimum value of shearing stress below which flow does not occur. This occurs when the suspension is allowed to stand quiescent for a length of time, which in some extreme cases need only be a few seconds.[43] The most recent straightforward demonstration of the ability of bentonite suspensions to sustain a load are the measurements of A. George Stern with his Eykometer (literally, yield meter)[44]. It appears from the work of Stern and others[41,45,46] that bentonite suspensions exhibit a yield value even when it is difficult to detect the gelled condition by visual examination and one would be inclined to designate the system as that of a fluid. The existence of this type of behavior for the bentonite suspensions used in this investigation has been indicated by the qualitative description given at the beginning of Chapter VI. At that point, the tendency of the suspensions to thicken and gel was considered as an indication of the presence of internal structure. Here will be discussed the case in which the gel structure is sufficient to sustain a load

[42] G. Broughton & L. Squires. J. Phys. Chem. 40:1041-3 (1936)
[43] Unpublished experiments of the author.
[44] A. George Stern. U. S. Bureau of Mines, Rept. Inv. 3495(1940)
[45] G. Broughton & R. S. Hand. Trans. Am. Inst. Min. & Met. Engrs. T. P. 1002 (1938)
[46] A. D. Garrison, Trans. Am. Inst. Min. & Met. Engrs. T.P. 1027 (1939)

and the relation of that structure to the fluid properties
of the material.

Bingham[47]

## 1. Historical Resume.

Bingham[47] was the first to relate yield value to fluid properties. He suggested that a minimum critical shearing stress necessary to start the flow of a material possessing rigidity should be subtracted from the total shearing stress applied to the system. Accordingly he writes the following equation as a modification of the fundamental equation for the relationship between rate of shear and shearing stress for liquids.

$$\frac{dv}{d\lambda} = \sigma = \mu \left( \tau - f \right)$$

(43)

where $f$ = the yield value, defined as the minimum shearing stress required to start flow.

$\mu$ = the mobility, the reciprocal of the slope of curve D Figure 3.

$\frac{dv}{d\lambda}$ = the velocity gradient which is equal to $\sigma$, the rate of shear.

$\tau$ = the shearing stress.

When an attempt is made to reduce experimental observations to this form investigators experience difficulty with the Bingham principle.

Buckingham[48] and Reiner,[49] working quite independently, have intergrated Equation 43 in much the same manner that the Poiseuille equation was obtained and thus derive the following

---

47 E. C. Bingham, Fluidity and Plasticity, (McGraw-Hill Book Co., New York, 1922) p. 217.

48 E. Buckingham. Proc. Amer. Soc. Test. Mats. 21:1154 (1921)

49 M. Reiner, Koll. Zeits. 39:80 (1926)

equation for flow through tubes:

$$Q_t = \frac{\pi R^4}{8 L \eta}\left(P - \tfrac{4}{3} p + \frac{p^4}{3 P^3}\right)$$  (44)

where     $p$ = the minimum critical pressure corresponding to the yield value necessary to start flow.

          $P$ = the total pressure causing flow.

Buckingham[48] apparently tried to test Equation 44 experimentally and as a result suggested that at very low rates, the flow occurs in plug form, being lubricated by a thin and very fluid envelope. He added a corrective term containing constants for the fluidity of the water envelope and its thickness. The constants as yet have never been evaluated. Green's[50] tests on clay and soil pastes had shown that the plug type of flow really exists. Scott Blair and Crowther[51] investigated the flow of clay and soil pastes quite extensively and found the existence of a yield value, i. e. the clay pastes would sustain a shearing stress below a certain critical value which led them to add a yield value term for the thin water envelope. As a result, Equation 44 now takes this form:

$$Q_t = \frac{\pi R^4}{8 L \eta}\left(P - \tfrac{4}{3} p + \frac{p^4}{3 P^3}\right) + \frac{\pi R^3 \varepsilon (P-a)}{2 L \eta'}$$  (45)

where     $\varepsilon$ = the thickness of the fluid film.

          $\eta'$ = the coefficient of viscosity of the fluid envelope

          $a$ = the yield value of the fluid envelope.

[50] H. Green, Proc. Am. Soc. Test. Mat. 20:450 (1920)
[51] G. W. Scott Blair, and E. M. Crowther, J. Phys Chem. 33: 321 (1929)

Scott Blair[52] holds that Equation 45 has been, in general, adequately confirmed from a qualitative and semi-quantitative standpoint. It is this work that is most generally quoted to offer confirmation of the Bingham principle.

For higher values of the shearing stress or pressures, the terms to the right of the dotted line drawn through Equation 45 can be neglected, and in effect Equation 46 is obtained.

$$\frac{q}{t} = \frac{\pi R^4}{8 L \eta} \left( P - \frac{4}{3} p \right) \tag{46}$$

Equation 45 represents a straight line with slope of $\eta$ with an intercept on the pressure axis at $4/3\, p$.

As a result of the uncertainty of the experimental data for the region just after flow has commenced, it has become customary for many investigators to plot the upper portions of the curve where reasonably straight line data appear. From this region, extrapolation to the stress axis gives an intercept that has been termed the yield value. Hatschek[56] has objected to this practice on grounds that the linearity may be only illusionary as due to the scale used in plotting. The discerning rheologists admit the validity of Hatschek's objection, but take refuge in the necessity and usefulness of the simplification pending development of a more exact and less cumbersome means of making the measurements. In some cases, the deviation from the Buckingham-Reiner flow curve is not great.

52 G. W. Scott Blair,"Industrial Rheology" (Blakiston, Son & Co.,Philadelphia, 1928) p.33
56 E.Hatschek, op. cit. pp. 209-15.

Houwink[53] considers that the Bingham relation has been
repeatedly confirmed and cites as examples the work of Wilson
and Hall[54] and Scott Blair and Crowther.[51]  The former authors
give flow pressure diagrams for suspensions of Tennessee ball
clay that show an intercept on the pressure axis.  The latter
authors have made the distinct contribution showing that suspen-
sions of rigid particles do show true rigidity, but fail to
confirm the curvilinear portion of the flow curve demanded by
the Buckingham-Reiner equation, 51.[55]

Van Nieuwenburg[57] suggests that the curved portion is
very rarely the most important part, a proposal with which
the author can hardly agree.  Van Nieuwenburg[58] also points
out that one of the first questions to be decided is the reality
of the yield value in order to distinguish between flow curves
of type B and type C shown in Figure 3.  For crystals and poly-
crystalline materials the existence of a yield value is very
definite.  However, passing to the

> "less rigid structures, where still are orientated
> micelles or groups of molecules, but no real crystals,
> we find that the reality of $f$ (yield value) begins
> to waver.  We shall be able to make a—vague—dis-
> tinction between configurations where still and such
> where no longer an uninterrupted skeleton of particles,

[53] R. Houwink, Elasticity, Plasticity, and Structure of Matter
  (University Press, Cambridge, 1937) p.346.
[54] R. E. Wilson and F P. Hall. J. Amer. Ceram. Soc. 5:916(1922)
[22] G. W. Scott Blair. Physics, 4:113 (1933)
[57] C. J. Van Nieuwenburg. First Report on Viscosity and Plasticity,
  p. 167.
[58] Ibid.,p.166.

in themselves undeformable, exists and we may
expect that the presence of such a skeleton
will be accompanied by the presence of a yield
value.  It is evident that then the phenomena
of thixotropy must be perfectly normal and that
this leads to a serious complication of the case.
With an undisturbed skeleton there is a yield
value: after powerful agitation, however, it dis-
appears completely.* In future work it will be
advisable to take this complication more into
account than has been done formerly."

Obviously, van Nieuwenburg has in mind the frequently
encountered middle case existing between his extremes: "an
undisturbed skeleton" and "after powerful agitation".  Houwink
discusses the observability of the yield value in his chapter
in the Second Report on Viscosity and Plasticity.[59]  He points
out that difficulty is usually experienced in detecting the
first appearance of flow and intimates that the investigation
may best be resolved into two parts, first, by appropriate
experimental arrangement the whole course of the $\sigma$ vs. $\tau$ curve
may be determined, then later investigations may lead to the
fixation of the yield point $\tau_f$ .  On the other hand, according
to Houwink, when the $\sigma$ vs. $\tau$ curve goes through the origin,
($\sigma=0$ , $\tau=0$) it is mandatory that there is no indication of a
yield point.

---

* The underscore is by the present author.
[59] R. Houwink.  Second Report on Viscosity and Plasticity, p.166.

2. The Relation of Yield Value to the Present Investigation.

With the assurance of the forehand knowledge that bentonite suspensions exhibit the yield value phenomena, this investigation was directed toward the careful determination of shearing stress- rate of shear data for this material over a range from very low to relatively large values. The expression of the data in terms of shearing stress and rate of shear is in accordance with the vigorous recommendation of the Amsterdam Committee on Viscosity and Plasticity.[60] The curves obtained by plotting the data do not show the existence of any yield value as required by Bingham, since in all cases they appear to pass through the origin as the values of shearing stress and rate of shear are made very small. It was expected that yield value would be indicated and the rheological curves would be of the Bingham type as illustrated by curve B in Figure 3. This behavior has been reported by Rieke and Tscheischvila[61], Broughton and Hand[20], Ambrose and Loomis[19] specifically for bentonite sols and by many others for clay suspensions of more or less indefinite but analogous composition.

The rheological curves obtained in this work all pass through the origin, therfore, Houwink's criteria indicates there is no yield value. Such an indication is in agreement with van Nieuwenburg's "presence-of-structure" criteria since

---

[60] Second Report. p. 171. see also M. D. Husey, J. Rheol. 3:196 (1932)

[61] R. Rieke & Ing. L. Tscheischvilli Ber d. Deut. Keram. Ges. 17: 1-46 (1936).

the suspensions have all had varying degrees of mechanical
working before the test, and during the test the rate of shear
would be expected to destroy any continuous structure present
in the suspensions. The equilibrium curves of the Series II
tests are plotted from data which derives from the initial
conditions of maximum structure in the case of the 18-hour
standing period, and zero structure in the case of the zero
standing period. Both cases arrive at the same fluidity after
approximately 15-20 minutes of shearing at any constant rate
and indicate no yield value. It appears that no matter how
small the rate of shear is made, the shearing stress is a
very small value, approaching zero as the rate of shear ap-
proaches zero. According to the Bingham principle, as the
rate of shear approaches zero the shearing stress approaches
some finite value which is the yield value.

By virtue of the above indications to the nonexistence
of yield value in the bentonite suspensions, it appears that
the uncertainty felt by van Nieuwenburg and Houwink towards
the "experimental observability of the yield value" on the
Bingham diagram has been confirmed, since prior knowledge
indicates that structural rigidity is a common manifestation
of aqueous bentonite suspensions, and has been detected here
by the qualitative experiments described in the beginning of
Chapter I. In view of this situation, the suggestion of Houwink
that the value of the yield point be fixed by a separate inves-
tigation was entertained. Following from this point, the ex-
periments in the next section were planned and executed.

3. Experimental Observation and Study of Yield Value.

Series IV Tests.

It was reasoned that if a material possessing a yield value was present in the cup of the Goodeve apparatus with the cone suspension in place, wen the rotation is started, the cone assembly will turn with the cup, until the opposing torque becomes sufficient to break the structure in the material tending to bind the cup to the cone. Under normal operation, even at the lowest speed of 1.25 r.p.m. the yield occurred so quickly that no exact measurements could be taken. As a means of circumventing this difficulty, an electric synchronous clock motor, self starting and geared to turn at 4 revolutions per hour, was mounted adjacent to the Goodeve instrument. A silk thread was fastened to a drum on the clock motor and wound around different drum-like sections of the lower cup assembly having different diameters. In this manner, four different combinations of diameters gave speeds of 0.007, 0.014, 0.030, and 0.059 r.p.m. A full circle protractor, reading to 0.5 degrees, was fitted to the lower cup assembly which permitted the determination of the angular deflection through which the lower cup had been turned. With this arrangement, when a material possessing a yield value was in the annular space of the cup and cone and the clock motor started, a certain number of degrees of twist could be observed on the lower scale and the corresponding deflection obtained on the upper scale fastened to the inner cone. The deflection registered by the inner cone for any given twist of the cup, is the measure of

the shearing torque that is exerted by the torsion wire upon
the material in the annular space. It can be expressed as
dynes per square centimeter in the conventional way by mul-
tiplying the degrees of deflection by the wire constant and is
called, as has been used consistently above, the shearing stress.
The shear that is suffered by the sample as a result of the
shearing stress is measured by the difference in reading of
the upper and lower scales. Since shear is a displacement
and is measured by a distance, it can be conveniently expressed
as degrees. The symbol for the shearing stress, $\tau$ , has been
used throughout this work; for the shear angle the symbol $\varphi$
will be used.

The arrangement described above is similar to that used
by Schwedoff[62] Hatschek and Jane,[63] McDowell and Usher,[64]
Richardson,[65] Evans and Reid,[66] Russell[67] and Brimhall and
Mixon.[68] These workers did not arrange to drive the apparatus
by a motor, but used the method only as an empirical means of
testing gel strength. Evans and Reid applied the twist manually,
in steps, and report that it was difficult to obtain constant
values and that time effects complicate the readings. *

[62] T. Schwedoff. J de Physique 8:381 (1899)
[63] E. Hatschek, and R. S. Jane. Kolloid. Zschr. 39:300 (1926)
[64] C. M. McDowell, & F. L. Usher. Proc. Roy. Soc. A,131:409(1931)
[65] E. G. Richardson, J. Agric. Sci. 23(II) 176 (1933).
[66] P Evans, and A. Reid. Trans. Min. and Geol. Inst. of India
      32:128 (1936)
[67] J. L. Russell. Proc. Roy. Soc. A. 154:557 (1936).
[68] B. Brimhall & R. M. Mixon. J Ind. & Eng. Chem. Anal. Ed.
      11:358 (1939)
* As this paper was being written, an article appeared by
  Hobson (J. Pet. Inst.,26:533-64 (1940)) describing the use
  of this type of apparatus driven by a very low speed,

The various bentonite suspensions were tested for the conditions of fluidity recorded in the headings of the data tables given below. Before any setting period, the suspensions were subjected to the shearing treatment in the structure breaker that was noted in the Series I tests to be sufficient to convert them into the most fluid condition. The temperature was maintained at 25°C. In all the tests wire MO was used and the separation between the walls was kept at 2.0 mm. When it was necessary for the sample to remain in the cup for extended lengths of time during the setting period, the cup was covered with moistened blotting paper or the bakelite cap. To avoid the possibility of disturbing the sample after a setting period, the end effect correction was omitted by not removing the material above the rim of the inner cone. The zero readings on the upper and lower scales were taken before and after the standing period and served as a partial check on possible disturbance of the test before it was started. When all was in readiness, a snap switch in the clock motor circuit was closed while the lower scale pointer was watched to see if irregular or jerky starting occurred. If such happened, the test was

---

synchronous electric clock motor in connection with the measurement of the gel strength of certain oil well drilling muds. Hobson's results are similar to those obtained here, except he fails to note the effect of varying the rate of loading that is described below. In addition, he has chosen to present his data as plots of the torque angle of the wire versus the total angle of the applied twist, which does not show the shear angle by which the sample is distorted, and also masks the indications of a range of elastic behavior.

repeated. When the lower scale pointer indicated an angle sweep of multiples of $5^o$, the upper scale was read quickly to obtain the corresponding deflection of the inner cone. The lag between the two readings was considered insignificant at the very low speed of rotation used which was constant at 0.030 r.p.m. for all tests. Readings were continued until the desired amount of data was obtained. The data obtained are reported as corresponding shear angles and shearing stresses for the various indicated setting periods.

The data given in Table 23 indicate that the 4% suspension develops only a very slight yield value after 18 hours of quiescent standing before the test was started. In this case, after a very slight initial maximum the shearing stress was constant at about 0.20 d./sq.cm. through a shear angle of approximately $100^o$. Since the shearing stress was so small the data could not be plotted conveniently in a graphical diagram. The curves of Figure 19 of the Series I tests for the 4% suspension show considerable difference between the material that was given 100 strokes in the structure breaker and the mildly disturbed material, which would lead one to expect that a quite apprecialbe yield value would be observed in the above test. Apparently, the concentration of the bentonite particles is insufficient to allow more than a very weak linking of structure throughout the entire mass of the suspension. However, the structure that is formed, even though very weak in texture, does seem to be sufficient to interfere considerably with the free motion of the liquid as is indicated by shift in the curves of

## Table 23

### Shearing Stress – Shear Data

#### 4% Suspension
18-Hour Setting Period.

| Temperature 25° | | Wire MO |
|---|---|---|
| Angle of Cup Twist | Shear Angle | Shearing Stress |
| deg. | deg. | d/sq.cm. |
| 0 | 0 | 0 |
| 5 | 4.1 | 0.23 |
| 10 | 9.1 | 0.23 |
| 20 | 19.1 | 0.23 |
| 30 | 29.1 | 0.23 |
| 40 | 39.2 | 0.20 |
| 50 | 49.2 | 0.20 |
| 60 | 59.2 | 0.20 |
| 70 | 69.2 | 0.20 |
| 80 | 79.2 | 0.20 |
| 90 | 89.2 | 0.20 |
| 100 | 99.2 | 0.20 |

## Table 24

### Shearing Stress – Shear Data
#### 5% Suspension

| Temperature 25° | 12 Hours Set | | 1 Hour Set | Wire MO |
|---|---|---|---|---|
| Angle of Cup Twist | Shear Angle | Shearing Stress | Shear Angle | Shearing Stress |
| deg. | deg. | d/sq.cm. | deg. | d/sq.cm. |
| 0 | 0 | 0 | 0 | 0 |
| 5 | 0.5 | 1.15 | 4.5 | 0.13 |
| 10 | 1.6 | 2.15 | 9.4 | 0.15 |
| 15 | 3.4 | 2.97 | 14.4 | 0.15 |
| 20 | 6.1 | 3.56 | 24.5 | 0.13 |
| 25 | 10.3 | 3.76 | 24.5 | 0.13 |
| 30 | 15.6 | 3.69 | 29.5 | 0.13 |
| 35 | 21.3 | 3.51 | 34.5 | 0.13 |
| 40 | 27.4 | 3.23 | 39.5 | 0.13 |
| 45 | 33.5 | 2.94 | 44.5 | 0.13 |
| 50 | 38.9 | 2.84 | 49.5 | 0.13 |
| 60 | 50.0 | 2.56 | 59.5 | 0.13 |
| 70 | 60.8 | 2.36 | 69.5 | 0.13 |
| 80 | 71.2 | 2.25 | 79.5 | 0.13 |
| 90 | 81.3 | 2.23 | 89.5 | 0.13 |
| 100 | 91.5 | 7.18(1) | 99.5 | 0.13(1) |

(1) Dropped to zero stress after rotation was stopped.

Figure 19. Since only a very slight yield value was observed on the 4% suspension after 18 hours standing in the apparatus, it was considered unnecessary to examine the suspensions of lesser bentonite concentrations.

Tables 24, 25, 26, and 27 contain the shearing stress-shear data that was obtained for the 5, 6, 7, and 8 per cent suspensions, respectively. The different setting periods that were employed are given at the column headings. The data of these tables are plotted in Figures 32, 33, 34 and 35 for the 5, 6, 7, and 8 per cent suspensions respectively. The indications of these figures can best be discussed by comparison with the typical stress-strain diagram used by the mechanical engineers for the expression of the tensile strength of iron, steel and other materials. A close similarity exists between the stress-strain diagram and the shearing stress-shear diagram shown by Figures 32, 33, 34 and 35.

A typical stress-strain diagram[69] is shown in Figure 36.
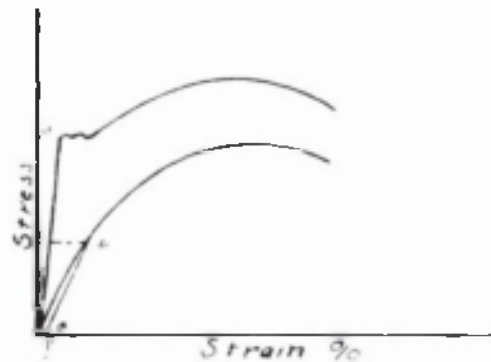


Figure 36.   Typical Stress-Strain Diagram for Metals.

69 O. W. Eshbach. Handbook of Engineering Fundamentals. (New York, John Wiley & Sons, 1936) p.5-05
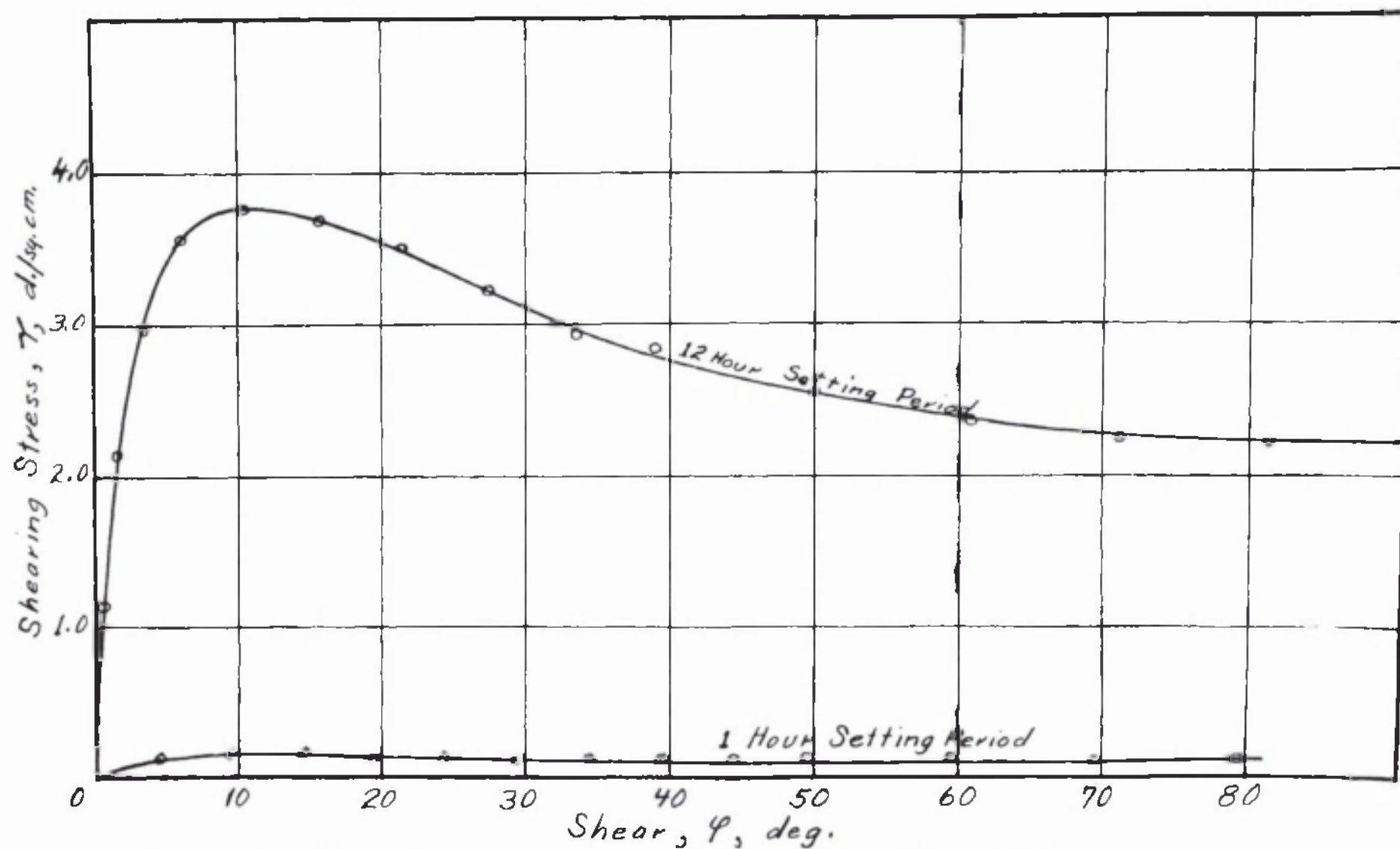
Figure 32. Shearing Stress - Shear Diagram for the 5% Suspension.
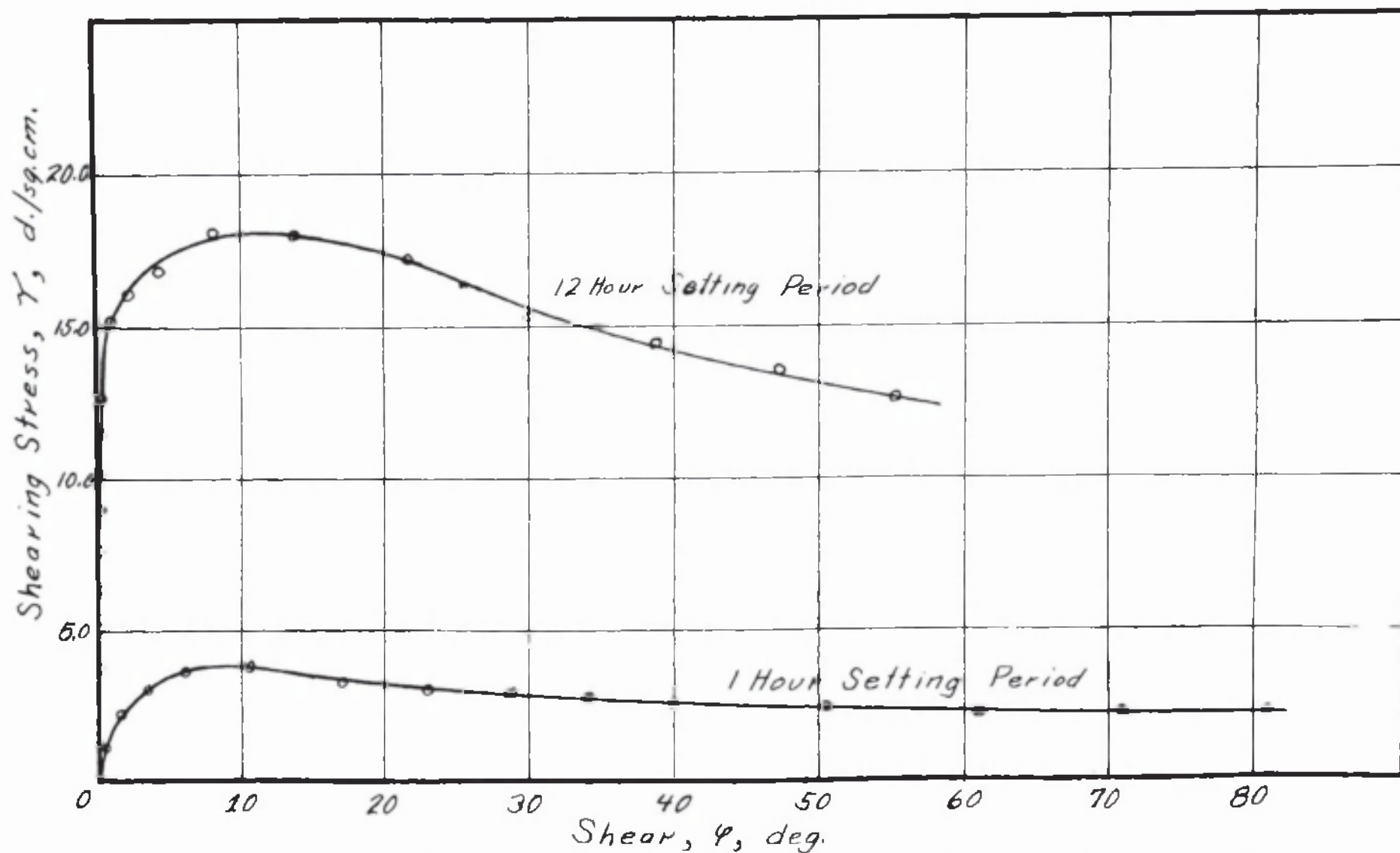
Figure 33. Shearing Stress - Shear Diagram for the 6% Suspension.
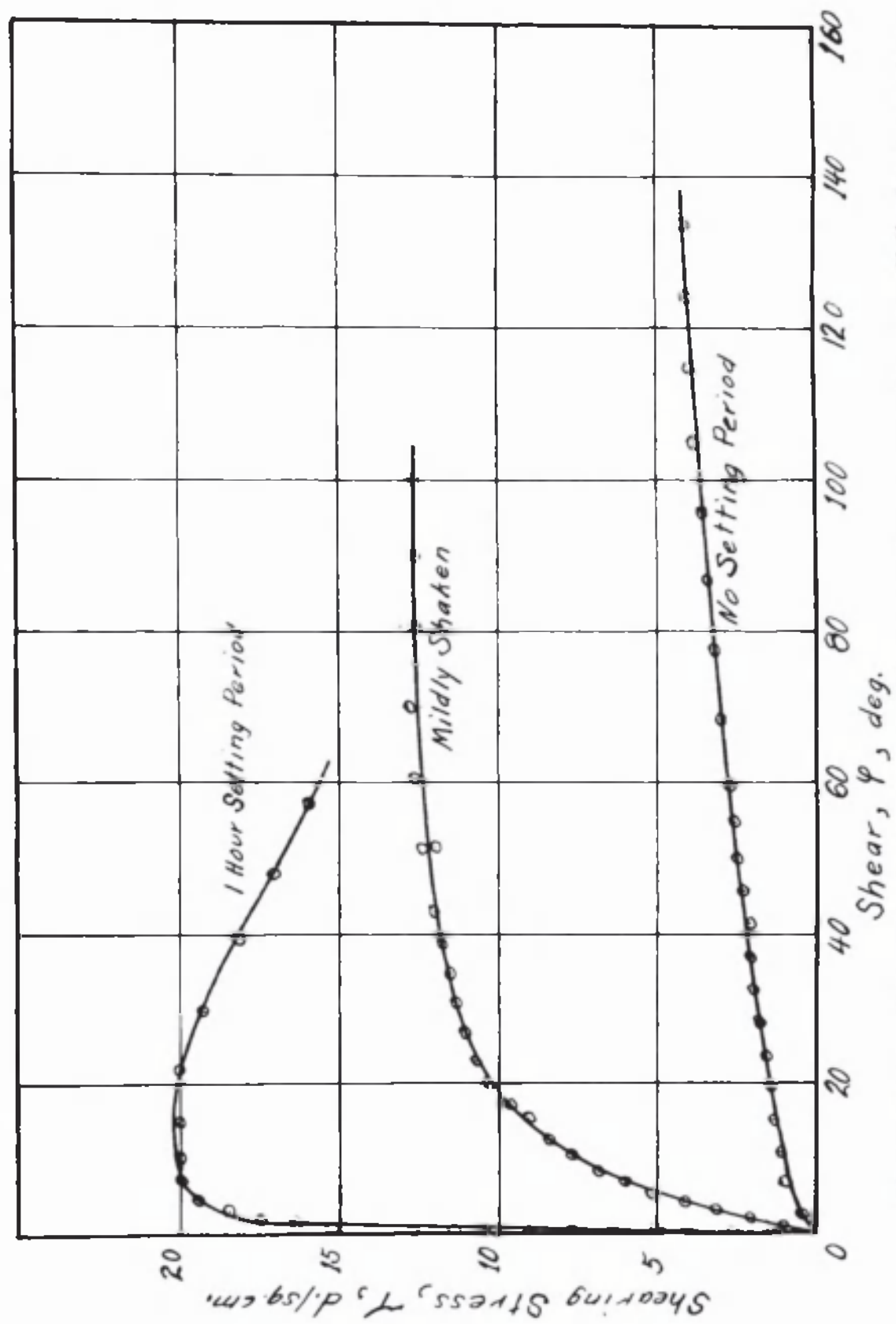
Figure 34. Shearing Stress – Shear Diagram for the 7% Suspension.
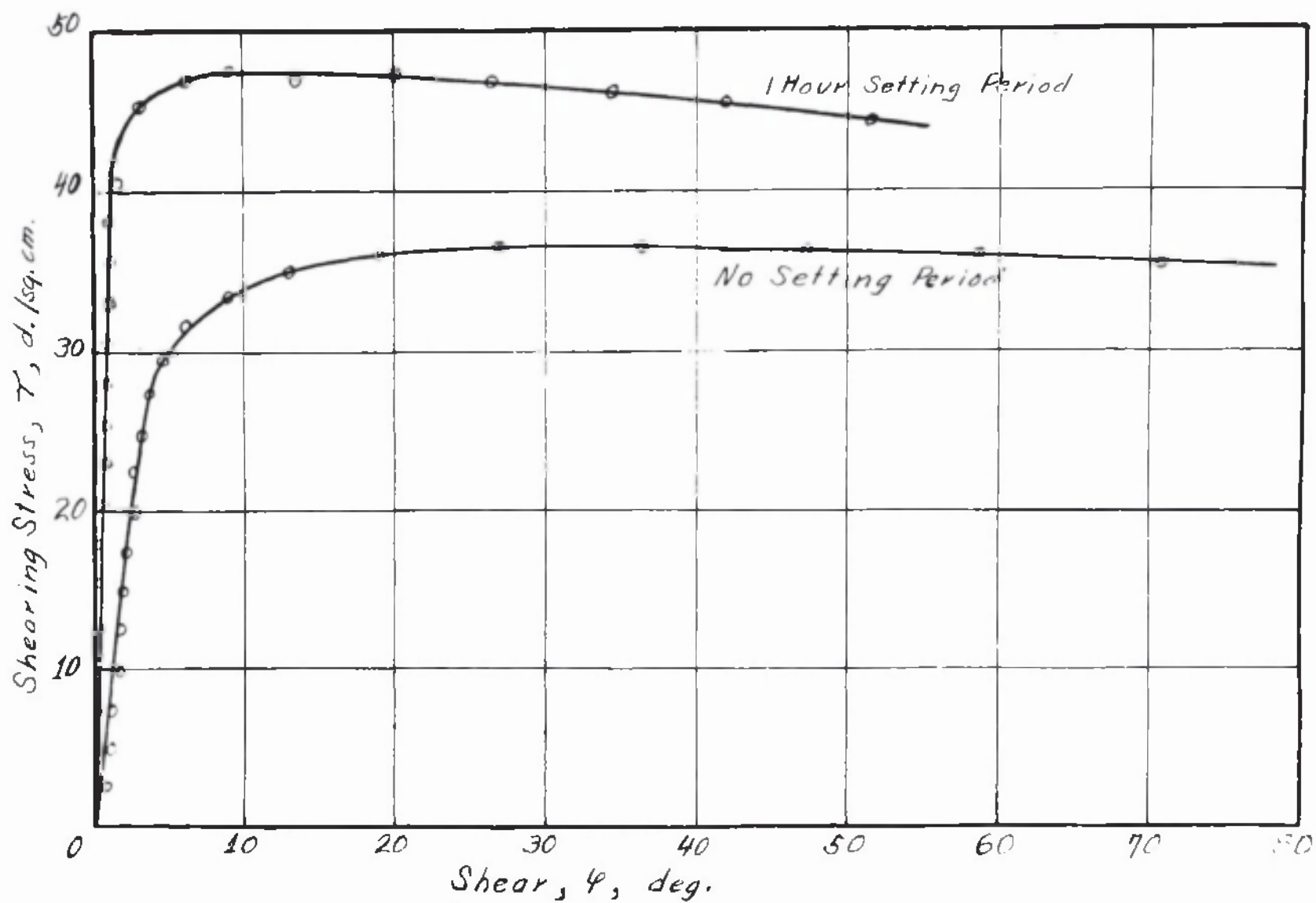
Figure 35. Shearing Stress - Shear Diagram for the 8% Suspension.

The chart's vertical axis is labeled "Shearing Stress, $\tau$, d./sq. cm." with values 10, 20, 30, 40, 50. The horizontal axis is labeled "Shear, $\varphi$, deg." with values 0, 10, 20, 30, 40, 50, 60, 70, 80. Two curves are shown, labeled "1 Hour Setting Period" and "No Setting Period".

Table 25

Shearing Stress - Shear Data.

6% Suspension

| Temperature 25° | | | | Wire MO |
|---|---|---|---|---|
| | 12 Hours Set | | 1 Hour Set | |
| Angle of | Shear | Shearing | Shear | Shearing |
| Cup Twist | Angle | Stress | Angle | Stress |
| deg. | deg. | d/sq.cm. | deg. | d/sq.cm. |
| 0 | 0 | 0 | 0 | 0 |
| 5 | 0 | 1.28 | 0.5 | 1.15 |
| 10 | 0 | 2.56 | 1.6 | 2.16 |
| 15 | 0 | 3.83 | 3.3 | 2.99 |
| 20 | 0.1 | 5.12 | 6.1 | 3.56 |
| 25 | 0.2 | 6.38 | 10.6 | 3.68 |
| 30 | 0.2 | 7.66 | 17.1 | 3.31 |
| 35 | 0.3 | 8.95 | 23.0 | 3.07 |
| 40 | 0.3 | 10.15 | 2?.8 | 2.86 |
| 45 | 0.3 | 11.41 | 34.2 | 2.76 |
| 50 | 0.4 | 12.69 | 39.8 | 2.61 |
| 60 | 1.0 | 16.12 | 50.6 | 2.40 |
| 70 | 4.4 | 16.60 | 61.3 | 2.22 |
| 80 | 13.8 | 16.96 | 71.3 | 2.22 |
| 90 | 30.1 | 16.35 | 81.3 | 2.22 |
| 100 | 47.3 | 13.50(1) | 91.5 | 2.18 |

(1) Dropped to a shearing stress of 0.10 d./sq.cm.
in 1 hour after rotation was stopped.

# Table 26

## Shearing Stress – Shear Data
## 7% Suspension

Temperature 25°                                                      Wire NO

| Angle of Cup Twist deg. | 1 Hour Set | | Wildly Shaken[1] | | No Set | |
|---|---|---|---|---|---|---|
| | Shear Angle deg | Shearing Stress d/sq.cm. | Shear Angle deg | Shearing Stress d/sq.cm. | Shear Angle deg. | Shearing Stress d/sq.cm. |
| 0 | 0 | 0 | 0 | 0 | 0 | 0 |
| 5 | 0 | 1.28 | 0.8 | 1.07 | 2.5 | 0.64 |
| 10 | 0 | 2.56 | 1.9 | 2.07 | 6.4 | 0.92 |
| 15 | 0 | 3.97 | 2.? | 3.12 | 10.6 | 1.13 |
| 20 | 0 | 5.11 | 3.? | 4.14 | 15.0 | 1.2? |
| 25 | 0 | 6.39 | 4.9 | 5.14 | 19.5 | 1.41 |
| 30 | 0 | 7.67 | 6.6 | 5.98 | 23.7 | 1.61 |
| 35 | 0.2 | 8.91 | ?.2 | 6.85 | 2?.2 | 1.74 |
| 40 | 0.2 | 10.12 | 10.1 | 7.64 | 32.5 | 1.92 |
| 45 | 0.3 | 11.43 | 12.2 | ?.38 | 37.0 | 2.05 |
| 50 | 0.4 | 12.70 | 15.4 | 9.11 | 41.5 | 2.2 |
| 55 | | | 16.9 | 9.74 | 45.9 | 2.3 |
| 60 | 0.7 | 15.20 | 19.8 | 10.28 | 50.2 | 2.5 |
| 65 | 1.3 | 16.30 | 22.9 | 10.75 | 54.8 | 2.6 |
| 70 | 2.0 | 17.41 | 26.7 | 11.07 | 59.6 | 2.7 |
| 75 | 3.0 | 18.45 | 30.8 | 11.30 | | |
| 80 | 4.5 | 19.35 | 34.9 | 11.52 | 68.5 | 2.0 |
| 85 | 6.9 | 20.0 | 3?.7 | 11.83 | | |
| 90 | 10.4 | 20.4 | 42.7 | 12.12 | 77.5 | 3.2 |
| 95 | 15.4 | 20.4 | | | | |
| 100 | 22.0 | 20.0 | 51.5 | 12.42 | 86.7 | 3.4 |
| 110 | 38.8 | 18.2 | 60.6 | 12.63 | 95.? | 3.6 |
| 120 | 57.4 | 16.0[2] | 70.? | 12.77 | 105.3 | 3.8 |
| 130 | | | 80.8 | 12.58 | 114.7 | 3.9 |
| 140 | | | 90.6 | 12.65 | 124.5 | 4.0 |
| 150 | | | 100.5 | 12.67[3] | 134.0 | 4.1[4] |

(1) Container inverted several times after standing approximately 200 hours.
(2) Dropped to a shearing stress of 1.41 d./sq.cm. in 20 minutes after rotation was stopped.
(3) Dropped to a shearing stress of 0.87 d./sq.cm. in 15 minutes after rotation was stopped.
(4) Dropped to a shearing stress of 0.95 d./sq.cm. in 5 minutes after rotation was stopped.

## Table 27

### Shearing Stress Shear Data
### 8% Suspension.

| Angle of Cup Twist | 1 Hour Set | | No Set[1] | |
|---|---|---|---|---|
|  | Shear Angle | Shearing Stress | Shear Angle | Shearing Stress |
| deg. | deg. | d/sq.cm. | deg. | d/sq.cm. |
| 0 | 0 | 0 | 0 | 0 |
| 10 | 0 | 2.56 | 0.5 | 2.43 |
| 20 | 0 | 5.12 | 0.9 | 4.88 |
| 30 | 0 | 7.68 | 1.0 | 7.41 |
| 40 | 0 | 10.24 | 1.5 | 9.84 |
| 50 | 0 | 12.80 | 1.6 | 12.39 |
| 60 | 0 | 15.36 | 1.7 | 14.93 |
| 70 | 0.2 | 17.87 | 2.0 | 17.43 |
| 80 | 0.5 | 20.4 | 2.6 | 19.8 |
| 90 | 0.5 | 22.9 | 2.5 | 22.4 |
| 100 | 0.6 | 25.4 | 3.0 | 24.8 |
| 110 | 0.6 | 28.0 | 3.7 | 27.2 |
| 120 | 0.7 | 30.6 | 4.6 | 29.5 |
| 130 | 0.9 | 33.0 | 6.1 | 31.7 |
| 140 | 0.9 | 35.6 | 8.9 | 33.5 |
| 150 | 0.9 | 38.1 | 13.1 | 35.0 |
| 160 | 1.3 | 40.5 | 19.0 | 36.1 |
| 170 | 1.4 | 43.3 | 26.9 | 36.6 |
| 180 | 3.1 | 45.3 | 36.5 | 36.5 |
| 190 | 6.2 | 47.0 | 47.3 | 36.4 |
| 200 | 13.5 | 47.0 | 58.8 | 36.1 |
| 210 | 26.4 | 46.9 | 70.7 | 35.6 |
| 220 | 42.0 | 45.6 | 82.8 | 35.1 |
| 225 | 51.7 | 43.3[2] | 88.7 | 34.8[3] |

(1) As obtained by 300 strokes in the Structure Breaker.
(2) After stopping rotation, returned to: 24.4 d/sq.cm.
                        in 10 minutes
                        23.5 d/sq.cm.
                        in 15 minutes
                        23.3 d/sq.cm.
                        in 20 minutes.
(3) After stopping rotation, returned to 7.3 d/sq.cm. in 27 minutes.

Two cases are recognized; one (represented by the upper curve) shows a relative constant stress at the yield point, as the strain is increased for a short distance, then advancing to a maximum and quickly dropping off as complete failure takes place. The first part of the curve obeys Hooke's Law of elasticity until yield occurs. Ideally, yield value can be defined as the value of the stress at which Hooke's law just fails. The second case is represented by the lower curve in Figure 36 which shows no definite point at which yield can be recognized since linearity does not exist. In this case yield point is defined arbitrarily as the stress which just causes 0.1 or 0.2% permanent elongation of the specimen. It is represented by the ordinate at point b, the line a b, being drawn parallel to the apparent linear section of the curve near the origin.

The shearing stress and shear determined in the Series IV tests and shown by Figures 32, 33, 34, and 35, correspond respectively to the stress and strain of Figure 36. Therefore, the criteria for the yield point used in connection with the stress-strain diagram can be used with shearing stress-shear diagrams of the bentonite suspensions.

The shearing stress-shear diagram for the 5% suspensions given by Figure 32 is most apparent with the test in which the material had previously set for 12 hours. In this case the first part of the curve does not show a linear section corresponding to the operation of Hooke's law, therefore it cannot be determined with any degree of certainty just where

yield occurs. The curve appears to be similar to the lower
curve of Figure 36 which would indicate that the yield point
is to be determined by an arbitrary specification as indicated
above for metals. However, it is more probable that yield
has taken place from the very start of the application of the
shear and reaches an ultimate value at approximately 3.80
dynes/sq.cm. The test in which the suspension previously had
set for 1 hour showed only a very slight maximum and it was
evident that the setting time was insufficient for a notice-
able yield value to develop. It is of interest to note that
after the maximum was passed the shearing stress dropped to
a much lower value which was constant. The footnote on Table
24 records that the shearing stress reduced to zero when the
forward motion of the lower cup was stopped at the conclusion
of the test. This would indicate that the material had been
completely converted into the liquid state.

The results of the shearing stress-shear determinations
with the 6, 7, and 8 per cent suspensions as shown by Figures
33, 34, and 35, respectively can be considered as a group. It
is seen that when the suspensions had been allowed to set before
the test for 12 hours in the case of the 6% suspensions and for
1 hour in the case of the 7 and 8 per cent suspensions the
curves rise almost coindicent with the axis indicating a large
shearing stress caused by only a slight amount of shear. This
portion of the curve appears to be linear up to a point at
which a relatively sudden break occurs whereupon it rapidly
bends to a maximum and then drops off as the shear angle becomes

larger and larger. This behavior appears to be similar to the upper wire of Figure 36 with the exception of the plateau at the end of the linear section. It is concluded that these suspensions are acting as solids and obey Hooke's law over the linear range. Yield takes place where the linear section ends which occurs at a shearing stress of approximately 14.0, 16.5 and 40.8 dynes/sq.cm. for the 6, 7, and 8 per cent suspensions respectively. The curve for a 1-hour set period with the 6% suspensions given in Figure 33 does not show the linear section that is obtained with the curve for the test preceded by the 12-hour set period. In this case it appears that yield has taken place from the onset of the shear increase, the shearing stress rising to maximum and dropping off to a constant value. A test with the 7% suspension shown in Figure 34, in which the material was shaken mildly before placing in the sample cup, has given a curve that rises from the origin to a constant value insofar as the test was taken. This curve does not possess a linear portion rising from the origin, hence it is concluded that the mild agitation before the start of the test had broken the continuous structure and the material was acting as a very viscous liquid under the influence of the very slow rate of shear.

A test with the 7% suspension is shown on Figure 34 in which the material had been given 200 strokes in the structure breaker previous to being placed in the viscometer cup. This is the equivalent of no setting period and shows that no structure exists within the experimental limits. It is of interest

to compare this curve with the curve for the no-setting
period determined in the same way using the 8% suspension
which is shown on Figure 35.  In this case, a section is
evident at the beginning which appears to be linear and would
give a yield value at about 27 d./sq.cm.  The maximum is ob-
tained somewhat more slowly  than in the former cases where
a yield point is evident and persists over a much greater
range of shear angle.  The same tendency for the flattened
maximum is present with the curve representing the 1-hour set
period test.  The behavior is considered to be the result of
the relatively (in comparison with the progressively more di-
lute 7, 6, and 5 per cent suspensions) more intense structure
building activity inherent with the 8% suspension which causes
the broken bonds to heal and re-form in the face of the in-
exorable forward increase of the shear angle.

The considerable difference between the curves of the
7 and 8 per cent suspensions obtained for the test with no
setting period is noteworthy and indicates that a critical
average spacial separation may exist between the bentonite
particles.  When the average separation of the bentonite
particles is less than this critical distance, the rate of
gelatin or structure formation is greatly speeded.  Bentonite
suspensions of 9 and 10 weight per cent concentration had
been prepared but were not used since they were almost un-
manageable, and could be poured only with difficulty from the
container even after very vigorous stirring.

In the foregoing interpretations of the shearing stress-

shear curves, it has been assumed without direct proof that true rigidity actually existed and that the shearing stress at which yield occurred, i. e. the yield value, could be determined by the "failure of Hooke's law" criteria. A direct confirmation of the ability of bentonite in water suspension to form a rigid gel and sustain a shearing stress or load is offered by the following experiment. A sample of the 7% bentonite suspension was given the customary treatment in the structure breaker, placed in the viscometer cup and the inner cone lowered into position. After a setting period of 165 minutes, a twist of 25.0° was given the lower cup. This twist was immediately registered by the scale on the inner cone. At the end of 105 minutes, after the twist was applied the inner cone scale reading was 24.9° and after 165 minutes 24.8°. This experiment has indicated quite conclusively that structure actually was present in the suspension. This behavior has been confined in several instances for setting periods of 5-10 minutes.

At first it would appear that the maximum found in the stress-shear diagrams for the bentonite suspensions could be considered as analogies of the ultimate tensile strengths found in metals, which are given by the maxima in Figure 36. However, this comparison is illusionary because it was found that the material in the region after the curve had indicated yield, but before it arrived at the maximum, is in what might be called a semi-liquid state. When the shear advance is

stopped in this region it was found that the shearing stress dropped slowly to some value greater than zero but less than the yield value. Consistent results could not be obtained, and because of time effects which tend to re-jel the material it was difficult to study this effect of stress release. However, it is sufficient to know that the material was unable to support the indicated shearing stress in this region. Thus the maximum cannot be called an upper yield value and related to the ultimate tensile strength as in metals practice.

In the footnotes given in Tables 24, 25, 26, and 28 observations are recorded that indicate the ability of the material to relieve the shearing stress after the yield point and maximum had been passed and the forward motion of the shear stopped. For the 5, 6 and 7 per cent suspensions, the stress seems to decrease over a period of time to a quite small value which is a reasonable approach to the zero stress expected when it is remembered that the suspension structure ceaselessly endeavors to re-establish itself. However, the 8% suspension showed rather large residual stress values when the shear was stopped which is considered to be due to the relatively greater tendency of the suspension to form structure. It is interesting to note that this unloading stress had dropped in 10 minutes to a value less than the yield value of the material. This could be construed to mean that the drop of the shearing stress to zero was arrested by the unrestricted formation of structure when the shearing action was stopped.

### 4. Observation of the Location of Yield.

It was of interest to determine whether the yield took place at the wall or in the main body of the geled material. Qualitative information was obtained by the following experiment, which represents the best results of a number of preliminary trials. A sufficient amount of the well dispersed bentonite suspension (7%) was placed in the cup to cover the top of the inner cone. The level of the bentonite suspension was then carefully lowered by means of the suction flask until the rim of the inner cone was just visible under the surface. This left the recess on the top of the inner cone filled with material, giving an unbroken and level surface from the center spindle to the cup wall. After allowing the material to set undisturbed for approximately 3 hours, a few specks of finely powdered anthracite coal were dropped on to the surface of the gel. When the clock motor was started no appreciable displacement of the black coal particles relative to one another could be observed until the yield point was reached. At this point, a definite line of demarcation was observed at about 1/3 the distance from the wall of the cone to the wall of the cup. It appeared that the material on the cup side (outer) of the line of demarcation was turning as a whole with the cup, while the material adjacent to the cone was undergoing concentric shearing. This experiment demonstrates that the yield takes place by means of a slip in the main body of the gel, and that the counterpart of tubular plug flow exists in the concentric conical apparatus.

This phenomena can be described as follows with the idealized diagram given in Figure 37 in which the particles of black are assumed to have been placed on the surface of the gel in a narrow radial filament. Stage 1 represents the filar position of the particules before the shear has been applied. At stage 2, the shear angle has been applied and the alignment of the particles indicates a slight retardation of the particles nearest the inner wall (it is assumed the outer wall rotates in the direction of the arrow) which decreases uniformly to the outer wall. This retardation is due to the elastic effect indicated by the linear section of the curves of Figures 33,34, and 35. When the shear angle has increased from stage 1 to stage 3, the gel is at the point of incipient shear which occurs along the indicated line of slip. This point would correspond to the end of the linear section on the curve shown by the shearing stress-shear diagrams. At stages 4 and 5, yield has occurred and the particles inside the line of slip are being displaced according to concentric laminar flow. Stage 5 is given to indicate the possible recession of the line of slip as the shearing action wears the particles from geled material at the boundary between it and the fluid material. This stage was not observed by the coal particles test since it was difficult to distinguish the relative displacements of the particles after $360^0$ of rotation had occurred.
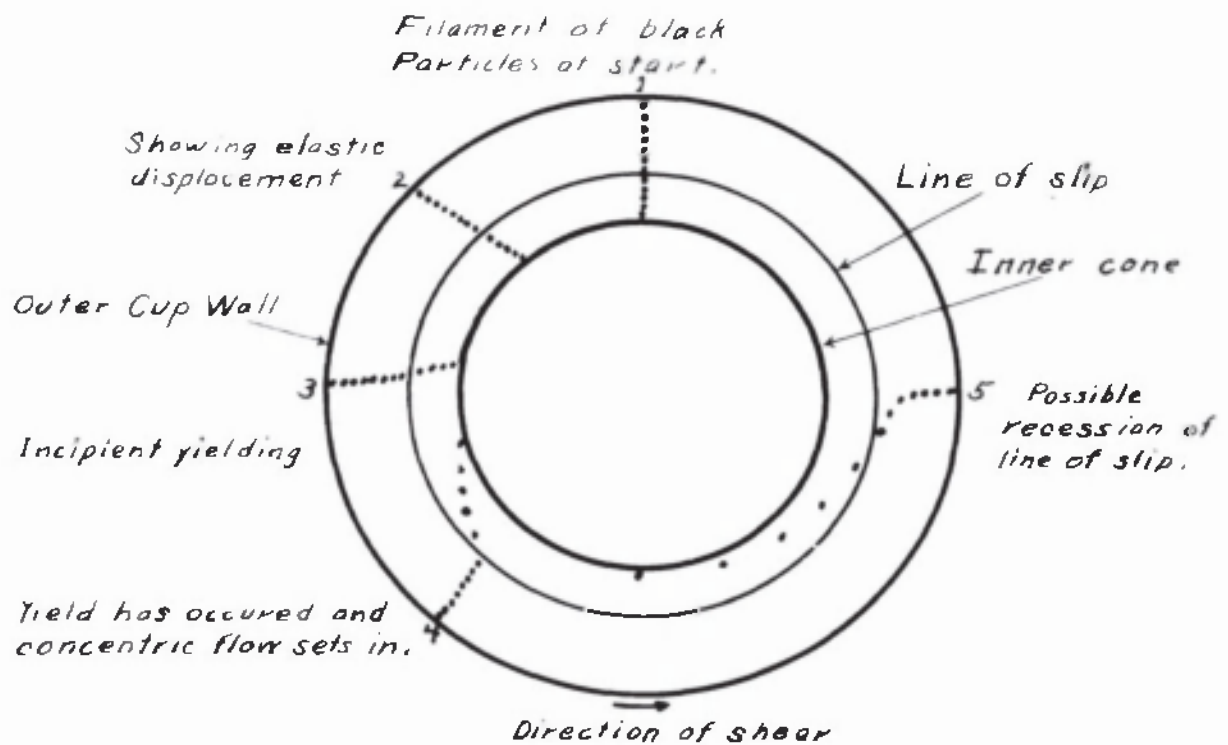
Figure 37. Idealized Diagram Showing the
Line of Slip in a Bentonite Gel Under-
going Shearing.

### 5. The Effect of the Rate of Shear on the Shearing Stress-Shear Diagram. Series V Tests.

It will be remembered that the determination of a shearing stress-shear diagram by observing the shearing stress caused by uniformly increasing the shear gives a rate factor. In the above diagrams this factor was a constant though very small rate of shear of such magnitude that the shearing stress could be observed without appreciable error for any given total value of the shear. It has been recognized that the rate of loading is one of the factors that must be specified in the determination of the tensile strength of metal.[70] Smekal[71] has indicated that the relation of the rate of loading must be considered in the determination of the yield value and plastic properties of crystals. In order to ascertain the importance of this factor in the shearing stress-shear measurements on the bentonite suspensions, the following experiments were performed.

In general, the procedure was that described for the determination of the shearing stress-shear diagrams of the Series IV tests. In the present case, tests were conducted at the four different speeds of rotation listed above in section 3, namely, 0.007, 0.014, 0.030 and 0.059 r.p.m. These different speeds of rotation afford the means of determining the effect

---

[70] A. S. T. M. Standard E8-33 (1933)
[71] A. Smekal. International Conference on Physics, London, II: 106 (1935).

of varying the rate of shear on shearing stress-shear measurements, since they are equivalent to rates of shear of 0.0078, 0.0155, 0.0333 and 0.0667 sec.$^{-1}$ respectively (at a separation of 2.0 mm.). The tests were performed upon the 7% suspension which was allowed to stand quiescent in the cup for exactly 1 hour before the application of the shear was started. The deflection readings of the inner cone were continued to a much greater range of shear than formerly as determined by the angle of sweep measured on the lower protractor. Reasonable agreement was obtained between the data of several runs made at each speed of rotation. However, since the complete data are quite extensive, Table 28 contains the data for the curves of Figure 38 which best represented the average. As before, the readings have been converted to dynes per square centimeters and shear angle.

It is seen from Figure 38 that the increase of the rate of shear has the effect of shifting the entire curve upwards on the shearing stress-shear diagram. The upwards shift seems to be roughly proportional to the rate of shear in the regions near the maxima. After the maxima has been passed, the curves decrease to a horizontal section that fluctuates about a constant value as the shear angle steadily increases. With the exception of the curve determined at a rate of shear of 0.0667 sec.$^{-1}$, the constant value is roughly proportional to the rate of shear.

The whole course of the curves shown in Figure 38 can be

## Table 28

Shearing Stress – Shear Data Showing the Effect
of Rate of Shear.
7% Bentonite Suspension.
1 Hour Setting Period.

Temperature 25°                                          Wire NO

| Angle of Cup Twist deg. | $\sigma = 0.078$ | | $\sigma = 0.0155$ | |
|---|---|---|---|---|
|  | Shear Angle deg. | Shearing Stress d./sq.cm. | Shear Angle deg. | Shearing Stress d./sq.cm. |
| 0 | 0 | 0 | 0 | 0 |
| 5 | 0 | 1.28 | 0 | 1.28 |
| 10 | 0 | 2.56 | 0 | 2.56 |
| 15 | 0.2 | 3.78 | 0 | 3.83 |
| 20 | 0.3 | 5.03 | 0.1 | 5.00 |
| 25 | 0.3 | 6.31 | 0.2 | 6.33 |
| 30 | 0.4 | 7.56 | 0.3 | 7.58 |
| 35 | 0.6 | 8.78 | 0.4 | 8.33 |
| 40 | 1.1 | 9.93 | 0.9 | 9.98 |
| 45 | 2.7 | 10.81 | 1.9 | 11.00 |
| 50 | 6.3 | 11.18 | 3.5 | 11.88 |
| 55 | 12.5 | 10.87 | 6.2 | 12.48 |
| 60 | 20.4 | 10.12 | 10.6 | 12.63 |
| 65 | 28.7 | 9.27 | 16.5 | 12.29 |
| 70 | 36.1 | 8.67 | 23.4 | 11.90 |
| 75 | 43.0 | 8.17 | 31.2 | 11.20 |
| 80 | 49.0 | 7.92 | 38.7 | 10.56 |
| 85 | 54.8 | 7.71 | 45.9 | 9.98 |
| 90 | 60.0 | 7.66 | 52.9 | 9.47 |
| 95 | 65.3 | 7.58 | 59.2 | 9.14 |
| 100 | 70.2 | 7.61 | 65.3 | 8.86 |
| 105 | 75.2 | 7.61 | 71.0 | 8.68 |
| 110 | 80.1 | 7.63 | 76.4 | 8.57 |
| 115 | 85.0 | 7.66 | 81.5 | 8.56 |
| 120 | 90.0 | 7.67 | 86.5 | 8.56 |
| 125 | 95.0 | 7.67 | 91.3 | 8.60 |
| 130 | 99.9 | 7.66 | 96.1 | 8.66 |
| 135 | 104.8 | 7.71 | 100.8 | 8.73 |
| 140 | 109.8 | 7.72 | 105.6 | 8.78 |
| 145 | 114.6 | 7.76 | 110.5 | 8.81 |
| 150 | 119.3 | 7.84 | 115.6 | 8.78 |

Table 28 Continued.

| Angle of Cup Twist deg. | σ = 0.078 | | σ = 0.0155 | |
|---|---|---|---|---|
| | Shear Angle deg. | Shearing Stress d./sq.cm. | Shear Angle deg. | Shearing Stress d./sq.cm. |
| 160 | 129.2 | 7.87 | 126.7 | 8.66 |
| 170 | 139.1 | 7.89 | 137.1 | 8.40 |
| 180 | 149.3 | 7.84 | 147.6 | 8.27 |
| 190 | 159.6 | 7.76 | 157.2 | 8.37 |
| 200 | 169.2 | 7.87 | 166.8 | 8.48 |
| 210 | 179.0 | 7.92 | 176.2 | 8.63 |
| 220 | 188.8 | 7.97 | 186.3 | 8.63 |
| 230 | 198.8 | 7.97 | 196.3 | 8.61 |
| 240 | 208.7 | 8.00 | 207.0 | 8.42 |
| 250 | 218.4 | 8.07 | 217.5 | 8.29 |
| 260 | 228.1 | 8.15 | 227.7 | 8.24 |
| 270 | 238.0 | 8.17 | 237.2 | 8.37 |
| 280 | 248.3 | 8.10 | 246.7 | 8.50 |
| 290 | 259.0 | 7.92 | | |
| 300 | 269.1 | 7.89 | 267.0 | 8.42 |
| 310 | 279.0 | 7.92 | 277.2 | 8.37 |
| 320 | 289.3 | 7.84 | 287.7 | 8.24 |
| 330 | 299.8 | 7.71 | 297.0 | 8.17 |
| 340 | 310.0 | 7.66 | 307.5 | 8.29 |
| 350 | 319.8 | 7.71 | 317.1 | 8.40 |
| 360 | 320.2 | 7.87 | 326.6 | 8.53 |
| 370 | 338.6 | 8.02 | 336.5 | 8.55 |
| 380 | 348.7 | 7.98 | 347.2 | 8.37 |
| 390 | 358.8 | 7.97 | 357.8 | 8.22 |
| 400 | 368.8 | 7.97 | 368.1 | 8.14 |
| 410 | 378.7 | 8.10 | 377.8 | 8.22 |
| 420 | 388.8 | 7.97 | 387.5 | 8.29 |
| 430 | 399.4 | 7.83 | 397.2 | 8.37 |
| 440 | 409.2 | 7.80 | | |

Table 28 Continued.

| Angle of Cup Twist deg. | $\sigma = 0.0333$ | | $\sigma = 0.0667$ | |
|---|---|---|---|---|
| | Shear Angle deg. | Shearing Stress d./sq.cm. | Shear Angle deg. | Shearing Stress d./sq.cm. |
| 0 | 0 | 0 | 0 | 0 |
| 5 | 0 | 1.28 | 0 | 1.28 |
| 10 | 0 | 2.56 | 0 | 2.56 |
| 15 | 0 | 3.84 | 0.1 | 3.81 |
| 20 | 0 | 5.12 | 0.1 | 5.08 |
| 25 | 0 | 6.40 | 0.1 | 5.36 |
| 30 | 0.2 | 7.61 | 0.2 | 7.61 |
| 35 | 0.2 | 8.88 | 0.3 | 8.87 |
| 40 | 0.4 | 10.12 | 0.6 | 10.07 |
| 45 | 0.7 | 11.32 | 0.8 | 11.28 |
| 50 | 0.9 | 12.55 | 0.8 | 12.59 |
| 55 | 1.7 | 13.63 | 1.1 | 13.80 |
| 60 | 3.1 | 14.59 | 1.1 | 15.09 |
| 65 | 5.0 | 15.36 | 1.4 | 16.28 |
| 70 | 7.7 | 15.96 | 2.0 | 17.4 |
| 75 | 11.6 | 16.25 | 3.2 | 18.4 |
| 80 | 16.8 | 16.20 | 4.6 | 19.3 |
| 85 | 22.8 | 15.92 | 6.9 | 20.0 |
| 90 | 29.6 | 15.48 | 10.6 | 20.3 |
| 95 | 36.6 | 14.97 | 15.5 | 20.4 |
| 100 | 43.8 | 14.38 | 21.7 | 20.1 |
| 105 | 51.0 | 13.82 | 28.9 | 19.5 |
| 110 | 58.3 | 13.71 | 37.1 | 18.6 |
| 115 | 65.5 | 12.65 | 40.4 | 17.8 |
| 120 | 72.7 | 12.08 | 53.9 | 16.9 |
| 125 | 79.4 | 11.64 | 61.9 | 16.13 |
| 130 | 85.9 | 11.25 | 70.4 | 15.15 |
| 135 | 92.2 | 10.93 | 78.5 | 14.45 |
| 140 | 98.1 | 10.70 | 86.4 | 13.71 |
| 145 | 103.8 | 10.50 | 93.8 | 13.10 |
| 150 | 109.5 | 10.33 | 100.7 | 12.61 |

Table 28 Continued.

| Angle of Cup Twist deg. | σ = 0.0333 | | σ = 0.0667 | |
|---|---|---|---|---|
| | Shear Angle deg. | Shearing Stress d./sq.cm | Shear Angle deg | Shearing Stress d./sq.cm. |
| 160 | 120.2 | 10.17 | 114.0 | 11.75 |
| 170 | 130.6 | 10.07 | 126.0 | 11.43 |
| 180 | 141.1 | 9.93 | 137.6 | 10.84 |
| 190 | 151.1 | 9.93 | 149.1 | 10.47 |
| 200 | 161.0 | 9.96 | 160.1 | 10.19 |
| 210 | 170.9 | 9.99 | 170.5 | 10.08 |
| 220 | 180.6 | 10.07 | 180.9 | 9.98 |
| 230 | 190.6 | 10.07 | 191.1 | 9.93 |
| 240 | 200.4 | 10.12 | 201.3 | 9.87 |
| 250 | 210.2 | 10.16 | 211.5 | 9.83 |
| 260 | 220.0 | 10.21 | 221.9 | 9.73 |
| 270 | 230.2 | 10.16 | 232.0 | 9.70 |
| 280 | 240.4 | 10.12 | 242.6 | 9.54 |
| 290 | 250.6 | 10.07 | 252.9 | 9.48 |
| 300 | 261.4 | 9.86 | 263.1 | 9.42 |
| 310 | 272.2 | 9.65 | 273.1 | 9.42 |
| 320 | 282.6 | 9.54 | 283.3 | 9.42 |
| 330 | 292.9 | 9.47 | 293.4 | 9.34 |
| 340 | 303.1 | 9.43 | 303.3 | 9.37 |
| 350 | 313.4 | 9.35 | 313.4 | 9.34 |
| 360 | 323.3 | 9.37 | 323.5 | 9.32 |
| 370 | 333.1 | 9.43 | 333.8 | 9.24 |
| 380 | | | 343.9 | 9.22 |
| 390 | 352.6 | 9.55 | 354.0 | 9.20 |
| 400 | 362.6 | 9.55 | 363.9 | 9.22 |
| 410 | | | 373.9 | 9.22 |
| 420 | 382.6 | 9.55 | 383.9 | 9.22 |
| 430 | 392.3 | 9.62 | 393.9 | 9.22 |
| 440 | 402.3 | 9.62 | 403.8 | 9.24 |
| 450 | 412.5 | 9.57 | 413.8 | 9.24 |
| 460 | 422.7 | 9.53 | 423.9 | 9.20 |
| 470 | 432.7 | 9.53 | 434.1 | 9.17 |
| 480 | 442.9 | 9.47 | 443.9 | 9.20 |
| 490 | 453.0 | 9.40 | 453.7 | 9.27 |
| 500 | 463.2 | 9.40 | 463.6 | 9.29 |
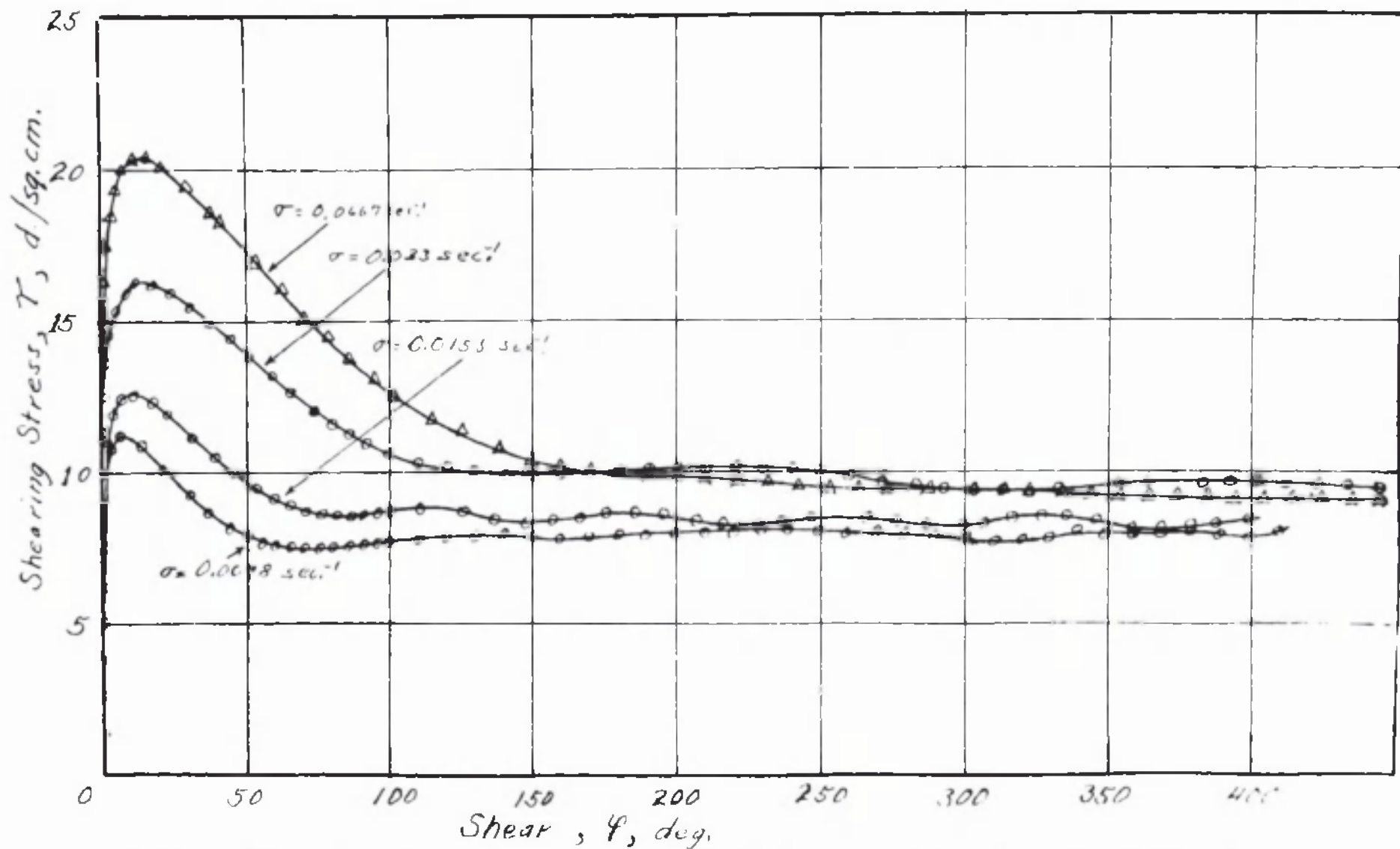
Figure 38  Shearing Stress - Shear Diagram Showing the Effect of Varying the Rate of Shear.

interpreted on the basis of three stages. In stage I, the shear is acting upon material that possesses the characteristics of an elastic solid. Thus for only a very small amount of shear, the shearing stress developed is quite large and is governed by Hooke's law. In the case of the curves in Figure 38, the scale used in plotting seems to mask the linearity that is required by Hooke's law; however, this behavior has been adequately indicated by the curves appearing in Figures 33, 34 and 35, hence it can be assumed to be present here. The failure of the suspension to obey Hooke's law at the yield point marks the beginning of stage II which can be designated as the elastico-viscous portion of the curve. This is regarded as due to the remaining structural elements that are fast breaking up tending to release the inner cone and allow it to return to its equilibrium position. This is opposed by the forward motion of the shearing action which as the last elements of continuous structure break up is unable to sustain the stress at the maximum and thus rapid decay occurs and the curve passes into stage III in which the shearing stress is due to the viscous character of the fluid material. The descending portion of the curve after the maximum is characterized by the completion of the transition from a solid material to a fluid material. The stress is being rapidly released and a higher rate of shear exists because of the rotation of the inner cone in the opposite direction to the rotation of the cone. Gel fragments are being reduced in size and possibly completely destroyed, and the material ultimately

arrives at the beginning of the horizontal section in which the viscous effect governs the shearing stress that is developed by the constant rate of shear.

The wave form of the curves that is obtained over the horizontal section is of interest since it indicates an alternate building up and destruction of structure. A possible hypothesis for the explanation of this behavior is as follows. During the greater-than-normal rate of shear generated as the inner cone returns towards its zero position turning against the outer cup more than the equilibrium amount of structure is destroyed and hence the inner cone carries beyond the equilibrium position. Inertia also aids in carrying the inner cone beyond the equilibrium position. Therefore, after the inner cone reverses its rotation the two surfaces turn together until the opposing force of the torsion wire brings the inner cone to rest again. During this period structural elements can form from wall to wall and it is probable that some will be stronger than others. These stronger elements tend to carry the inner cone beyond the equilibrium position until the mounting shearing stress causes their failure whereupon the load is transferred to the weaker structural elements and progressive decay results. Again the inner cone turns against the outer rotation f the outer cup and the greater-than-normal rate of shear carries the inner cone beyond the equilibrium position and the cycle thus repeats itself.

The indications are that these suspensions obey Hooke's law of elasticity. It appears to be feasible to use the failure

to obey the law as a criterion for the determination of shearing stress at the yield point. Since the instrument was incapable of affording the sensitivity needed to examine critically the section of the curve that is deemed linear, only cursory conclusions can be made in regards to the effect of varying the rate of shear. The maxima in Figure 38 show a profound response to a change in the rate of shear. However, since the maxima are not accepted as the true yield point, it is necessary to look to the Hooke's law criteria for indication of the yield point and its response to changes of rate of shear. It cannot be said with certainty just where the curves rising from the origin in Figure 38 cease to be linear. In Figure 39, the first few points for the curves at the highest and lowest rates of shear, 0.0667 and 0.0068 sec.$^{-1}$, respectively, have been plotted using larger units on the shear angle axis. It would appear that the departure from linearity takes place at about the same shearing stress with both curves which could indicate that the yield value is independent of the rate of shear.

It is of interest to note in Figure 39 that the higher rate of shear has given a greater shearing stress for a given shear angle. For example, at the shear angle of 0.1$^{\circ}$, the shearing stress is 1.9 d./sq.cm. and 3.8 d./sq.cm. for the lower and higher rates of shear respectively. It appears that this behavior is evidence of a relatively slow relaxation time which governs the decrease of the shearing stress to a constant value when a shear is applied to the bentonite gel.
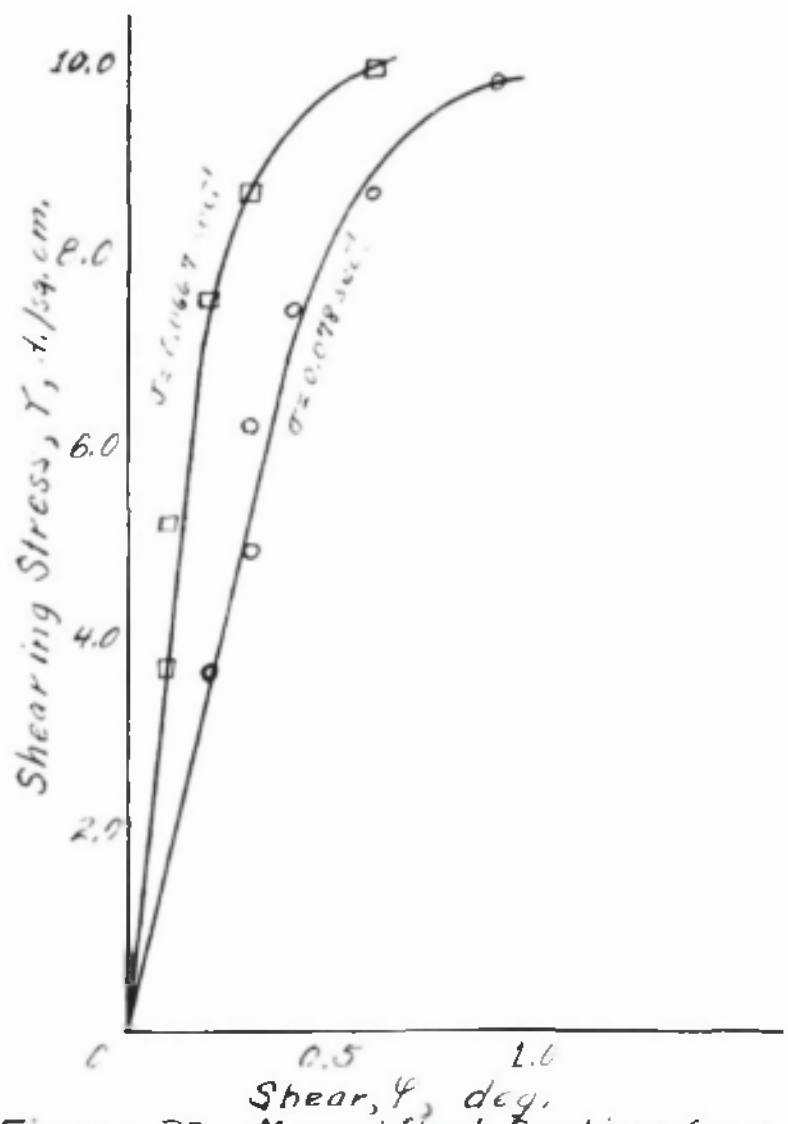
Figure 39. Magnified Section from near
Origin of Figure 38.

At the higher rate of shear in Figure 39, the shearing stress did not have time enough to decrease to the smaller value that was obtained by the smaller rate of shear. Undoubtedly this effect continues beyond the yield point and contributes considerably to the attainment of the maxima shown in Figure 38.

The relation of relaxation time and the coefficient of elasticity of a body to its viscosity was given by Maxwell[72] in 1868. Subsequent investigations by Schwedoff[73] and others indicated that the experimental conditions seldom conformed to the necessary assumptions and that in general, the matter was not as simple as Maxwell had indicated. The elastic regidity of suspensions and gels has been the subject of investigations by Hatschek and Jane,[74] Michaud,[75] McDowell and Usher,[76] Freundlich and Seifritz,[77] Brimhall and Hixon.[78] These workers have given only slight attention to the possibility of measurable relaxation times and its relation to the coefficient of elasticity. Scott Blair[79] has observed its influence in the measurements made for yield stresses on flour doughs. However, it does not appear to have been reported in relation to the determination of the yield stress of clay or bentonite

[72] J. C. Maxwell. Phil. Mag. 35:129 (1868)
[73] T. Schwedoff. J. de Physique 8:341 (1889)
[74] E. Hatschek and R. S. Jane. Koll. Z. 39:300(1926).
[75] M. H. Michaud. Compt. rend. 174:1282 (1922) 175:196 (1922)
[76] C. M. McDowell and F. L. Usher. Proc. Roy. Soc. A131:409, 564 (1931).
[77] H. Freundlich and W. Seifritz. Z. Physik. Chem. 104:232(1923)
[78] B. Brimhall and R. M. Hixon. Ind. Eng. Chem. Anal. Ed. 11: 358 (1939)
[79] J. W. Scott Blair. Physics, 4:113 (1933)

suspensions.  It appears that any rational determination of
the yield stress should take these factors into consideration.
Unfortunately, the Goodeve instrument was of insufficient
sensitivity to allow more than the indication of this inter-
esting effect.

CHAPTER X

DISCUSSION AND CONCLUSION REGARDING THE FLUID
PROPERTIES OF BENTONITE SUSPENSIONS.

1. In Relation to the Bingham Concept.

The work in the foregoing chapters has established a
number of facts concerning the fluid nature of the bentonite
suspensions.  Since the bentonite suspensions used in this
investigation are regarded as typical of so-called anamolous
flow, the information that has been obtained will have an ap-
plication to the many other materials that exhibit this be-
havior.

The rheological diagrams obtained in Chapters VI and VII
indicate that the fluid behavior of the bentonite sols of con-
centrations greater than 2% is non-Newtonian because a curved
relationship is found to exist between the shearing stress
and the rate of shear.  This curved relationship is described
by a parabolic equation of the type suggested by Ostwald and
de Waele.[31]  Particular attention is given the fact that
the rheological curves rise from the origin.  This means that
at zero rate of shear the shearing stress is zero, and that
the rheological curve is the same as curve C in Figure 3.

It has been generally held that highly structural bentonite
suspensions exhibit flow properties that conform to those pre-
scribed by Bingham, illustrated by curve B in Figure 3.

If the Bingham theory is valid for these suspensions then
it is logical to expect that the rheological diagrams show an
intercept on the stress axis and are described by Equation 43

or an equation of its same general form. No indication of this behavior is obtained, therefore, it is concluded that the bentonite suspensions used in this investigation do not exhibit the Bingham type of flow.

On the remote possibility that the bentonite suspensions employed, were not capable of developing sufficient structural rigidity to allow the existence of a yield point, the experiments of Chapter IX were conducted with the viewpoint of proving the reality of the yield value. This endeavor was given greater significance in view of the uncertainty expressed by von Nieuwenburg and Houwink concerning the fixing of the yield point on the rheological diagram representing the Bingham type of flow. The results of the tests demonstrated conclusively that a yield value could be detected in the 6, 7, and 8 per cent suspensions, and could not be detected under the conditions of the test with the suspensions of lesser concentrations. The existence of the yield point in the 6, 7, and 8 per cent suspensions could be considered as partial indication that the material conforms to the Bingham type of flow behavior.

In relation to the Bingham concept, the results of these two experimental approaches point to an apparent contradiction. Stated concisely, the contradiction is as follows: particular bentonite suspensions have been shown to possess a yield value which is not indicated by the flow curves that have been experimentally determined and found to curve into the origin as the rate of shear was made smaller.

It is evident that variables used to measure the charac-
teristics of solid and fluid states have been erroneously merged
by Bingham in his hypothesis for the explanation of the fluid
behavior of the highly structural materials such as the bento-
nite suspensions investigated here. The following considerations
will show the reason for this statement and indicate the un-
satisfactory physical basis for the Bingham hypothesis.

The elastic behavior of the solid state is characterized
by the relation between the variables, shearing stress and shear,
and affords the physical basis for the concept of yield value
as pointed out in section 3 of Chapter IX. On the other hand,
the fluid state is most conveniently described by the relation
between the variables, shearing stress and rate of shear, which
has been discussed fully in Chapter I. Bingham's suggestion
that the solid state of gel materials can be characterized by
the distance along the shearing stress axis of a rheological
or viscosity diagram seems quite illogical because he has sub-
stituted rate of shear for shear, on the other axis. It is
true that the application of a shearing stress, less than the
yield value, will allow the observation of the rigidity of
the solid material, but it does not follow from the Bingham
diagram that the application of successively smaller rates of
shear will allow the detection of the solid state by a residual
shearing stress, as the rate of shear becomes infinitely small
and finally zero. Since the rate of shear can be maintained
as long as desired, the corresponding shear angle is necessarily
large, and hence the structure causing the rigidity must be in
a broken or ruptured condition. The broken condition of the

structure is obtained for even infinitely small rates of shear including the limiting value of zero rate of shear since there is no limit to the length of time the rate of shear acts. It follows therefore that on the viscosity diagram the shearing stress is always zero at zero rate of shear and, consequently there can be no yield value in the Bingham sense.

It is emphasized, however, that the existence of a yield point is not denied these materials, but rather it is the existence of the yield point on the rheological diagram that is emphatically rejected.

It is not surprising that the Bingham interpretation has received considerable support when it becomes apparent that the greater majority of the investigators employed experimental methods wherein the material was subjected to shearing stress loads applied by pressure heads in capillary apparatus or torque loads in the concentric cylinder apparatus. Under such conditions the shearing stress is the independent variable and a minimum critical value could be observed at which yield occurred. Obviously these experiments were shearing stress-shear determinations in which the shear was not considered. It must be remarked that data for shearing stress-rate of shear observations taken immediately after yield are in no place reported in the literature.

The diagram given in Figure 40 can be used to illustrate what takes place when a material such as a bentonite gel is subjected to a very small rate of shear. It is assumed that the gel has developed considerable structure and may be deemed to
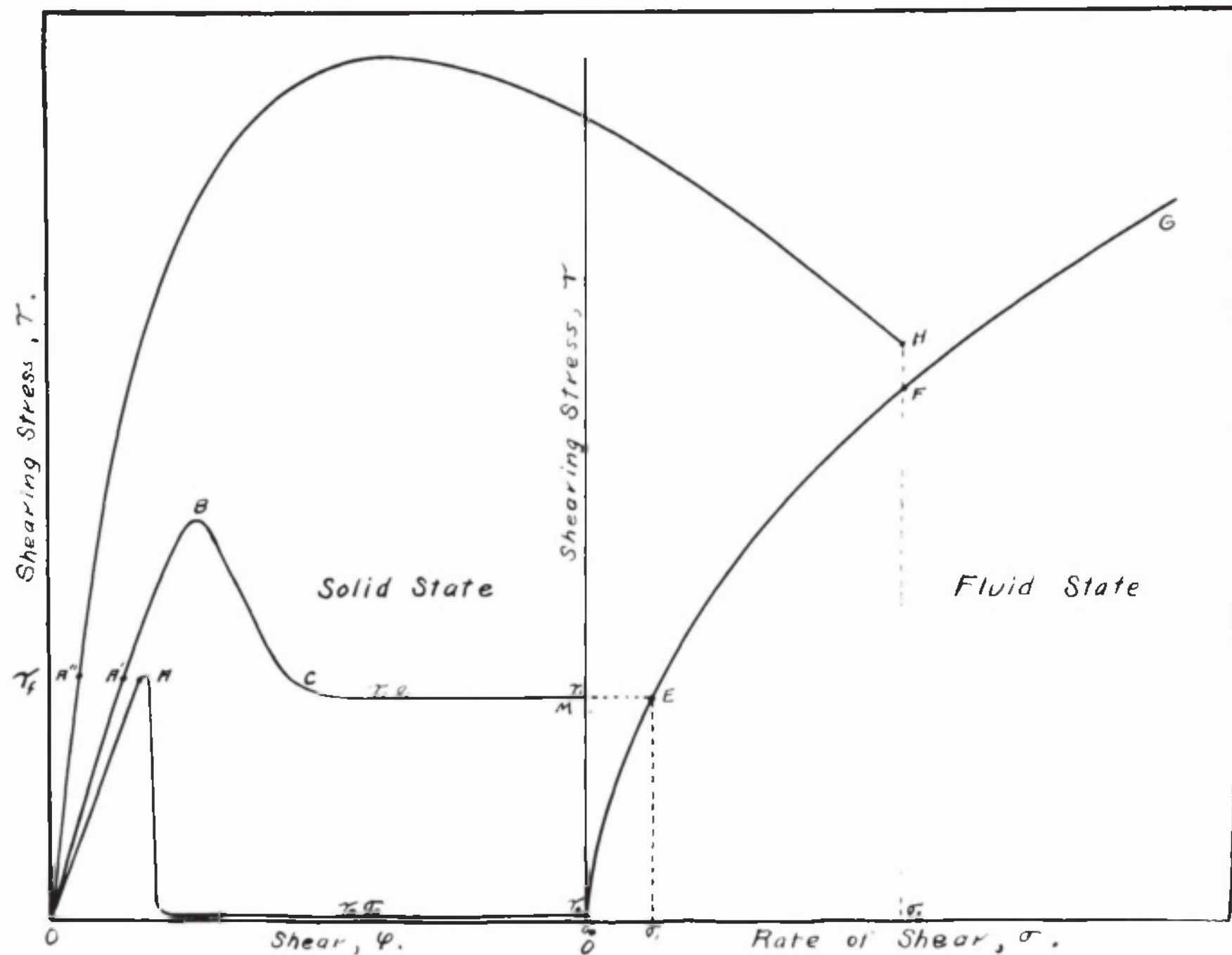
Figure 40. Diagrammatic Representation of the Relationship Between the Solid State and Fluid State for Suspensions.

be in the solid state. The relationships given in Figure 40 are diagrammatic, but are based upon the form of the curves obtained in the Series II and V tests. The diagram on the left represents the measurements that are properly made on the solid condition of the material with the variables shearing stress and shear; while the diagram on the right represents the usual rheological diagram for the liquid state. When an increasing shear is applied to the structurally rigid material, the stress increases uniformly from the zero value up to say, point A′ whereupon yield occurs and the transition from the solid state to the liquid state commences. It is assumed the rate at which the shear angle is generated operates at a speed that does not allow sufficient time for complete relaxation to occur, therefore the stress increased along line O A′. The gel-sol transition that begins at A′ lasts until C at which point equilibrium is reached between the destruction of the structure and its inherent tendency to heal. Since the uniform increasing of the shear occurs as a rate of shear, there exists a point on the rate of shear axis of the coordinate system on the right, that corresponds to the rate at which the shear was applied to make the observations on the solid state. This point corresponds to the extension of the stress at equilibrium indicated by the section C E, to the right until it reaches the curve O E F G at point E. The abscissa at point E represents the rate of shear $\sigma$ , at which the shearing stress-shear observations were made. The whole curve O E F G represents the shearing stress-rate of shear relationship for the liquid created

by the transition between A' and point C.

It is of interest to consider the probable course that will be indicated on Figure 40 when a very low and a relatively high rate of shear is employed. In the first case when a vanishingly small rate of shear is applied to the solid gel, the shearing stress increases in accordance with its elastic behavior to point A where yield will take place. Since at the extremely slow rate of shear there will be sufficient time for complete relaxation of all the structural linkages, the shearing stress will not rise above the value at A. After the collapse of all continuous structural linkages, the shearing stress will drop almost vertically to a vanishing small shearing stress represented by the horizontal line extending to the right to intersect with the line O E F G at the abscissa value that represents the vanishingly small rate of shear, $\sigma_0$ .

When the rate at which the shear applied is quite large, the curve on the shearing stress, shear side of Figure 40 is passed over almost instantaneously. At the very high rate of shear, time for complete relaxation is insufficient therefore the shearing stress increases along the line O A''. At A'' yield occurs, but is not distinct since the vigor of the shearing action almost instantaneously carries the shearing stress through the maximum to point H on the rheological diagram. At point H, the structure is destroyed by the shearing forces and the shearing stress gradually drops to point F on the rheological curve which represents the equilibrium condition.

## 2. Summary and Conclusions.

An examination of the basic principles of viscosity measurements indicated the importance of using the fundamental units of rate of shear and shearing stress for the characterization of the fluid behavior of bentonite suspensions.

Calibration experiments on the Goodeve viscometer using standards with certified coefficients of viscosity have shown that the instrument affords a means for applying a definitely known rate of shear to the sample and measuring the effect as a shearing stress.

A structure breaker was designed and constructed to give means of attaining a reproducible fluid condition with the highly structural bentonite suspensions.

The study showed that under a constant sustained rate of shear the shearing stress developed by a bentonite suspension tends to attain an equilibrium between the destructive action of the shearing surfaces and the tendency of the bentonite to develop structural rigidity.

The rheological curves determined under equilibrium conditions are not Newtonian with concentrations of bentonite greater than about 2% weight, and seem best related to the parabolic equation as recommended by Ostwald and de Waele.[31/]

The concept of thixotropy was related to the rate at which gel structure is formed in the suspensions. Its effect was demonstrated by a diagram showing the open loops obtained with a cyclic increase and decrease of the shearing stress-rate of shear observations.

The existence of yield values was demonstrated by means of the relation between the variables of shearing stress and shear, for the suspensions containing 6 weight per cent and greater of bentonite.

The study of the yield value has indicated that measurable elastic effects are present in bentonite gels and that such effects afford a convenient criterion for the determination of the shearing stress at the yield point.

Indications were obtained that a relaxation time was closely associated with observations determining the relationship between shearing stress and shear for the bentonite gels.

Observations of shearing stress at very low rates of shear formed the basis for the conclusion that the bentonite suspensions do not conform to the fluid behavior postulated by Bingham.

The apparent contradiction induced by the observation of a yield value and the curvilinear shearing stress-rate of shear relationship intersecting the origin on the rheological diagram served to bring attention to the impropriety of the yield point on the shearing stress axis of the rheological diagram. As a result, the Bingham concept must be denied.

A diagram indicating the relationship of the rigid state which manifests a yield point to the fluid condition obtained after a shearing stress surpasses the yield value has been proposed, based upon data obtained experimentally.

## ACKNOWLEDGMENTS.

# VITA.

Carl Kerby Stoddard

Doctor of Philosophy, 1941.

December 20, 1907.

Place of Birth: Reno, Nevada.

Secondary Education:

Attended high schools Nevada and California; graduating
from Berkeley High School, Berkeley, California, June, 1927.

Collegiate Institutions attended:

University of Nevada, 1929-34.   B. S. in chemistry 1934.

University of Nevada, 1934-36.   M. S. in chemistry 1936.

University of Maryland, 1938-40.

Positions held:

Prior to graduation from high school, the author spent
a number of months working in the mills of the Columbia
Steel Corporation at Pittsburg, California.   After gradua-
tion from high school and before entering college, he was
employed for 15 months by the Union Oil Company in the
inspection laboratory located at Oleum, California.
During undergraduate years at the University of Nevada,
the author was employed testing petroleum products for
the Nevada State Pure Food and Drugs Department.  Through
association with his father, a mining engineer, incidental
employment and experience with the mineral industries has
formed a considerable part of the environmental background
of the author.   After receiving the bachelor's degree he

was awarded a fellowship in chemistry at the Nevada
State Agricultural Experiment Station. The work was
related to the study of plant poisons that occasionally
c use large stock losses in the semi-acid grazing lands
of the west. This fellowship also allowed his enrollment
in the Graduate School of the University of Nevada in
candidacy for the master's degree. From July 1936 to
December 1937 he was employed as junior engineer for the
Gold and Silver Circle Mines Inc., at Midas, Nevada,
where his duties were the conducting of underground and
surface surveying, map making, fire assaying, and metal-
lurgical testing. During the period from January 1938
to June 1938, he assisted as instructor in chemistry at
the University of Nevada. In June 1938, he entered the
Graduate School of the University of Maryland having re-
ceived a cooperative fellowship with the U. S. Bureau
of Mines and the University of Maryland. At present he
is employed as research chemist by the American Society
of Mechanical Engineers for studies in relation to the
intercrystalline cracking of boiler plate steel.